BOUNDARY MODE FRICTIONAL PROPERTIES OF ARTICULAR CARTILAGE: FUNCTIONAL IMPLICATIONS OF LUBRICIN LOCALIZATION

A Dissertation

Presented to the Faculty of the Graduate School

of Cornell University

In Partial Fulfillment of the Requirements for the Degree of

Doctor of Philosophy

by

Jason Paul Gleghorn

January 2008

© 2008 Jason Paul Gleghorn

BOUNDARY MODE FRICTIONAL PROPERTIES OF ARTICULAR CARTILAGE: FUNCTIONAL IMPLICATIONS OF LUBRICIN LOCALIZATION

Jason Paul Gleghorn, Ph. D.

Cornell University 2008

Lubrication of cartilage involves a variety of physical and chemical factors, including lubricin, a synovial glycoprotein shown to be a boundary lubricant. It is unclear how lubricin boundary lubricates a wide range of bearings from tissue to artificial surfaces, and if the mechanism is similar for soluble and bound lubricin.

The objective of this research was to investigate lubricin as a mediator of articular cartilage boundary mode frictional properties. The central hypothesis of this dissertation was that the boundary mode friction coefficient is mediated by localization of lubricin at the tissue surface. In order to determine the frictional properties of cartilage, a linearly oscillating cartilage-on-glass friction apparatus was designed and validated, and a novel extension of the Stribeck curve, a 'Stribeck surface,' was created to map cartilage lubrication modes. The first aim identified the ability of exogenous lubricin to lubricate articular cartilage and characterized the differential roles of bound and soluble lubricin. The second aim investigated the ability of endogenously synthesized lubricin to lubricate cell-alginate constructs generated from chondrocytes, meniscal fibrochondrocytes, and mesenchymal stem cells. The last aim determined the functional effects of short term exposure to TGF-β, IL-1β, and OSM on the frictional properties of cartilage explants.

These studies demonstrate that molecular modification of the tissue surface by localization or removal of lubricin altered the boundary mode frictional properties of cartilage. Additionally, localization of lubricin at the tissue surface is not a simple

adsorption mechanism, with aggregation, steric arrangement of the molecule, and electrostatic interactions possibly playing a role in lubricin's boundary lubricating ability. These findings point to two distinct mechanisms by which lubricin lubricates, one mechanism involving lubricin bound to the tissue surface and the other involving lubricin in solution. The results presented herein suggest that production of extracellular matrix capable of localizing lubricin may be just as or more important than lubricin production in the lubrication of engineered tissues. Further, the recovery of lubrication for catabolically exposed tissue by exogenous lubricin may be therapeutically important to combat high tissue friction found in injury and disease.

BIOGRAPHICAL SKETCH

Jason was born and raised in southeastern Massachusetts with his parents Tom and Mary and sister Anissa. He received a B.S. degree with distinction in Mechanical Engineering with a minor in Organizational Leadership from Worcester Polytechnic Institute. Prior to starting graduate studies, Jason lived and traveled abroad in Thailand and Costa Rica. He also spent a memorable year teaching 7th grade special education science in New Bedford. For several years, Jason was also active with the National Search and Rescue Team. One of Jason's other passions has been his involvement with the National Youth Science Camp where he originally attended as a delegate from Massachusetts in 1996 and went on to contribute in a variety of positions from Assistant Director to invited speaker over the past 10 years.

In 2001, Jason started his PhD at the University of Massachusetts Medical School in Worcester, MA. Since relocating to Cornell alongside his academic advisor, Larry Bonassar, Ph.D., Jason has continued his service to the community as a firefighter and Paramedic. In addition to his dissertation research, he has participated in an exciting range of projects from cartilage injury to novel tissue engineering scaffolds with imbedded microstructure. Jason will continue as a post-doctoral fellow with Brian Kirby, Ph.D. at Cornell's Micro/Nanofluidics Laboratory in the Sibley School of Mechanical and Aerospace Engineering.

To my family.

ACKNOWLEDGMENTS

I would like to extend a sincere thank you to my mentor and advisor, Lawrence Bonassar, Ph.D., for his encouragement and guidance throughout my graduate studies. I am indebted to Larry for believing in me and teaching me. Before I met Larry, I had never touched cartilage nor seen a cell. In the last 6+ years, I have grown significantly, in knowledge, scientific insight, and abilities in the lab, due in no small part to Larry's encouragement. It has been an honor to learn from someone who is so excited and passionate about research.

I would also like to thank the additional members of my advisory committee: John Booker, Ph.D. and Cornelia Farnum, D.V.M., Ph.D.. Jack and Nelly continually challenged me, reminding me of the "big picture" and taught me to think both like an engineer and a scientist. Their expertise, advice, and wisdom solidified the research presented in this dissertation. I am very grateful for their time and enthusiasm.

Larry gave me many opportunities to build my skills through participation in a number of remarkable collaborations and research endeavors with people who have taught me a great deal. Thank you to Abe Stroock, Mario Cabodi, Nakwon Choi, Valerie Cross, Itai Cohen, Mark Buckley, Suzanne Maher, Tim Wright, Steve Doty, Russ Warren, and Scott Rodeo.

I wish to acknowledge my co-authors: Carl Flannery, Ph.D. and Aled Jones, Ph.D. who were instrumental in my work, providing valuable insights and support as I developed my research ideas.

I thank the past students, of which I am the last, from the Center for Tissue Engineering at UMass Med School: Nick, JP, Nichole, and Rani, as well as the present Bonassar lab and biomechanics group at Cornell. You have all challenged me, provided sound advice, and allowed me to learn from you.

I thank Kim Bothi for her endless support and assistance. Thank you for

challenging me everyday while keeping me sane and committed to my dreams.

Most importantly I thank my family, and in particular my mother and father who in addition to support, love, guidance, and opportunity, gave me the greatest gift of all, an education.

This research was primarily funded by the NASA Graduate Student Researchers Program (NNG04-GN57H). Additional funding was provided by Wyeth Research, the University of Massachusetts Medical School, and Cornell University.

TABLE OF CONTENTS

LIST OF FIGURES

CHAPTER 1

CHAPTER 2

CHAPTER 3

CHAPTER 4

CHAPTER 5

APPENDICIES

LIST OF ABBREVIATIONS

AFM	atomic force microscopy
ANOVA	analysis of variance
ASC	ascorbate
BCA	bicinchoninic acid
BMP-2	bone morphogenetic protein-2
BMP-4	bone morphogenetic protein-4
BSF	bovine synovial fluid
CACP	camptodactyly-Arthropathy-Coxa vara-Pericarditis syndrome
CHO	chinese hamster ovary
cm/s	centimeter per second
CO_2	carbon dioxide
CON	articular chondrocytes
DAQ	data acquisition
DMAB	p-dimethylaminobenzaldehyde
DMEM	dulbecco's Modified Eagle's Medium
DMMB	dimethylmethylene blue
DOL54	'dowstream of the liposacroma-associated fusion oncoprotein' 54
EC50	half maximal effective concentration
ECM	extracellular matrix
EDTA	ethylenediamine tetraacetic acid
ELISA	enzyme-linked immunosorbent assay
ESF	equine synovial fluid
FBS	fetal bovine serum
FGF-2	fibroblast growth factor-2
g	gram
GAG	glycosaminoglycans
GF	gage factor
HA	hyaluronic acid
HAPO	hemangiopoietin
HGNC	human gene nomenclature committee
HSD	honestly significant difference (Tukey's HDS test)
Hz	Hertz
IHC	immunohistochemical
IGF-I	insulin-like growth factor-I
IL-1	interleukin-1
IL-6	interleukin-6
IL-1b	interleukin-1 beta
kD	kiloDalton
kg	kilogram
kHz	kilohertz
kPa	kilopascal
LGP-I	lubricating glycoprotein I
MEN	meniscal fibrochondrocytes
mm	millimeter

mm/s	millimeter per second
M	molar
μg/ml	microgram per milliliter
mM	millimolar
μm	micrometer
μm/s	micrometer per second
MPa	megapascal
MMP	matrix metalloproteinase
MSC	mesenchymal stem cells
MSF	megakaryocyte stimulating factor
ng/ml	nanogram per milliliter
nm	nanometer
OA	osteoarthritis
OSM	oncostatin M
Pa	pascal
PBS	phosphate buffered saline
PDGF	platelet-deriver growth factor
PRG4	proteoglycan 4
RA	rheumatoid arthritis
rh	recombinant human
RMS	root mean square
SAPL	surface-active phospholipid
SD	standard deviation
SEM	standard error of the means
SF	synovial fluid
SVD	singular value decomposition
SZP	superficial zone protein
TBS	tris buffered saline
TGF-β1	transforming growth factor - Beta 1
TNF-a	tumor necrosis factor – alpha
U/ml	units per milliliter
VSCR	variable slope concentration-response
ww	wet weight

LIST OF SYMBOLS

Symbol	Variable or parameter	Dimensions
$^{\circ}C$	degrees Celsius	$L^2 M T^{-2}$
ε_N	compressive normal strain	---
E_Y	Young's modulus	$M L^{-1} T^{-2}$
η	dynamic viscosity	$M L^{-1} T^{-1}$
h	fluid film thickness	L
H	Hersey number	---
H_A	aggregate modulus	$M L^{-1} T^{-2}$
k	hydraulic permeability	$L^3 T M^{-1}$
k_{ij}	load cell decoupling calibration matrix	---
L_j	load matrix	$M L T^{-2}$
L_N	normal force	$M L T^{-2}$
L_{N0}	initial L_N, $L_N(t\rightarrow 0)$	$M L T^{-2}$
L_{Neq}	equilibrium L_N, $L_N(t\rightarrow \infty)$	$M L T^{-2}$
L_S	shear force	$M L T^{-2}$
μ	friction coefficient	---
$\mu(t)$	instantaneous friction coefficient	---
μ_0	initial μ, $\mu(t\rightarrow 0)$	---
μ_{min}	minimum μ	---
μ_{eq}	equilibrium μ, $\mu(t\rightarrow \infty)$	---
ω	shaft rotation rate	T^{-1}
P	mean pressure	$M L^{-1} T^{-2}$
R_a	average surface roughness	L
τ	relaxation time constant	T
τ_N	relaxation time constant of $L_N(t)$	T
τ_μ	relaxation time constant of $\mu(t)$	T
σ	stress	$M L^{-1} T^{-2}$
σ_{eq}	equilibrium stress	$M L^{-1} T^{-2}$
v	surface speed	$L T^{-1}$
V_j	voltage matrix	$M L T^{-2}$
V_N	load cell normal channel voltage	$M L T^{-2}$
V_S	load cell shear channel voltage	$M L T^{-2}$

CHAPTER 1
INTRODUCTION

1.1 ARTICULAR CARTILAGE

Structure

Articular cartilage is a highly hydrated tissue that covers the articulating ends of bones. Cartilage is comprised of chondrocytes and a complex heterogeneous extracellular matrix (ECM) consisting of a network of collagen, proteoglycan, and other small molecules. The primary physiological function of cartilage, performed by the ECM, is to provide a low friction interface that distributes compressive loads across diarthrodial joints[133]. While factors such as low cell density, a dense ECM, and limited vascular supply contribute to the tissue's poor regenerative capabilities, cartilage is able to withstand decades of use.

Cartilage consists primarily of water (65-80%) and the ECM comprises approximately 90% of the tissue dry weight[64]. By dry tissue weight, cartilage ECM is comprised mainly of proteoglycans and collagen, aggrecan and type II collagen being the most abundant respectively[45,104]. Proteoglycans consist of a large core protein with covalently bonded, sulfated glycosoaminoglycan (GAG) chains. In the case of aggrecan, the most prevalent large molecular weight proteoglycan found in cartilage, the core protein is non-covalently bound via link protein to long hyaluronic acid (HA) chains[148]. Fibrils of type II collagen, the second most ubiquitous ECM constituent, are covalently crosslinked by type IX collagen[46] forming a collagen network within the tissue. Entanglement of HA and the collagen mesh, in addition to smaller bridging molecules between collagen and aggrecan, such as decorin, biglycan, and fibromodulin[15,65,99], aid in confining the aggrecan within the ECM[157].

The complex structure of the ECM is regulated by chondrocytes, the other main component of cartilage. Chondrocytes are found throughout the ECM, and vary in organization and phenotype with depth from the articular surface[7,33]. At the superficial zone, a dense population of chondrocytes is present with low metabolic rates, compared to those cells deeper into the tissue[6,184,194]. Conversely, the density of middle and deep zone chondrocytes is less than the superficial cells, but they have higher biosynthetic rates of ECM molecules[149,184]. While superficial zone chondrocytes produce fewer ECM macromolecules, a phenotypic characteristic of those cells is the production of lubricin, a biomolecule shown to impart boundary lubrication properties to the tissue[175].

Cartilage matrix metabolism occurs from a variety of physical and biochemical signals that act cooperatively to regulate the balance between anabolic and catabolic activity in ECM turnover. Synovial cytokines, soluble signaling proteins, act via autocrine and paracrine mechanisms to initiate biosynthesis of matrix molecules or the release of proteases for ECM remodeling. In addition to signals received via soluble factors, chondrocytes also obtain physical signals through interactions directly with the ECM[114,187]. Chondrocytes use various heterodimer membrane proteins called integrins to bind to the type II collagen fibrils[154], in addition to other matrix molecules including fibronectin, vitronectin, and tenascin[99,113,116]. While the chondrocytes do not bind directly to the cartilage proteoglycans, the cell surface receptor CD44 does bind to HA[65,100] in the ECM. As a result of these physical connections to the ECM, mechanotransduction occurs, which modulates chondrocyte phenotype, metabolism, and response to mechanical load[114] altering ECM organization and composition[101].

Function

Interactions between the hydrated proteoglycans and the constraining collagen network give rise to the tissue's time and frequency dependent behavior including: biphasic compressive[134], biphasic frictional[49], and flow-independent tensile and shear properties[61]. Material properties such as compressive and shear moduli and hydraulic permeability vary throughout the depth of the tissue and correspond to the local ECM structure and composition[17,28,159].

Resistance to compressive loads is governed by the hydraulic permeability of the tissue and the GAG dependent electrostatic events, producing a strain-rate dependent modulus[1,93]. Compression of the tissue causes pressurization of the interstitial fluid within the ECM that is dissipated as the fluid is exuded from the tissue. The hydraulic permeability, which describes the ease with which a pressure gradient can drive fluid through the tissue, governs the shift between fluid load support and matrix load support as fluid exudation occurs. After the interstitial fluid has reached equilibrium, the cartilage equilibrium compressive properties are dictated by the electrostatic repulsion between neighboring charged GAG chains[19], thereby reducing compaction of the ECM. Following unloading of cartilage, the fixed charge of the concentrated GAG chains produces an osmotic pressure difference that assists in rehydration of the tissue[42], with osmotic swelling kept in check by the collagen network[64]. In a similar manner, fluid pressurization and flow through the tissue cause a time-dependent frictional response producing a low initial friction coefficient when fluid pressurization is high that monotonically increases to an equilibrium friction coefficient as fluid equilibrium within the tissue is achieved[103]. The time scale for the biphasic frictional response is dependent on the sample size and magnitude of the applied load; however, equilibrium of articular cartilage occurs on the order of tens of minutes. Further discussion of cartilage frictional properties and lubrication can be

found later in this chapter.

Conversely, tensile and shear properties are dominated by the solid ECM matrix, primarily the collagen architecture, and are thought to be independent of fluid flow effects. The tensile modulus of cartilage has been shown to be one or two orders of magnitude greater than the compressive modulus[92]. The shear properties likewise are governed exclusively by the properties of the matrix as shear does not induce volumetric changes, bulk fluid flow, or pressure gradients.

Pathology

Composition of the ECM and the resulting mechanical properties change with age, injury, and disease. A decrease in proteoglycan core protein size and shortening of GAG chains occur with age[122] in addition to enzymatic and non-enzymatic crosslinking of collagen[8] and decreasing mitotic and biosynthetic activity of chondrocytes[123]. Cartilage injury induces disruption of the collagen matrix and significant proteoglycan loss at the site of injury. These changes with age and injury lead to the deterioration of mechanical properties and predisposition of the cartilage to develop osteoarthritis (OA).

In addition to increasing age and joint trauma, prevalence of OA correlates with increasing weight and repetitive mechanical loading[99]. In the United States, more than 21 million people were diagnosed with OA in 2005[51] of which more than two thirds are over age 65. By age 75, features of OA are observed almost universally throughout the population[144].

OA is a degenerative joint condition that results in an imbalance between catabolic and anabolic pathways[9] leading to fissures in the cartilage surface, collagen fibrillation, ulcerations, and loss of tissue[16,145]. In this disease state, synthesis of new

ECM components does not keep pace with degradation, as an increase in catabolism of matrix components via metalloproteinases (MMPs) such as collagenases and aggrecanases is observed[99,121,122].

Another arthritic disease prevalent in society is rheumatoid arthritis (RA), an autoimmune disease typified by chronic joint inflammation and synovial hyperplasia. Features of RA include overgrowth of synovial tissue and formation of pannus[30,130] with destruction of the cartilage and bone credited to MMPs, aggrecanases, and serine and cysteine proteases such as capthepsins released from the pannus[31,186]. RA is a progressive disease leading to joint dysfunction[120] that, at least in part, may be due to degradation of lubricin[43], a molecule possessing chondroprotective[155] and boundary lubricating ability[83].

While the mechanisms underlying degeneration of cartilage in OA and RA are the subject of intensive research, it is evident that disruption in joint mechanics and synovial metabolism possibly contribute to the initiation and progression of these diseases. Thus, maintenance of cartilage's tribological properties is of great significance to retard the onset and progressive degenerative processes of arthritis.

1.2 DIARTHRODIAL JOINT TRIBOLOGY

Tribology involves the study of friction, lubrication, and wear of materials. While a significant understanding of lubrication mechanisms for the minimization of friction and wear exists for most traditional materials, such mechanisms are not well understood for biological tissues. This is due, in part, to the added complexity of a biological friction interface, complicated by inhomogeneous mechanical and material properties, an ECM that remodels, and interactions with macromolecules localized in synovial fluid or at the tissue surface that may act independently, synergistically, or

competitively to lubricate the tissue.

Modes of Lubrication

Friction is a force that acts opposite in direction to the relative tangential motion of two surfaces and is modulated by interactions between the two surfaces. The friction coefficient μ is a quantitative measure that describes the dimensionless ratio between the tangential friction force and normal force ($\mu = F_f / F_N$). This ratio is not a material property, but rather, a relationship that is dependent upon the two surface materials, the lubricant used, and the operating conditions.

Lubrication of an interface occurs within distinct modes (i.e., boundary, mixed, and hydrodynamic). The Stribeck curve (Figure 1.1), classically used to describe the various lubrication modes of a rotating journal bearing, relates friction coefficient μ to Hersey number H, a non-dimensional number comprised of the lubricant dynamic viscosity η, the shaft rotation speed ω, and the mean pressure P[66].

In boundary mode, the regime where μ is greatest, friction and wear between two surfaces are determined by the properties of the surfaces, and the properties of the lubricant other than bulk viscosity[177]. In industrial bearings this occurs in situations of high P, low ω, and low η causing significant solid-solid contact as the two surfaces interact directly. During boundary mode lubrication, the mean separation distance between the two surfaces is often less than the asperity height, or average surface roughness R_a. As a result, boundary mode is surface dependent and thus the lubrication mechanisms are related to surface chemistry. Boundary mode is characterized by an invariant μ over a range of ω, η, and P[37,110].

In contrast, when the friction and wear properties are determined by the properties of the lubricant solution, in particular viscosity, hydrodynamic mode

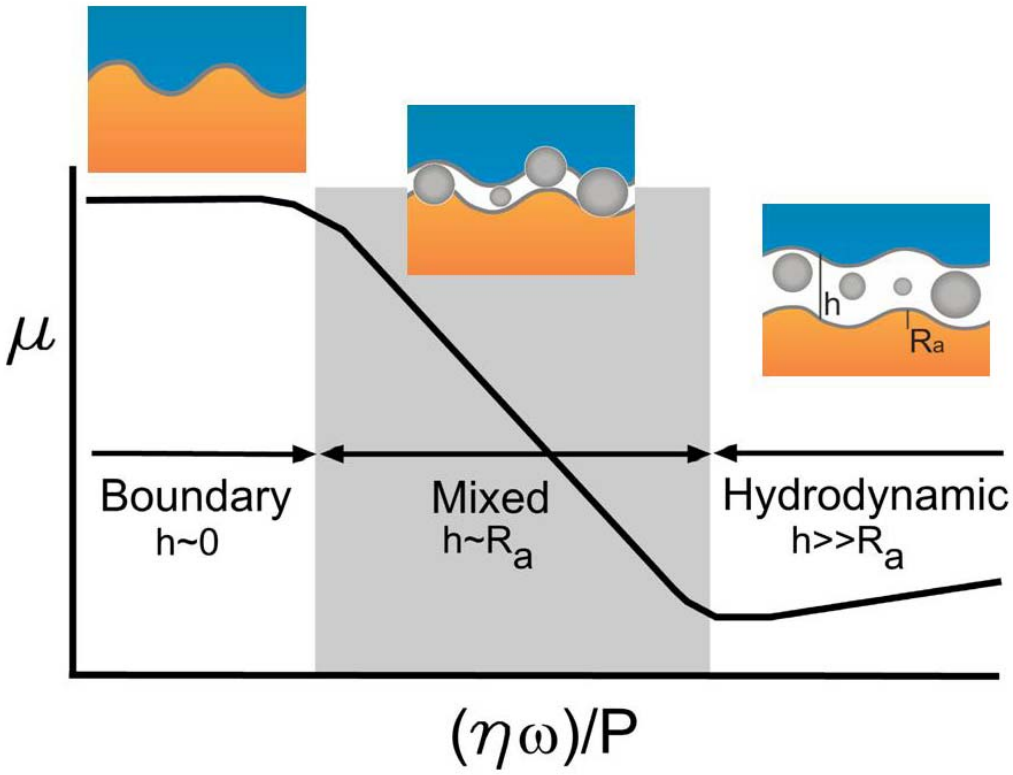

Figure 1.1: Sketch of a Stribeck curve relating friction coefficient μ to the Hersey number**,** a non-dimensional expression of dynamic viscosity (η), shaft speed (ω), and mean contact pressure (P) for a typical journal bearing. Lubrication modes of a system are related to asperity-asperity interaction and fluid separation of two surfaces as suggested by the inset cartoons.

occurs. In this lubrication mode, a fluid film completely separates the surfaces and the pressure generated within the fluid carries the applied load[177], with friction arising entirely from shearing the viscous fluid. Lubrication mechanisms in hydrodynamic mode are dominated by fluid mechanics. The start of hydrodynamic mode is noted on the Stribeck curve with a Hersey number which produces a minimum μ, as a result of no solid-solid contact. Hersey numbers that maintain a fluid film (i.e. greater than the initial) allow hydrodynamic mode.

Mixed mode lubrication represents the transition from boundary to hydrodynamic modes with the separation distance between the two surfaces on the order of R_a. Mechanisms of lubrication within this regime are involved in the formation of a fluid film, and μ decreases with η and ω and increases with P.

Cartilage Lubrication

Cartilage lubrication is even more complicated! Lubrication of cartilage has been thought to occur in hydrodynamic[117], mixed[110] and boundary[24,69,152,175] modes as well as in combination[135,151]. Several mechanisms for cartilage lubrication have been proposed including "weeping"[125,126], "boosted"[182], "elasto-" and "micro-elastohydrodynamic"[38,39], "squeeze film"[47,71] and "biphasic" lubrication[2,4,49]. While there is currently no universal agreement as to the mechanisms by which cartilage maintains a low friction interface, consensus does exist that cartilage operates primarily in boundary and mixed modes with fluid pressurization within the tissue and interface playing a significant role in the frictional properties of the tissue.

Experimental studies have found cartilage to have an exceptionally low friction coefficient upon initial loading ($\mu = 0.002\text{-}0.02$)[11,24,27,49,90,91,109,111,126,180]. If load is maintained for long periods of time, μ becomes significantly elevated (0.2-

0.4)[49,115,126,182]. Termed biphasic lubrication due to the fluid and solid phases, this temporal dependence in μ is apparently due to fluid pressurization as originally hypothesized by McCutchen[126] and others[2,49,118] and experimentally shown by Krishnan et al[103]. Experiments have shown this biphasic response to be altered as a result of loading rate, time of compressive load application prior to sliding, porosity of the tissue, and lubricant used[13,49,103].

Cartilage boundary lubrication is believed to occur only if fluid equilibrium is achieved, with initial frictional response of cartilage in hydrodynamic or mixed modes. In fact, to achieve boundary lubrication many experiments are conducted after tissue relaxation at relatively slow surface speeds (< 5 mm/s) and moderate loads without validation of lubricating mode. This level of control over lubrication mode is not sufficient to study potential biomolecules, as different modes of lubrication are dominated by different mechanisms. This approach to creating boundary lubrication results in experiments being carried out over a wide range of operating parameters (v and P), using various bearings from material-material to cartilage-cartilage, making comparisons within and between experiments challenging.

Synovial Fluid

Synovial fluid, the physiologic joint lubricant, consists of a wide range of constituents including carbohydrates, proteins, lipids, and soluble signaling factors. The main viscosity determinant of the fluid is the molecular weight and concentration of hyaluronic acid (HA)[5]. While the viscosity of the solution may assist in mixed and/or possible hydrodynamic modes, where bulk lubricant properties participate in the reduction of μ, other molecules affect boundary lubrication of articular cartilage. In 1970, Radin et al found that the protein fraction in the synovial fluid and not the

HA was responsible for the boundary lubrication properties of synovial fluid[152]. This protein fraction was analyzed and a glycoprotein, named lubricating glycoprotein I, and later, lubricin, was identified[175]. Additional experiments with synovial fluid have shown that digestion with trypsin, an enzyme that non-specifically cleaves proteins, completely removes the fluid boundary lubricating ability[79,83].

In addition to lubricin, other molecules have been proposed to be boundary lubricants found in synovial fluid, including surface-active phospholipids (SAPLs), chondroitin sulfate, and HA[13,60,69,147]. While their effectiveness as boundary lubricants is somewhat controversial[79] it is possible these molecules play a role, synergistically, additive, or antagonistically with lubricin to modulate μ.

1.3 LUBRICIN

Human lubricin, a mucinous glycoprotein (~227 kD) structurally composed of a 1,404 amino acid core protein encoded by 12 exons[48,78,84,175], is extensively glycated with O-linked negatively charged β(1-3)Gal-GalNac oligosaccharides partially capped with NeuAc[52,82] (Figure 1.2). This oligosaccharide rich domain, referred to as the mucin-like domain, is encoded by exon 6 and consists of >70% of the amino acid composition of lubricin[82]. The amino- and carboxyl-terminal ends of the lubricin molecule are globular, cysteine-rich domains[129], which play a role in matrix binding and aggregation[48,89].

Lubricin is encoded by the proteoglycan 4 (PRG4) gene (HGNC:9364) and is homologous to other post translational products referred to as superficial zone protein (SZP), megakaryocyte stimulating factor (MSF) precursor, camptodactylyarthopathy-coxa vera-pericarditis (CACP) protein, 'downstream of the liposarcoma-associated fusion oncoprotein' 54 (DOL54), hemangiopoietin (HAPO), and

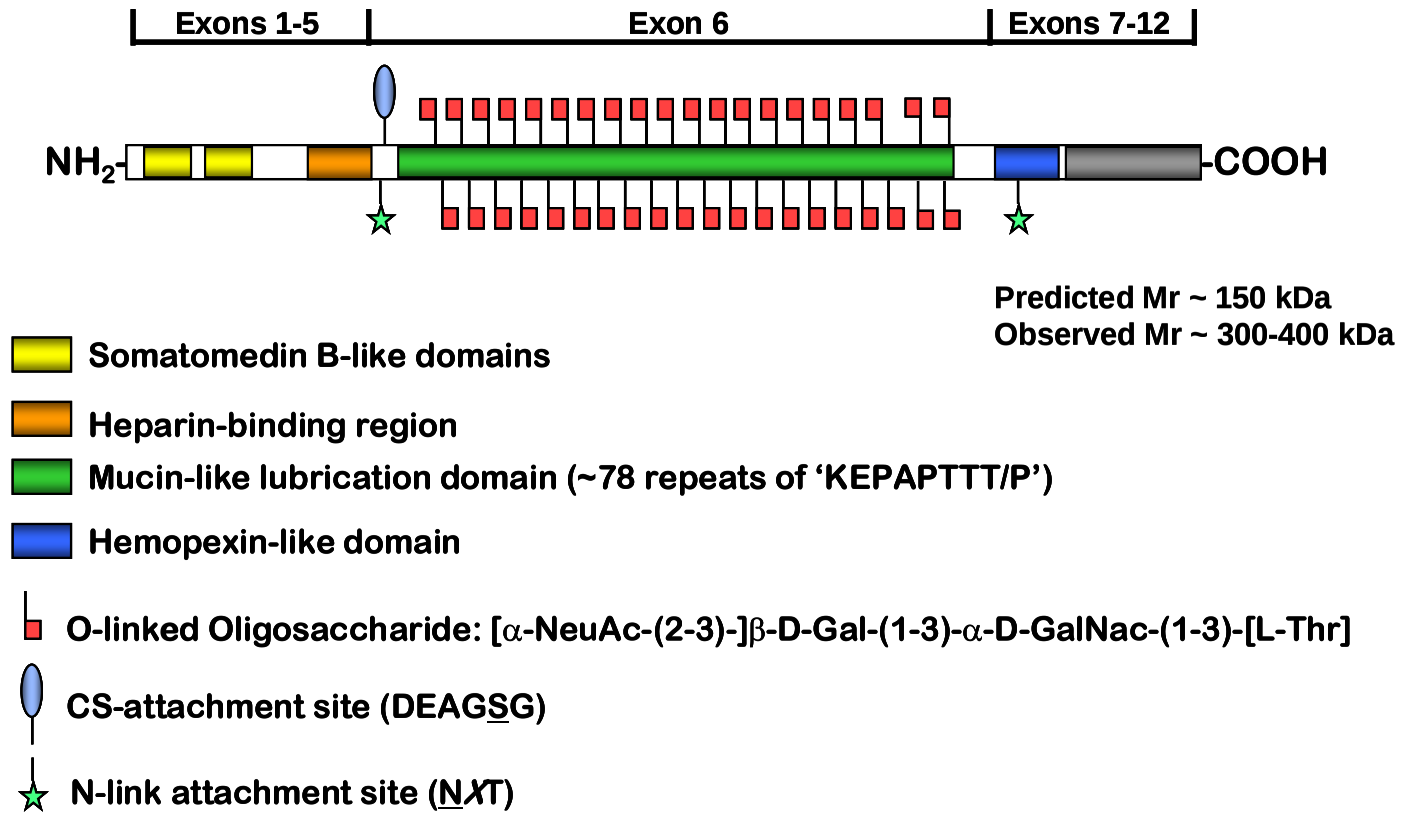

Figure 1.2: Illustration of the structure of full-length lubricin**,** a lubricating glycoprotein found in synovial fluid. (Adapted from Jones et al, 2007).

PRG4[48,75,78,84,112,105,119,129,155]. The name "lubricin" was first given to a lubricating glycoprotein, LGP-I, isolated from synovial fluids[174]. However, the molecule also is expressed by superficial zone chondrocytes and not by middle or deep zone cells[48,164,165] where it is termed SZP. MSF and HAPO are homologous proteins identified in areas of the body outside of the joint with functions independent of joint maintenance. MSF was purified from human urine and found to stimulate growth of platelet forming cells in vitro[129], while HAPO was identified as a factor capable of inducing growth of hematopoetic and endothelial progenitor cells[112]. CACP protein, expressed by truncating mutations in the PRG4 gene in patients with CACP syndrome, exhibits none of the functional characteristics of lubricin. Patients with CACP exhibit fibrosis, non-inflammatory synovial hyperplasia, and premature joint failure[119]. These features are also apparent in lubricin knockout mice[155]. Currently, nomenclature in the literature still has not converged, with most people utilizing the name lubricin or PRG4 when referring to protein products from the PRG4 gene that are expressed and secreted by cells found in diarthrodial joints including: superficial zone chondrocytes[48,164,165], synoviocytes[165,170], meniscal fibrochondrocytes[166] and tenocytes[153].

Lubricin has been identified to play several important roles in the maintenance of joint metabolism including boundary lubrication of cartilage, chondroprotection, and inhibition of synovial cell overgrowth. In boundary mode, lubricin has demonstrated the remarkable ability to lubricate latex-glass[49,76,109,126,178], cartilage-material[49,110,183], and cartilage-cartilage[25,34,90,110,162] bearings possibly by electrostatic repulsion between apposing surfaces[76,77,172,175]. However, to date a clear mechanism has not been elucidated. This lubricating ability is due to the mucin-like domain of the molecule, as glycosidase digestion of lubricin causes a loss of boundary lubrication[76,82] in a latex-glass bearing. Additionally, it is unclear if the noted

localization of lubricin at the surface of articulating tissues is necessary for boundary lubrication, or if the greater than 30 μg/ml lubricin in synovial fluid (as initially purified from bovine synovial fluid[175]) acts to produce the low friction coefficients observed.

Distinct from its boundary lubricating role, lubricin acts as a chondroprotective agent by enabling the synovial fluid network to absorb energy, deform, and slowly dissipate strain energy when it complexes with HA[85]. From a biomechanical perspective, the importance of lubricin is evident. However, lubricin's role in the prevention of synovial overgrowth by protecting articulating areas from cell adhesion and infiltration[155] is equally important. This role is evidenced by CACP syndrome patients who cannot synthesize lubricin. Overgrowth of the synovium and pannus formation is evident in CACP patients, and their synovial fluid aspirates do not lubricate a latex-glass bearing as effectively as non-pathologic human synovial fluid[80]. Additionally, in RA, where pannus on the cartilage surface is profuse, loss of boundary lubricating ability is also noted, due to the proteolytic degredation of lubricin by cathepsin B, a cysteine protease abundant in RA synovial fluid[43].

Modulation of lubricin expression and synthesis has been illustrated by biochemical and biophysical mediators. Dysregulation of lubricin metabolism by cytokines, such as interleukin-1 (IL-1) and tumor necrosis factor-alpha (TNF-a) produce decreased expression and synthesis of lubricin[48,88,94,142]. Oncostatin M (OSM), a member of the IL-6 cytokine family, yields an up-regulation of lubricin expression and synthesis[88]. Members of the transforming growth factor-beta superfamily, including bone morphogenic protein-2 & 4 (BMP-2, BMP-4) and transforming growth factor-beta (TGF-β) as well as insulin-like growth factor-I (IGF-I), fibroblast growth factor-2 (FGF-2), and platelet-derived growth factor (PDGF), all typically anabolic cytokines, have been shown to up-regulate lubricin expression and

synthesis[32,48,94,138,142]. Biomechanical stimuli including dynamic shear and compression on bovine cartilage explants have shown expression of lubricin by middle and deep zone chondrocytes, which typically do not express the molecule[139,140]. Surface motion studies on tissue engineered constructs[58] and studies of continuous passive motion in a whole joint bioreactor[141] have also noted an up-regulation of lubricin synthesis from the tissues. In contrast, down-regulation of lubricin expression is observed in some animal models of arthritis[43,193].

While biochemical and biomechanical stimuli have been shown to effectively moderate lubricin expression and synthesis, a clear understanding of the functional consequences of lubricin regulation and localization in normal and pathologic states is needed to develop therapeutic strategies to improve joint longevity and function.

1.4 RESEARCH OBJECTIVES

The overall objective of this work was to investigate lubricin as a mediator of articular cartilage boundary mode frictional properties. The central hypothesis of this dissertation is that the boundary mode friction coefficient is mediated by localization of lubricin at the tissue surface.

Specific Aims

Specific Aim 1 (Chapter 2):

To develop an in vitro cartilage friction testing apparatus with control of surface speed, normal strain, and tissue congruity to enable measurement of cartilage boundary mode μ.

A linearly oscillating cartilage on glass friction apparatus was designed and validated to measure cartilage friction coefficients. Due to the linear nature of the

sliding, a uniform sliding speed was achieved over the entire surface of the tissue. In addition a glass counterface provided a surface that has a low surface roughness compared to the cartilage (~ 5 nm for glass, ~ 5 μm for cartilage), an ability to be machined readily, and an extensive history of use as a counterface in the literature. Experiments with fresh and previously frozen tissue in addition to bovine and equine synovial fluid were conducted to validate experimental results with those seen in the literature as well as to establish baseline sample handling and storage procedures. Cartilage explants were tested under a variety of entraining speeds and normal strains with or without a pivot joint to ensure cartilage-glass congruity. A novel extension of the Stribeck curve, a 'Stribeck surface,' was created to map cartilage lubrication modes, which demonstrated cartilage in boundary and mixed lubrication modes. This analysis provided operating values within the speed-strain space for a pivoted sample holder that produced boundary mode lubrication.

Specific Aim 2 (Chapter 3):

To test the hypothesis that exogenous recombinant human lubricin (rh-lubricin) will differentially alter boundary mode μ if it is bound at the tissue surface or soluble in the bulk lubricant.

Varying concentrations of exogenous recombinant human lubricin (rh-lubricin) were added as a lubricant in the cartilage-glass friction apparatus to determine a concentration-dependent response of equilibrium μ in boundary mode. To investigate the relative contributions of rh-lubricin in the bound and soluble forms, two additional experiments were performed. In the first experiment, μ was evaluated, using PBS as a lubricant, following endogenous lubricin extraction and subsequent incubation in either equine synovial fluid or 50 μg/ml rh-lubricin. This experiment determined the

ability of surface localized lubricin to lubricate cartilage compared to localized synovial fluid constituents. In the second experiment, ionic strength of the lubricating solution was altered to control localization at the tissue surface. Rh-lubricin solutions (50 and 150 μg/ml) at three different ionic strengths (0.14M, 0.5M, 1.5M NaCl) were utilized as lubricants to determine the lubrication effect of either bound and soluble lubricin or just soluble lubricin. This aim focused on identifying the ability of exogenous lubricin to lubricate articular cartilage and on elucidating the differential role of lubricin when surface localized versus soluble.

Specific Aim 3 (Chapter 4):

To test the hypothesis that endogenous lubricin, produced from different cellular types will alter boundary mode μ_{eq} in an alginate-cell system.

Chondrocytes, fibrochondrocytes, and differentiated mesenchymal stem cells (MSCs)) were encapsulated within alginate disks and cultured for up to six weeks. Traditional biochemical (GAG and hydroxyproline content) and biomechanical (aggregate modulus and permeability) markers indicated normal tissue growth[23,107]. Assaying for lubricin with enzyme-linked immunosorbant assay (ELISA) and immunohistochemistry (IHC) yielded minimal localization of lubricin within the bulk or at the surface of the construct. However, significant lubricin concentrations were found in the media for all cell types, with MSCs secreting 10 fold more lubricin than other cell types. Friction testing of samples demonstrated no change in μ_{eq}; however a subsequent soak in ESF and retest with PBS as a lubricant, μ_{eq} decreased. Lubrication was abolished following a lubricin extraction protocol.

This aim was focused at understanding the ability of differentially synthesized endogenous lubricin, from different cellular types, to lubricate a cell-alginate construct

over time in culture. While the data did not fully support the hypothesis, this model system demonstrated difficulties that heterogeneous populations of chondrocytes, meniscal fibrochondrocytes, and MSCs had in retention and assembly of secreted lubricin. This occurrence is not present in cell-alginate constructs containing chondrocytes from distinct zonal layers in cartilage[97], and has not previously been investigated for meniscal fibrochondrocytes or MSCs.

Specific Aim 4 (Chapter 5):

To test the hypothesis differential tissue surface localization of endogenously produced lubricin by TGF-β1, IL-1β, and oncostatin M (OSM), will alter boundary mode μ of cartilage explants.

Cartilage explants were exposed to 10 ng/ml TGF-β1, IL-1β, and OSM for 24 or 48 hours. TGF-β and OSM lowered, while IL-1 increased, μ_{eq} over time in culture. OSM and IL-1 caused a loss of proteoglycan from the tissue as measured with the DMMB-dye assay, and TGF-β did not alter proteoglycan content over 48 hours of exposure. The functional lubrication of TGF-β and OSM, even with OSM causing abundant proteoglycan loss, is consistent with studies demonstrating increased synthesis and surface localization of lubricin following a 48 hour incubation with those cytokines[88]. Additionally, extraction of endogenous lubricin with 1.5M NaCl demonstrated an increase in μ_{eq} for all treated explants. A subsequent soak in synovial fluid recovered the μ_{eq} to values prior to endogenous lubricin extraction and μ_{eq} was further reduced for all samples when synovial fluid was used as a lubricant. These studies contribute to the understanding of how metabolism and localization of lubricin translates to functional alterations in friction coefficient for tissue exposed to commonly upregulated cytokines in injury and arthritis.

CHAPTER 2

LUBRICATION MODE ANALYSIS OF ARTICULAR CARTILAGE USING STRIBECK SURFACES[§]

2.1 ABSTRACT

Lubrication of articular cartilage occurs in distinct modes with various structural and biomolecular mechanisms contributing to the low friction properties of natural joints. In order to elucidate relative contributions of these factors in normal and diseased tissues, determination and control of lubrication mode must occur. The objectives of these studies were (1) to develop an in vitro cartilage on glass test system to measure friction coefficient, μ, (2) to implement and extend a framework for the determination of cartilage lubrication modes, and (3) to determine the effects of synovial fluid on μ and lubrication mode transitions. Patellofemoral groove cartilage was linearly oscillated against glass under varying magnitudes of compressive strain utilizing phosphate buffered saline (PBS) and equine and bovine synovial fluid as lubricants. The time dependent frictional properties were measured to determine the lubricant type and strain magnitude dependence for the initial friction coefficient ($\mu_0 = \mu(t\rightarrow 0)$) and equilibrium friction coefficient ($\mu_{eq} = \mu(t\rightarrow\infty)$). Parameters including tissue-glass co-planarity, normal strain, and surface speed were altered to determine the effect of the parameters on lubrication mode via a 'Stribeck surface'. Using this testing apparatus, cartilage exhibited biphasic lubrication with significant influence of strain magnitude on μ_0 and minimal influence on μ_{eq}, consistent with hydrostatic pressurization as reported by others. Lubrication analysis using 'Stribeck surfaces'

[§] Gleghorn, J.P. and Bonassar, L.J. "Lubrication Mode Analysis of Articular Cartilage Using Stribeck Surfaces," J Biomech, in review.

demonstrated clear regions of boundary and mixed modes, but hydrodynamic or full film lubrication was not observed even at the highest speed (50 mm/s) and lowest strain (5%).

2.2 INTRODUCTION

Articular cartilage is a load bearing tissue that provides a low friction interface as bones articulate during joint motion[18]. The low friction coefficients μ of the cartilage-cartilage bearing are important for reduction of cartilage damage and wear[49] over several decades to mitigate the irreversible loss of structure and mechanical function due to aging and pathologic conditions such as osteoarthritis (OA). In addition to concerns of mechanical wear, modulation of frictional shear is important, as numerous studies have shown that tissue octahedral shear stress modulates cell biosynthesis and matrix assembly through mechanotransduction[86,87,181]. Thus, it is crucial to understand cartilage friction and lubrication for normal, fibrillated, roughened, and eroded tissue found with age and disease[18]. Lubrication of idealized incompressible materials can be understood in the context of specific modes (i.e., boundary, mixed, and hydrodynamic). Classically, the relationship between the operating parameters (dynamic viscosity η, shaft rotation rate ω, and mean pressure P) and the friction coefficient μ for a typical rotating journal bearing can be displayed on a "Stribeck curve"[66] that defines the respective lubrication modes (Figure 1.1). In "boundary mode" (typically at high load and/or low speed), μ is invariant over a range of surface speeds, normal loads, and viscosities[37,110], with surface chemistry dominating the mechanism of lubrication. In contrast, "hydrodynamic mode" (typically at high speeds and/or low loads) μ is dominated by fluid mechanics, with increases in μ observed due to viscous forces in the fluid film. The transition from

high μ to low μ due to the formation of a fluid film and increasing material separation is termed "mixed mode" lubrication where both surface chemistry and fluid mechanics contribute to friction.

In contrast to the ideal case, articular cartilage lubrication is complicated by the relatively high compliance and permeability of the tissue[49,109], the presence of potential biolubricants localized in synovial fluid and at the tissue surface[12,70,89,152,164,173], and a dynamic tissue surface continually altered due to the mechanical and biochemical environment of the joint. It has long been accepted that several lubrication modes occur within the joint[36,110156,191]. In addition, the biphasic nature of cartilage allows for hydrostatic fluid load support upon initial tissue loading[49,103], with cartilage deformation and fluid flow into/from the interface due to tissue permeability potentiating possible elastohydrodynamic[38], squeeze film[68,72], boosted[182] and weeping[108,127,152] mechanisms of lubrication. As the fluid load support diminishes, boundary mode becomes the dominant regime[127] with interactions between cartilage-cartilage[14] and cartilage-biomolecules[25,111,152] playing a critical role in successful boundary lubrication.

Numerous friction testing paradigms have been utilized over the last eighty years in an effort to understand the remarkable frictional properties of cartilage and the role of biomolecules in cartilage lubrication. These devices have allowed investigation of various aspects of cartilage lubrication, but are not without limitations. For example, the examination of lubricant properties in artificial bearings including latex-glass[49,76,109,126,178] allows for tightly controlled interface geometry but is unable to capture the role that interactions between biological lubricants and the tissue play in modification of μ. In contrast, investigations using whole joints[25,43,141,156] display the inverse problem, with production of a physiological environment and biomolecule

interactions but difficulty in controlling experimental parameters to control lubrication mode. Other systems which utilize cartilage-material[49,110,183] or cartilage-cartilage[25,34,90,110,162] systems allow for control of interface geometry while simultaneously investigating lubricant-tissue interactions.

While different methods are used to measure μ, control of experimental variables is critical for proper investigations and comparisons of putative biolubricants. Since μ is simply a ratio between frictional and normal forces rather than a material property, results will depend on operating conditions[110,162], materials utilized[55,146], surface properties[21,29], normal loading and motion time-history[49,50], and interface geometries[34]. As mechanisms of lubrication vary significantly in different lubrication modes, an effective experimental set-up will allow for the control over such parameters to reliably produce a desired lubrication regime. Toward this end, the objectives of these studies were (1) to develop an in vitro cartilage on glass test system to measure cartilage friction coefficients over a wide range of surface speeds and compressive strains while controlling interface congruity, (2) to implement and extend a framework for the determination of cartilage lubrication modes using 'Stribeck surfaces', and (3) to determine the effects of synovial fluid on μ and lubrication mode transitions.

2.3 METHODS

Cartilage Explant & Lubricant Preparation

Full-thickness patellofemoral groove cartilage from nine bovine stifle joints [Gold Medal Packing, Syracuse NY] of 3 - 10 day old animals was harvested with precautions taken to avoid contacting the surface of the tissue. Cartilage blocks were either processed immediately into samples (referred to as "fresh") or frozen at -20˚C

prior to use. At the time of experimentation with the frozen cartilage, the tissue was thawed in PBS at 37˚C with a water bath for 1 hour prior to further processing into samples (referred to as "previously frozen"). Cartilage disks, 6 mm in diameter, were created from the full-thickness cartilage utilizing standard biopsy punches with attention taken to create a right cylinder with a visually flat cartilage surface to minimize fluid wedge generation due to irregular sample topography. Samples were removed from the biopsy punches with compressed air, placed in phosphate buffered saline (PBS) [Invitrogen, Carlsbad, CA], and immediately tested (previously frozen) or placed in tissue culture (fresh) with a standard media formulation[55] at 37˚C and 5% CO_2 atmosphere for less than three days until friction testing.

Lubricants used in these studies were PBS, bovine synovial fluid (BSF), and equine synovial fluid (ESF). BSF was sterilely aspirated from bovine stifle joints mentioned above while ESF was similarly aspirated from stifle joints of animals [College of Veterinary Medicine, Cornell University, Ithaca NY] being euthanized for pathologies not affecting the selected joint, under Cornell University Institutional Animal Care and Use Committee guidelines. The synovial fluid was visually inspected to ensure it was free of blood and contaminants, pooled from a total of 15 joints (BSF from 8 animals, ESF from 10 animals), aliquoted, and stored at -20°C for a maximum of three months prior to use. At the time of experimentation, frozen synovial fluid was thawed in a water bath at 37°C.

Friction Testing Apparatus

Cartilage friction coefficient μ was determined with a custom apparatus (Figure 2.1) modeled after a classic pin on plate test configuration by linearly oscillating a cartilage disk against a piece of glass. The four main components of the

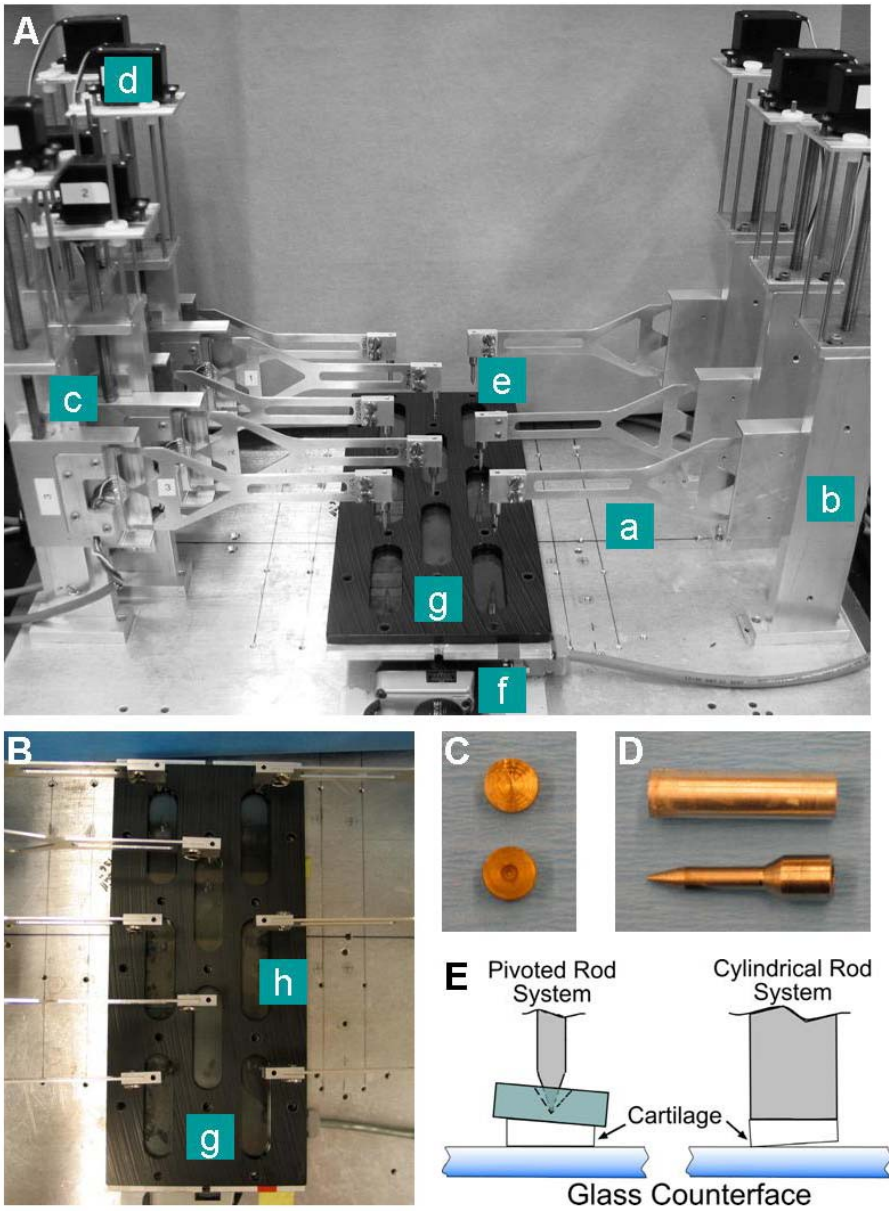

Figure 2.1: Photographs (A – side view, B- top view) of the custom friction instrument designed to measure friction coefficients over a wide range of surface speeds and compressive loads. The instrument consists of a custom designed biaxial load cell (a), mounted to a tower (b) allowing translation in the normal direction via a compound screw (c) and servomotor (d). The end of the load cell has a pin with a point (e) that interacts with the sample holder. A linear stage (f) oscillates a glass counterface (h) against cartilage within individual sample wells created by a delrin plate (g). The cartilage sample holder is either glued to a brass disk (C – top)) which interacts with the pointed pin (D - bottom) via the conical hole on the reverse (C – bottom) or the end of a cylindrical rod (D –top) as seen in the cartoon (E).

apparatus are the load cell tower, the custom biaxial load cell, the sample holder with either a fixed cylindrical rod (Figure 2.1D,E) or a pivoted rod system (Figure 2.1C,D,E), and the oscillating table (Figure 2.1A&B) that allow for both mapping and replication of various lubrication modes. The use of a biaxial load cell to measure normal and shear forces enables use of multiple load cells with one oscillating table to run eight friction tests simultaneously.

A custom Matlab [The MathWorks Natick, MA] script was used to calculate friction coefficients from the measured normal and shear voltages from the load cell strain gages over the course of the experiment. A typical experiment consists of translating the table at a constant speed (surface speed) and applying a step in normal strain ε_N. A poroelastic model[95] was fit to the compressive stress relaxation in the tissue allowing for calculation of a Young's modulus E_Y and permeability k. To better understand the temporal effects in the lubrication process, after each step displacement of strain, $\mu(t)$ was fit to a biphasic model for cartilage lubrication[49,103], which yielded $\mu_0 = \mu(t \rightarrow 0)$, $\mu_{eq} = \mu(t \rightarrow \infty)$, and the time constant for the transition, τ_μ (Figure 2.2A). To visualize and characterize the lubrication mode of cartilage, a "Stribeck surface"[185] was generated relating μ_0 and μ_{eq} (Figure 2.2B) to commonly controlled operating parameters (surface speed and ε_N).

Experimental Design

To determine the cartilage temporal friction properties (μ_0, μ_{eq}, τ_μ), fresh and frozen cartilage samples (n=8) were articulated against glass at a constant surface speed (0.33 mm/s) for a length of 36 mm at varying compressive normal strains, ε_N, of 10, 20, 30 and 40% using the pivoted rod system. The normal strain was applied either in a single step displacement to the total desired ε_N or applied in multiple 10%

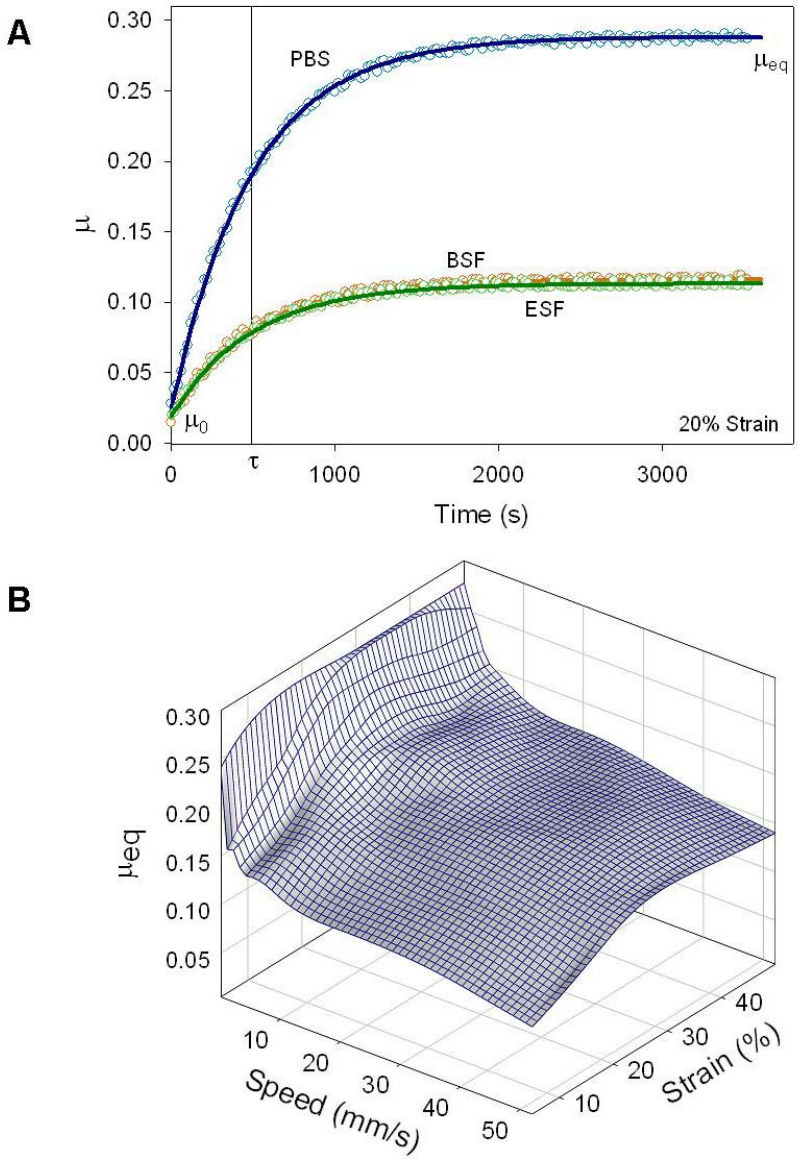

Figure 2.2: The temporal friction profile (circles) and poroelastic model fit to the data (line) of cartilage (A) lubricated with either PBS, equine synovial fluid (ESF) or bovine synovial fluid (BSF) with v = 0.33 mm/s and ε_N = 20%. Parameters obtained from the models are $\mu_0 = \mu(t \rightarrow 0)$, $\mu_{eq} = \mu(t \rightarrow \infty)$, and the relaxation time constant τ. All model fits had $R^2 > 0.97$ and RMSE < 0.042. A Stribeck surface (B) (representative of 4 created) maps lubrication mode by determining μ_{eq} for cartilage lubricated with PBS over a range of surface speeds and compressive strains.

ε_N steps. Samples were lubricated with a bath of PBS, ESF, or BSF and submerged in the lubricant solution throughout testing. The duration of the tests, determined from preliminary studies, was dependent on ε_N with sample relaxation times of at least 4 times the τ_N for that experiment.

The dependence of μ_0 and μ_{eq} on the experimental set-up was investigated and visualized with Stribeck surfaces. To determine if congruency between the tissue and the glass was an important variable to control in these experiments, friction tests were carried out using either the cylindrical rod or pivoted rod cartilage holder (Figure 2.1C,D,E). Previously frozen cartilage (n=4) was articulated against glass using PBS as a lubricant for a range of surface speeds (0.1 to 2 mm/s) and ε_N (5, 10, 20, 30, 40, 50%). A μ_{eq} Stribeck surface was created, and the transition between boundary and mixed mode lubrication was identified. Boundary mode lubrication was identified as the region of speed-strain space in which μ_{eq} was maximal and invariant. Using the pivoted rod, the effect of lubricant on μ_0 and μ_{eq} was determined by constructing Stribeck surfaces over a range of speeds (0.1 mm/s < v < 50 mm/s) and strains (5% < ε_N < 50%).

Statistical Analysis

All data are presented as mean +/- SD. A t-test was utilized to analyze E_Y data to determine the effect of lubricant type (PBS, ESF, BSF). The effect of lubricant type and applied strain on τ_N, τ_μ, k, μ_0, and μ_{eq} was determined using a two factor analysis of variance (ANOVA) with Tukey's HSD post hoc test. A three factor ANOVA with Tukey's HSD post hoc test was utilized to determine the effect of the cartilage sample holder, v, and ε_N on μ_{eq}, as well as, the effect of lubricant type (PBS, ESF), v, and ε_N on μ_{eq} and μ_0 from the Stribeck surfaces. All statistical analyses were carried out

using SigmaStat [SPSS Inc, Chicago, IL] with calculated p values being considered significant for $p<0.05$.

2.4 RESULTS

Temporal Response

Normal load temporal profiles were similar for all lubricants tested and were consistent with poroelastic/biphasic stress relaxation with τ_N ranging from approximately 406 +/- 37 seconds at 10% ε_N to 950 +/- 45 seconds at 40% ε_N. No statistical difference was seen for the model fit parameters, L_{N0}, L_{Neq}, τ, for all tested lubricants at each applied ε_N. Additionally calculated Young's modulus and hydraulic permeability were similar for all tested samples with $E_Y = 0.39$ +/- 0.14 MPa and $k = 2.8$ +/- 0.6 x 10^{-15} m^2 Pa^{-1} s^{-1}.

The temporal friction coefficient of the cartilage increased logarithmically from a μ_0 to μ_{eq} for all lubricants tested (Figure 2.2A). The $\mu(t)$ values for ESF and BSF lubricants were very similar and lower than $\mu(t)$ values for PBS at all points and the time constant, τ_μ, for $\mu(t)$ data for all lubricants were comparable. τ_μ ranged from 415 +/- 20 s to 990 +/- 40 s for 10 to 40% ε_N respectively which was similar to τ_N calculated from the $L_N(t)$ data for all the applied ε_N tested.

At low sliding speed (v = 0.33 mm/s), the equilibrium friction coefficient was dependent on the applied ε_N ($p<0.01$) and the lubricant tested ($p<0.001$); however, no significant differences were found in μ_{eq} as a result of the manner ε_N was applied (Figure 2.3A&B). Application of $\varepsilon_N = 10\%$ produced lower μ_{eq} values ($p<0.01$) for all lubricants tested (PBS = 0.218 +/- 0.015, ESF = 0.071 +/- 0.012, BSF = 0.068+/- 0.013) compared to μ_{eq} resulting from ε_N magnitudes greater than 20% (for example at $\varepsilon_N = 30\%$: PBS = 0.280 +/- 0.010, ESF = 0.116 +/- 0.009, and BSF = 0.114 +/- 0.009).

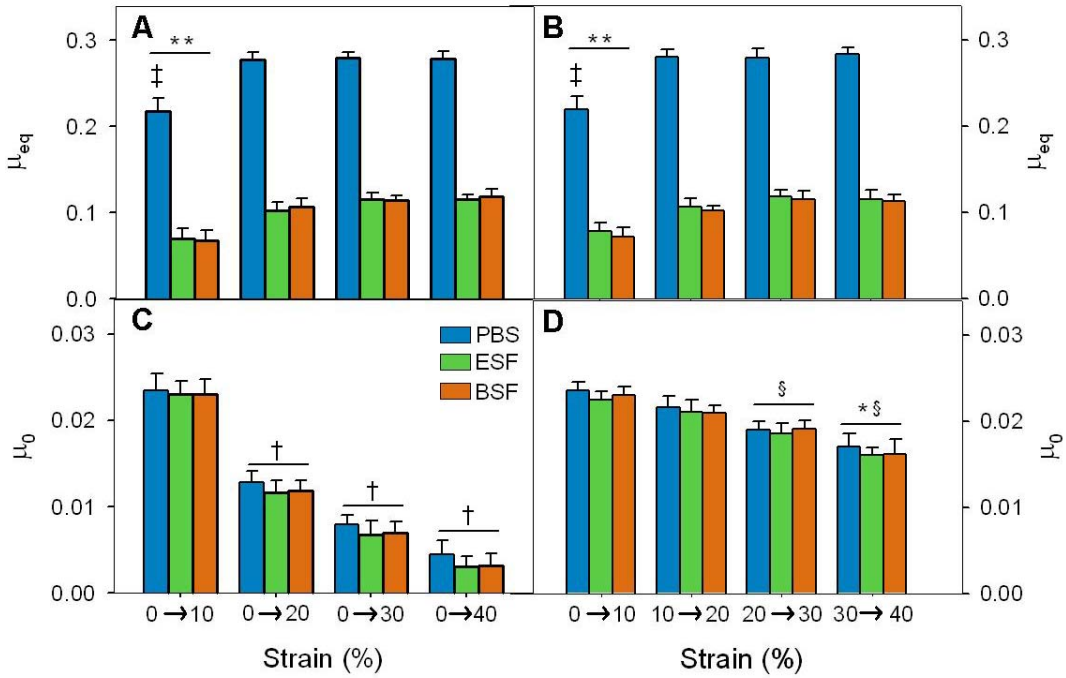

Figure 2.3: μ_{eq} (A&B) and μ_0 (C&D) values for cartilage lubricated with either PBS, ESF, or BSF with a surface speed of 0.33 mm/s and compressive strains applied in either large (A&C) or small (B&D) increments. Data represented as mean +/- SD with n = 8 (** = $p<0.001$ for $0\rightarrow10$ vs all other applications of strain, ‡ = $p<0.001$ for PBS vs ESF and BSF, † = $p<0.02$ compared to all others in C, § = $p<0.05$ for strain increment vs $0\rightarrow10$, and * = $p<0.05$ for strain increment vs $10\rightarrow20$).

For all applied ε_N, μ_{eq} were similar for ESF and BSF lubricants but larger for PBS.

The initial friction coefficient for all lubricants tested was dependent on the magnitude of the applied strain with μ_0 decreasing as the ε_N increased (Figure 2.3C&D). No significant difference was found between lubricant groups for a given ε_N regardless of the magnitude or manner applied; however, a general trend of lower μ_0 for ESF and BSF lubricated samples was noted for ε_N applied in a single step. At a given compressive strain, μ_0 was dependent on the manner ε_N was applied, with μ_0 lower for a single ε_N step (PBS = 0.005 +/- 0.002 with 40% applied strain resulting in ε_N = 40%) compared to an applied ε_N step function (PBS = 0.017 +/- 0.002 with 10% applied strain resulting in ε_N = 40%).

Stribeck Framework

Stribeck surfaces were generated to investigate the μ_{eq} transition from boundary to mixed mode lubrication due to the two different systems to hold the cartilage samples (Figure 2.4A&B). Boundary mode lubrication for cartilage lubricated with PBS occurred within a larger speed-strain variable space for the pivoted rod system compared to the fixed rod system. The pivoted rod system produced boundary mode with speeds as high as 1.1 mm/s compared to the fixed rod (v = 0.75 mm/s) under high ε_N (> 30%). Additionally, boundary mode was achieved at ε_N as low as 15% for the pivoted system compared to ε_N = 20% for the fixed system at low speeds (v < 0.5 mm/s). The mixed mode regime was steeper for the fixed rod system producing μ_{eq} values of approximately 0.194 +/- 0.044 under 30% ε_N at 2 mm/s compared to 0.230 +/- 0.032 for the pivoted rod under the same operating conditions.

Stribeck surfaces generated for μ_0 and μ_{eq} illustrate differences based upon the

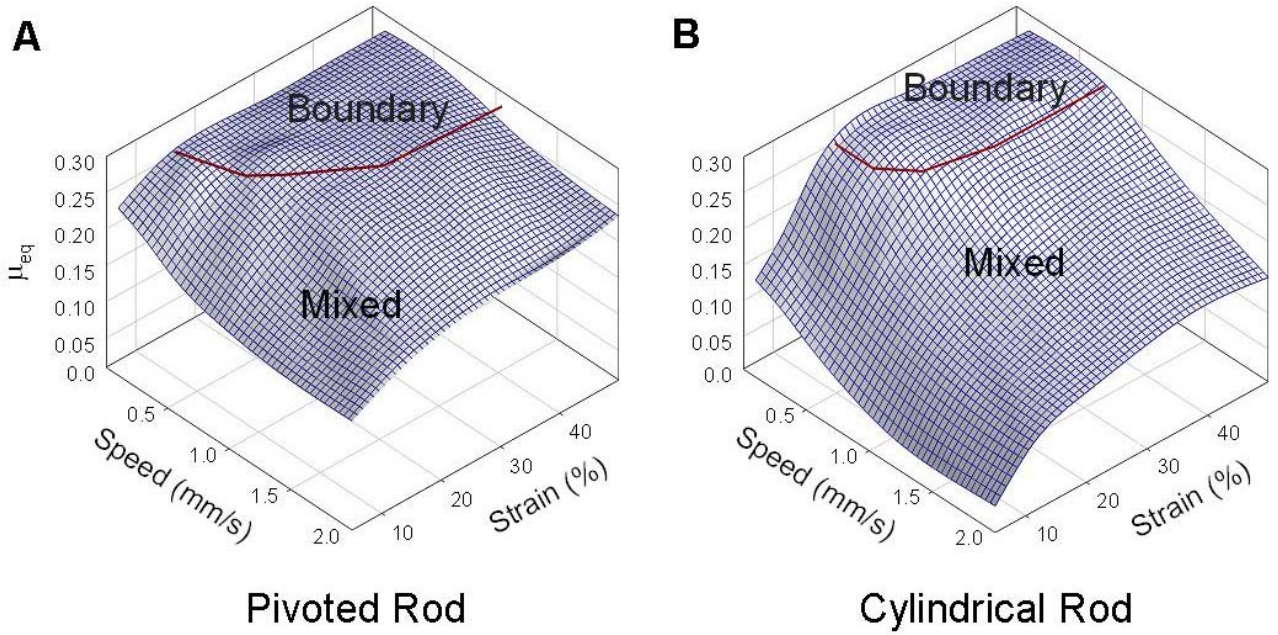

Figure 2.4: A Stribeck surface constructed from the mean μ_{eq} of 4 samples tested for a cartilage-glass bearing lubricated with PBS where the cartilage sample was mounted into the instrument with either a pivoted rod (A) or a fixed rod (B). The superimposed red line on the surface represents the boundary between lubrication modes.

type of lubricant (Figure 2.5A&B). Areas of high strain and low speed on the Stribeck surfaces produced a near constant μ_{eq} for both lubricants (ESF = 0.115 +/- 0.01, PBS = 0.279 +/- 0.009) and a decrease in μ_{eq} in regions of lower strain and higher speed. The area of decreasing μ_{eq}, mixed mode, produced greater variation in the data, in particular for regions of the ε_N-v space where $\varepsilon_N < 15\%$. For both PBS and ESF, μ_0 varied little over the strain-speed space investigated and no difference was noted in μ_0 for either lubricant. However, a significant difference in μ_{eq} at all points between the two lubricants was noted. For both PBS and ESF, μ_{eq} was not as low as μ_0 for any speed-strain combination with the lowest μ_{eq} value (0.039 +/- 0.028) being approximately two times larger than the highest μ_0 (0.020 +/- 0.004).

The boundary lubrication domain on the μ_{eq} Stribeck surfaces approximated an elliptical cross-section bounded at $\varepsilon_N = 15\%$, v =0.1 mm/s and $\varepsilon_N = 50\%$, v = 1.0 mm/s in PBS. The region of boundary mode was significantly smaller in ESF with bounds at $\varepsilon_N = 30\%$, v =0.1 mm/s and $\varepsilon_N = 50\%$, v = 0.75 mm/s.

2.5 DISCUSSION

This study documents the development and validation of a novel device to study the frictional behavior of articular cartilage in a linear pin on plate configuration. Using this system, temporal profiles in μ were noted, consistent with the notion of biphasic or pressure-borne lubrication of cartilage[49,103] with μ increasing from a minimum to an equilibrium value. The μ_0 observed instantaneously after load application was as low as 0.014 +/- 0.006 and μ_{eq} at fluid depressurization was 0.281 +/- 0.011 for cartilage lubricated with PBS, similar to other reports[49,50,103]. The Stribeck surfaces for lubricated cartilage followed trends similar to traditional Stribeck curves of material-material interfaces, with areas of high strain and low speed

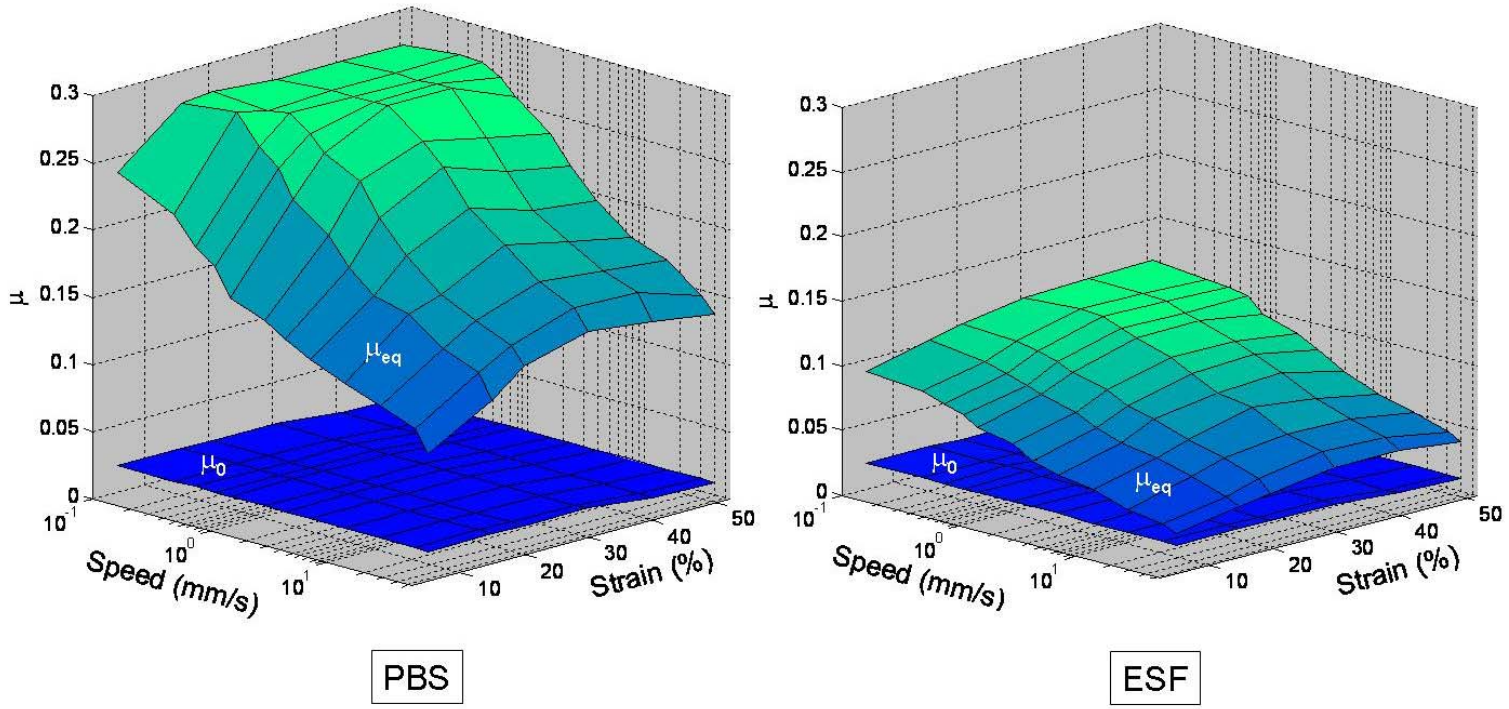

Figure 2.5: Stribeck surfaces for μ_{eq} and μ_0 for cartilage lubricated with either PBS (A) or ESF (B). Each surface is constructed from the mean of 4 samples.

producing boundary mode lubrication and areas of higher speed and lower strain producing mixed mode lubrication. The creation of the Stribeck surface, coupled with the simultaneous control of ε_N, v, and interface congruity, extends the previous work done by Linn[110] to enable the visualization and mapping of cartilage lubrication modes.

Interface geometry affected cartilage lubrication mode and transitions between modes (Figure 2.4), with a pivoted cartilage sample holder producing a larger boundary mode regime with transitions to mixed mode occurring at higher v and lower ε_N compared to tissue mounted with a fixed sample holder. Additionally, in mixed mode lubrication, the cylindrical rod Stribeck surface had a larger gradient, thereby producing lower μ_{eq} for a given set of operating conditions compared to the pivoted rod as observed from the Stribeck surfaces. Thus while consolidation[41] and depth dependent compressive moduli[28] enable the tissue to potentially achieve a high degree of conformation to the counterface, these data suggest differences in the manner by which fluid separation occurs between the fixed and pivoted rods.

Temporal investigations of the biphasic lubrication of articular cartilage were utilized to determine the sensitivity of sample preparation and storage on μ_0 and μ_{eq}. In this system, fresh and previously frozen cartilage behaved similarly, producing comparable μ_0 and μ_{eq}. μ_0 was dependent on strain rate (and thus tissue pressurization), which is consistent with other studies[20,103], while μ_{eq} was independent of strain rate. The biphasic lubrication time constant, τ_μ, was similar to the compressive stress relaxation time constant, τ_N, underscoring the fact that cartilage lubrication is coupled with fluid movement within the tissue. The addition of synovial fluid, both equine and bovine, affected μ_{eq} but had little effect on μ_0 suggesting that upon instantaneous loading, fluid pressurization and exudation at the tissue-glass interface governs μ_0 with an insensitivity to potential boundary lubricating and

viscosity modifying synovial fluid molecules.

Stribeck surfaces comparing μ_{eq} and μ_0 for PBS and ESF reveal differences in μ_{eq} based upon lubricant, but minimal differences are observed in μ_0 over the operating variable space for both lubricants. While μ_{eq} is larger for cartilage lubricated with PBS compared to ESF, it is also important to note that the boundary mode regime is larger for PBS compared to ESF. A proposed explanation for differences in overall μ_{eq} magnitude and the transition from boundary to mixed mode may be found due to the synovial fluid composition. The decrease in μ_{eq} in boundary mode can be attributed to molecules such as lubricin which have been shown to act as boundary lubricants[76,173]; whereas, a shift of load support from asperity contact to a fluid film, as observed by the boundary to mixed transition, is enhanced with an increase in viscosity due to molecules such as hyaluronic acid found in the synovial fluid[152]. Over the entire v-ε_N space tested, cartilage maintained either a boundary or mixed lubrication domain, with μ_{eq} not achieving the low μ_0 of a fully hydrated cartilage sample. The lack of ability to achieve full film lubrication following tissue depressurization, potentially due to the tissue's permeability allowing efflux of fluid from the cartilage glass interface into the tissue, is consistent with other theoretical and experimental studies[4,72,110,127].

The operating conditions of the friction test play a role in the mode of lubrication as illustrated by the Stribeck surfaces. Articular cartilage undergoes biphasic lubrication due to fluid pressurization which has a time history[49] and a strain rate dependence. At times immediately following the application of ε_N, lubrication is dominated by tissue pressurization with little variation in μ_0 noted for lubricant type (PBS, ESF, or BSF), v, or ε_N. Conversely, when relaxation of fluid pressurization occurs, lubrication mode is sensitive to operating parameters of the friction test (v, ε_N, and co-planarity) and not governed by tissue pressurization parameters (strain rate). In

addition, the Stribeck surface is asymmetric, with alterations to v or ε_N modulating μ_{eq} differently. As a result of the dependence of operating parameters on μ_{eq}, it is apparent that fluid equilibrium within the tissue is necessary but not sufficient for true boundary mode lubrication to occur. These data, pointing to the need for tight control over experimental variables, offer a potential suggestion as to why friction coefficients of cartilage reported in the literature range broadly (0.002-0.4) not only from system to system but within systems utilizing the same operating conditions[11,25,27,49,90,91,102,103,109,111,115,126,180,182].

While the studies documented here have only directly investigated the μ_{eq} effects of ε_N (rate and magnitude), v, and co-planarity on lubrication mode by Stribeck surfaces, additional dependences on lubricant η[192] and tissue surface roughness[4,50,192] do exist. Alterations to the tissue and synovial fluid due to disease or injury can include changes in viscosity, composition, modulus, and surface features; all of which may influence the lubrication of the tissue due to differences in the manner fluid films are able to be developed and sustained, as well as changes in lubricant-cartilage interactions. In order to understand the importance of synovial fluid components and tissue structure in cartilage tribology as well as identify lubrication mechanisms, investigation of the operational variable space for a particular friction apparatus coupled with tight control over experimental and control parameters is necessary.

This system and analysis paradigm allows for the control of lubrication mode enabling mechanistic and screening investigations of putative biolubricants for normal and diseased tissue. Control of operating variables and interface geometry enable investigations of multiple types of lubricated tissue and tissue engineered replacements, in addition to evaluation of materials for tissue replacement including hydrogels, foams, and commonly used hemiarthroplasty materials. Lastly, due to the ability to run multiple friction tests in parallel, control over the environment by

placing the apparatus in an incubator would facilitate long term investigations of tissue wear and alterations to lubrication modes with tissue development.

2.6 SUPPLEMENTARY MATERIAL

Friction Testing Apparatus

The four main components of the friction testing apparatus included one or more load cell towers, custom biaxial load cells, sample holders, and an oscillating table.

The load cell tower oriented the custom load cell correctly and allowed for translation of the load cell in the normal direction. The load cell mounted onto the freestanding tower via a dovetail track. A custom compound screw, formed by butt-end brazing a 1/4-28 threaded rod with a 8-1.0 threaded rod, allowed for the translation in the normal direction along the dovetail track at 98 μm/revolution. The compound screw was controlled by a servo motor [Parallex, Rocklin, CA] located on the top of the tower. The servomotor was controlled by a custom prototype circuit board and programmable Basic Stamp [Parallex]. The set-up allows for translation of the entire load cell in the normal direction and thus application of normal strains to the tissue.

The custom biaxial load cell was an instrumented cantilever beam that measures normal and shear loads. The load cell was designed using SolidWorks [SolidWorks, Concord, MA] and finite element analysis was performed using Cosmos [SolidWorks] to ensure maximum loads (24.5 N {normal direction}, 0.735 N {shear direction}) could be applied to the load cell without yielding or torsion. The load cell was instrumented with two full Wheatstone bridges placed along orthogonal axes, with one bridge to measure strains from normal forces and one to measure strains

resulting from frictional shear forces. The Wheatstone bridges were comprised of semi-conductor strain gages (SS-060-022-550P {normal bridge} SS-060-033-2000PU {shear bridge}, Micron Instruments, Simi Valley, CA) with high gage factors (GF=150 +/- 10 {normal bridge}, GF=155 +/- 10 {shear bridge}) resulting in high sensitivity to bending of the load cell. The load cell, machined from Aluminum 6061, included cutouts to concentrate stress in the bending beam. The beam geometry in combination with the highly sensitive Wheatstone bridges, created a load cell which was 100 times more sensitive to applied load in the shear direction than in the normal direction.

Load cell signal processing and conditioning was handled by custom and commercial equipment. Voltage signals from the two Wheatstone bridges on each load cell entered a custom prototype circuit board with copper cladding as a ground plane. The circuit board consists of the Wheatstone bridge balancing circuits, bridge excitation voltage regulation circuits, and shielded signal throughput circuits. Load cell voltage signals then enter an eight channel strain gage conditioning board [SC-203-SGU, National Instruments, Austin TX] where they pass through a 1.6 kHz high pass filter and into an instrumentation amplifier for a gain of 10. The signal was directed to a DAQ card [PCI-6034E, National Instruments] for data acquisition. All signal conduits were shielded to reduce the effects of external noise. A custom LabView [National Instruments] virtual instrument was utilized to interface with the DAQ board, apply a 5 Hz fourth-order low-pass Butterworth filter, perform data compression, and record the data at a sampling frequency of 10 Hz.

The sample holder was an important component of the friction apparatus allowing for coplanarity between the tissue and the glass, minimizing fluid wedge formation and allowing various lubrication modes to occur. Current cartilage friction testing set-ups found in the literature utilize both a gimbal system[49,76,109,126] and a fixed

system[102,162,183] to bring the two materials together. Two different sample holders were tested in these experiments: a cylindrical rod (fixed rod) which mounts the tissue sample similarly to a fixed system, and a custom pivot pin-disk holder. The custom pivoted sample holder (pivoted rod) was an 8 mm brass disc roughened on one side to assist in gluing the cartilage sample with cyanoacrylate gel glue [Henkel Consumer Adhesives, Avon, OH], and another side with a blind conical hole. The custom biaxial load cell interacted with the sample holder through a vee bearing where the conical hole accepted a pointed stainless steel pin attached to the load cell. The angle of the conical hole on the sample holder was approximately 3 times that of the angle of the point on the stainless steel pin. This interface allowed a point compressive load to be applied to the sample, with free rotation and no moments at this joint to enable co-planarity of the cartilage and glass surfaces.

The last major component of the friction apparatus was the oscillating table which translated the glass counterface against the cartilage sample. Any planar material (0.25 inch thick borosilicate glass, Ra = 5nm +/- 0.17nm using a MicroXAM non-contact 3D optical profilometer [ADE Phase Shift, Tucson AZ] in this case) can be placed into a recess in an aluminum plate and sandwiched with O-rings and a machined Delrin plate. This configuration created a watertight sample well where a test lubricant can be added to lubricate and hydrate the tissue. This assembly, with eight individual sample wells, was attached to a linear stage [Newmark, Mission Viejo, CA] and controlled by a motion control card (NI7344, National Instruments) and a PC running NI Motion (National Instruments). The stage was capable of speeds of 500 μm/s to 5.2 cm/s with controllable acceleration and deceleration profiles.

Instrument Calibration

Calibration of each load cell consisted of loading both directions of the load cell, either singularly or simultaneously, with a known load via a calibration jig (Figure 2.6). A matrix was calculated which describes the output voltage as a function of applied load while accounting for the bidirectional coupled strain effects due to bending of the beam. The applied load and loading patterns were randomized and loads ranged from 0 to 2 kg for the normal direction from 0 to 75 g for the shear direction. Experimental data in the normal load (L_N), shear load (L_S), and output shear voltage (V_S) and the L_N, L_S, and output normal voltage (V_N) spaces were fit with an orthogonal distance regression plane calculated using singular value decomposition (SVD) for linear minimization (Figure 2.7). This "plane of best fit" described the relationship between output voltage and applied load as follows:

$$\begin{bmatrix} V_S \\ V_N \end{bmatrix} = \begin{pmatrix} k_{11} & k_{12} \\ k_{21} & k_{22} \end{pmatrix} \begin{bmatrix} L_S \\ L_N \end{bmatrix} \tag{2.1}$$

where V is the voltage from the Wheatstone bridges in both directions, L is the applied load in both directions and the k matrix represents the unique decoupled stiffness matrix for a particular load cell. The relationship between voltage and load was linear since the load cell was manufactured from a linearly elastic isotropic material. The load cell was linear in both axes (through 2 kg normal direction and 75 g shear direction) with excitation voltages of 13V (shear bridge) and 1.5V (normal bridge).

Data Analysis

A typical experiment consisted of translating the table at a constant speed (Figure 2.8A) and applying a step in normal strain (Figure 2.8B), causing stress

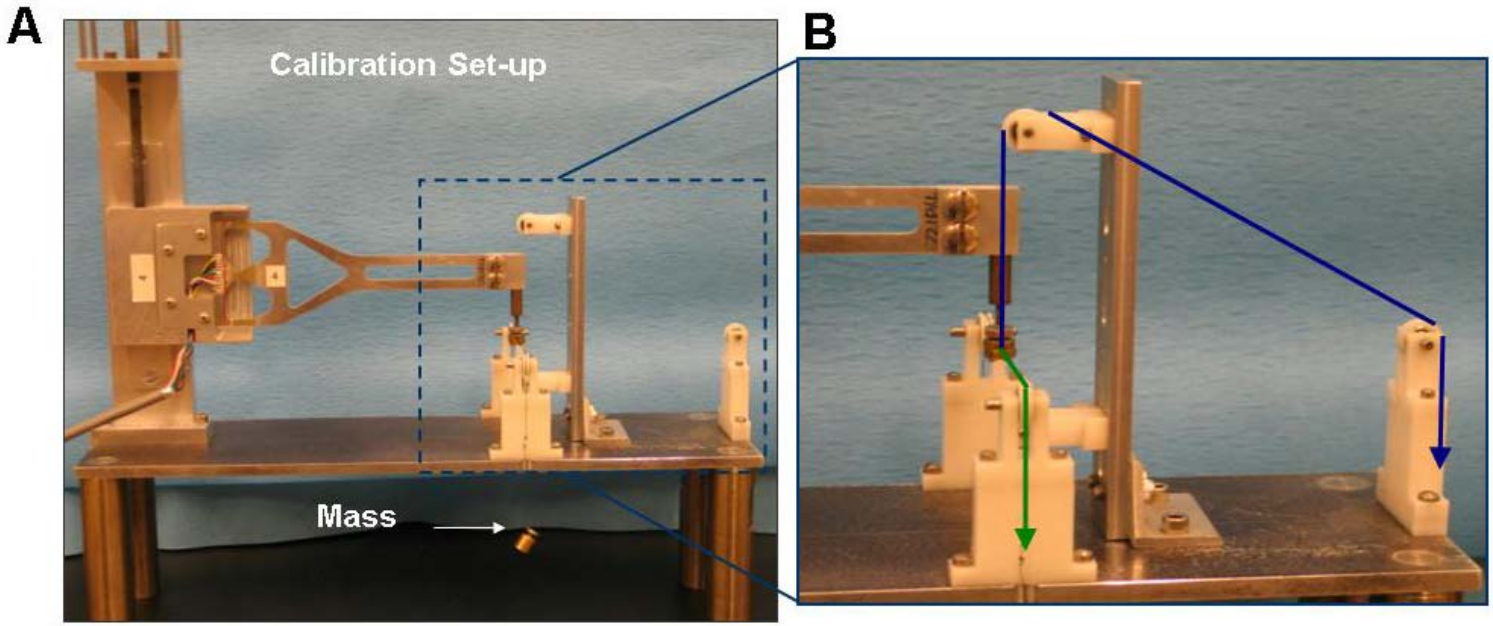

Figure 2.6: Photograph of the calibration set-up (A) where a series of masses attached to the load cell via strings apply loads in orthogonal directions (normal and shear) with the use of wheels to control direction of force. Superimposed arrows on the zoomed view (B) shows the path of the string for the various masses (green = shear, blue = normal).

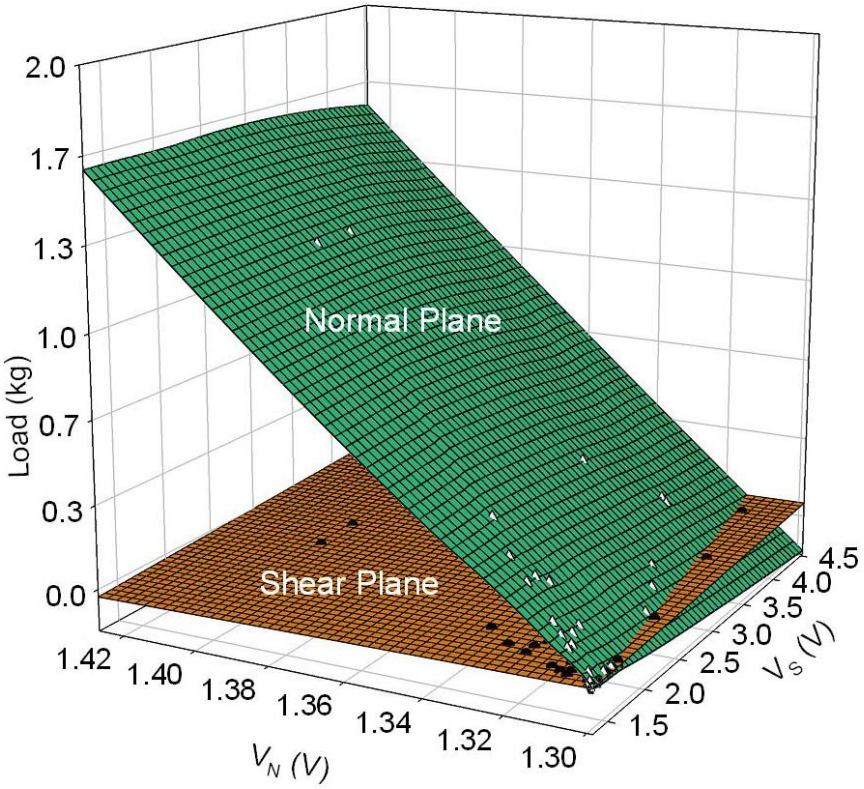

Figure 2.7: Plot of the voltage outputs for the normal (V_N) and shear (V_S) channels vs the applied calibration load. The equation of the resulting plane of best fit defines the calibration of the load cell.

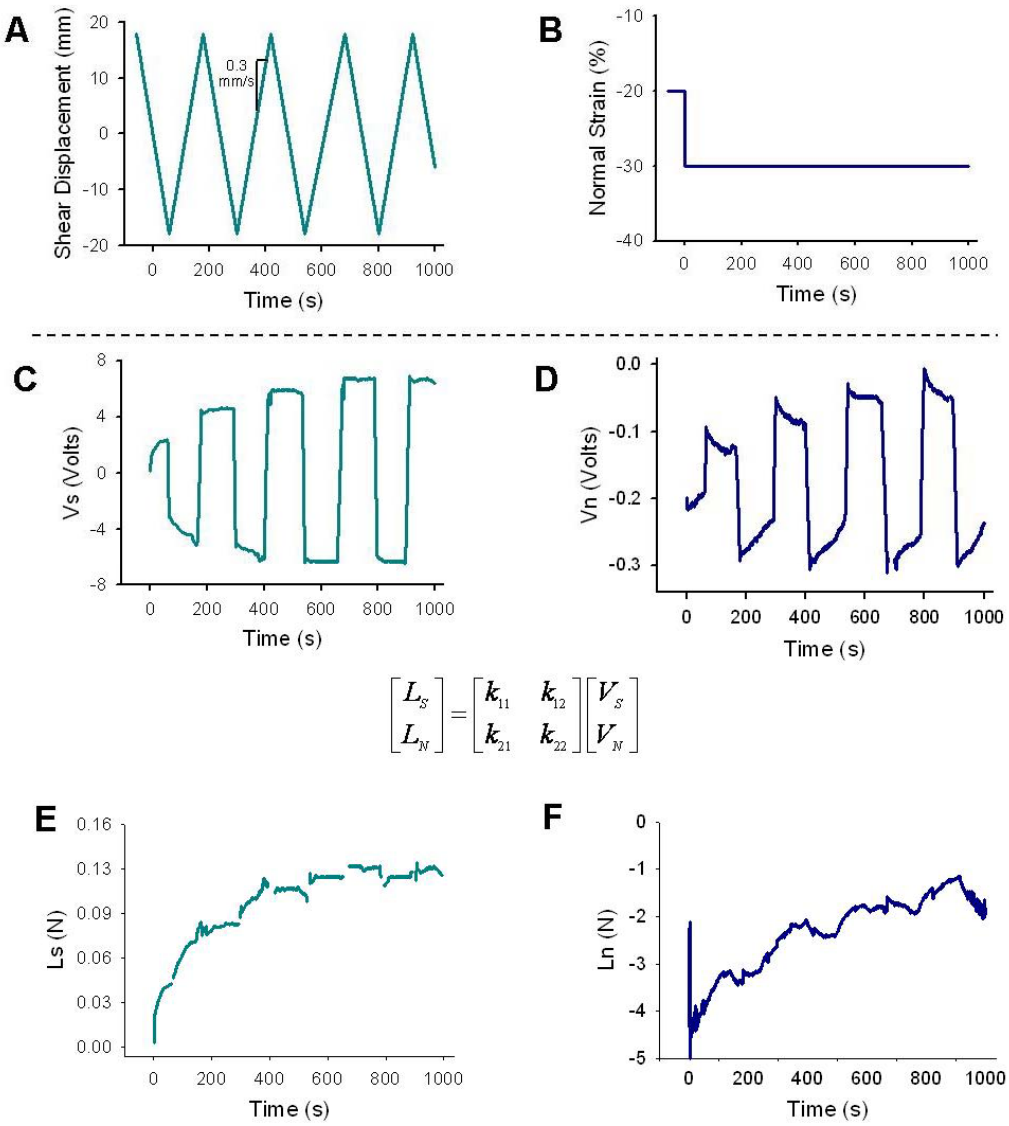

$$\begin{bmatrix} L_S \\ L_N \end{bmatrix} = \begin{bmatrix} k_{11} & k_{12} \\ k_{21} & k_{22} \end{bmatrix} \begin{bmatrix} V_S \\ V_N \end{bmatrix}$$

Figure 2.8: Process utilized to obtain shear and normal loads form the instrument as illustrated with example data obtained from a typical experiment. A table oscillates at a constant speed (A) and a step input in strain is applied (B). Over the course of the experiment the shear (C) and normal (D) channels of the load cell are recorded. Following the experiment, the voltages are decoupled into temporal shear (E) and normal (F) loads via the decoupling matrix.

relaxation in the tissue over time. The recorded time series of voltage signals for the normal and shear channels (Figure 2.8C&D) were transformed into shear and normal (Figure 2.8F) loads through $[\mathbf{k}]^{-1}$, the inverse decoupled stiffness matrix of the load cell. The shear load data was rectified and further processed to eliminate the extraneous data collected by the load cell as the direction of its deflection changed when the oscillating table reverses direction (Figure 2.8E). The normal load data for a range of ε_N was converted to normal stress, σ, through the sample geometry and fit with a poroelastic model[95] that allowed for the calculation of a Young's modulus and hydraulic permeability of the tissue. The instantaneous friction coefficient $\mu(t)$ (Figure 2.2A) was calculated using a simple Coulomb friction relationship where the friction coefficient for any given point in time is the magnitude of the shear load divided by the magnitude of the normal load $\{\mu(t) = |L_S(t)|/|L_N(t)|\}$. Similarly, a poroelastic/biphasic model[49,103] was then fit through the $\mu(t)$ data to calculate parameters including the initial ($\mu_0 = \mu(t\rightarrow 0)$) and equilibrium ($\mu_{eq} = \mu(t\rightarrow\infty)$) friction coefficients, in addition to the time constant τ (Figure 2.2A).

CHAPTER 3

BOUNDARY MODE LUBRICATION OF ARTICULAR CARTILAGE BY RECOMBINANT HUMAN LUBRICIN[‡]

3.1 ABSTRACT

Lubrication of cartilage involves a variety of physical and chemical factors, including lubricin, a synovial glycoprotein that has been shown to be a boundary lubricant. It is unclear how lubricin boundary lubricates a wide range of bearings from tissue to artificial surfaces, and if the mechanism is the same for both soluble and bound lubricin. In the current study, experiments were conducted to investigate the hypothesis that recombinant human lubricin (rh-lubricin) lubricates cartilage in a dose dependent manner and that soluble and bound fractions of rh-lubricin both contribute to the lubrication process. An rh-lubricin dose response was observed with maximal lubrication achieved at concentrations of rh-lubricin greater than 50 μg/ml. A concentration-response variable-slope model was fit to the data, and indicated that rh-lubricin binding to cartilage was not first order. The pattern of decrease in equilibrium friction coefficient indicated that aggregation of rh-lubricin or steric arrangement may regulate boundary lubrication. rh-lubricin localized at the cartilage surface was found to lubricate a cartilage-glass interface in boundary mode, as did soluble rh-lubricin at high concentrations (150 μg/ml) but, the most effective lubrication occurred when both soluble and bound rh-lubricin were present at the interface. These findings point to two distinct mechanisms by which rh-lubricin lubricates, one mechanism involving lubricin bound to the tissue surface and the other involving lubricin in solution.

[‡] Gleghorn, J.P., Jones, A.R.C., Flannery, C.R., and Bonassar, L.J. "Boundary Mode Lubrication of Articular Cartilage by Recombinant Human Lubricin," J Orthop Res, in review.

3.2 INTRODUCTION

Articular cartilage is responsible for the transfer of high compressive loads while maintaining a low friction bearing in diarthrodial joints over several decades of life. Lubrication of cartilage involves a variety of physical and chemical factors, including matrix architecture[21,169,183] and synovial macromolecules[60,69,146,172]. One such synovial fluid constituent, lubricin, has been shown to be, at least in part, responsible for the boundary lubrication of articular cartilage[163]. Nevertheless, the mechanism of cartilage lubrication by lubricin is not fully understood.

Lubricin, a mucinous glycoprotein, is encoded by the proteoglycan 4 (PRG4) gene and is homologous to other post translational gene products referred to as megakaryocyte stimulating factor (MSF) precursor, camptodactylyarthropathy-coxa vera-pericarditis (CACP) protein, 'downstream of the liposarcoma-associated fusion oncoprotein' 54 (DOL54), hemangiopoietin (HAPO), superficial zone protein (SZP), and proteoglycan 4 (PRG4)[48,75,78,84,105,112,119,129,155]. Lubricin is localized in the synovial fluid[174] and at the surface of multiple synovial tissues including cartilage[48,164,165], meniscus[164], and tendon[153]. Lubricin monomers consist of a multi-domain core protein with a central mucin-like domain that is extensively glycosylated with O-linked β(1-3) Gal-GalNac oligosaccharides[82], and globular cysteine-rich protein domains at the N- and C-terminus[48]. The termini of the molecule are believed to play a role in binding and aggregation[48,89] while the mucin-like domain is responsible for the boundary lubrication properties of the molecule[82].

The functional role of lubricin has been investigated previously with lubricin purified from synovial fluid[76,162,175] (referred to as "purified"). This purified lubricin is polydisperse with extended and less-extended forms observed[173]. Determination of the structure of human lubricin has enabled the production of a full-length

recombinant human lubricin (referred to as "rh-lubricin"), expressed from a Chinese hamster ovary (CHO) cell line as a monodisperse lubricin solution. This rh-lubricin may have great potential as a therapeutic agent, but the functional characteristics of the molecule are unknown.

A decrease in boundary mode friction coefficient (μ) has been observed in the presence of purified lubricin for latex-glass[49,76,109,126,178] and cartilage-cartilage[162] bearings. Previous studies have established localization of endogenous lubricin at or within the cartilage superficial zone and removal of lubricin from the surface of cartilage by changes in the ionic environment[89], suggesting that lubricin ionically binds to select extracellular matrix (ECM) macromolecules. The chemisorption of lubricin to the articular cartilage surface would seem to be integral to its role as a boundary lubricant. However, purified lubricin has been shown to decrease μ in artificial bearings with lubricin physiosorbed on surfaces and in the bulk solution[76]. Thus it is unclear how lubricin lubricates a wide range of bearings from tissue to artificial surfaces, and if the mechanism is the same for both soluble and bound lubricin.

This study investigates the hypothesis that recombinant human lubricin lubricates cartilage in a dose dependent manner and that soluble and bound lubricin both contribute to the lubrication process. To test these hypotheses, the objectives of this study were to (1) characterize the effect of human recombinant lubricin on the frictional properties of intact cartilage in a cartilage-glass bearing, and (2) to investigate the relative contributions of soluble and bound fractions of lubricin by measuring friction coefficients at multiple doses in a range of ionic strength solutions.

3.3 METHODS

Cartilage Explant Harvest & Lubricant Preparation

Full thickness bovine patellofemoral grove cartilage from six 1-10 day old calves was removed from the subchondral bone with a scalpel and subsequently frozen prior to testing. At the time of experimentation, the tissue was thawed and equilibrated for one hour in phosphate buffered saline (PBS) [Invitrogen, Carlsbad, CA] supplemented with a protease inhibitor cocktail [complete protease inhibitor cocktail, Roche Applied Science, Indianapolis, IN] in a water bath at 38˚C. A biopsy punch and scalpel were used to create 6mm diameter by 2mm thick disks with the articular surface intact. Samples were either friction tested (referred to as "non-extracted") or subjected to a lubricin extraction protocol[89] consisting of incubation in 1.5M NaCl [Sigma, St. Louis, MO] in PBS at 4˚C for 1 hour followed by equilibration in PBS for 1 hour prior to friction testing (referred to as "extracted").

Lubricants utilized for these studies included PBS, equine synovial fluid (ESF), and rh-lubricin. Utilizing guidelines approved by the Cornell University Institutional Animal Care and Use Committee, ESF was sterilely aspirated from equine stifle joints as described previously[55]. Contaminant free aspirates were pooled (6 joints from 4 animals aged 4 months to 5 years), aliquoted, and stored at -20ºC. On the day of friction testing, ESF was thawed in a water bath at 38˚C, vortexed, and utilized as a lubricant.

Full-length rh-lubricin was purified from the culture medium of a lubricin-expressing Chinese hamster ovary (CHO) cell line by heparin affinity and anion exchange chromatography as described previously[89]. Western blotting and total protein staining after gel electrophoresis assessed purity of rh-lubricin and concentration was determined by BCA protein assay (Pierce, Rockford, IL). Aliquots

of 200 and 300 μg/ml rh-lubricin in PBS were stored at -20ºC until friction testing. At the time of experimentation, the rh-lubricin was thawed at 38˚C in a water bath and serially diluted with PBS to create rh-lubricin lubricant solutions from 0-300 μg/ml. Two additional rh-lubricin solutions were created with altered ionic strengths of 0.5M and 1.5M NaCl for both 50 and 150 μg/ml rh-lubricin solutions.

Friction Testing

A custom cartilage on glass friction testing apparatus as described previously[54] was utilized to determine the initial (μ_0) and equilibrium (μ_{eq}) friction coefficients of cartilage in boundary mode lubrication. Briefly, the apparatus linearly oscillated cartilage against glass at one entraining speed (v = 0.33 mm/s) and a range of normal strains (20% < ε_N < 40%) utilizing different lubricants to measure the time-dependent normal ($L_N(t)$) and shear ($L_S(t)$) loads. The normal strain was initially applied (20%) and subsequently increased in 10% increments following a relaxation period of three times the previously determined stress relaxation time constant (τ_N). The instantaneous friction coefficient ($\mu(t)$) was calculated ($L_S(t)/L_N(t)$) producing a logarithmically increasing temporal friction profile, and a poroelastic model was fit to the $\mu(t)$ data to determine μ_0, μ_{eq} and τ_μ (Figure 3.1). Similarly, a poroelastic model was fit to the stress relaxation data ($\sigma(t)$), calculated from the sample geometry and $L_N(t)$ data, to determine σ_{eq} and τ_σ in order to calculate a Young's modulus (E_Y)[55,95]. All friction testing was conducted utilizing operating variables (v, ε_N) that produce boundary mode lubrication in this system[54].

Experimental Design

A series of experiments was conducted to investigate the dose dependent and

localization dependent lubrication abilities of rh-lubricin (Figure 3.1).

Experiment I: To determine the concentration-response behavior of rh-lubricin, a dose response curve was constructed for boundary mode μ_{eq} and μ_0 of an extracted cartilage-glass bearing lubricated with a range of rh-lubricin solutions from 0-300 μg/ml (n=6 per rh-lubricin concentration, with 14 concentrations tested). The frictional properties of the extracted cartilage-glass lubricated with ESF were also determined as a control in order to compare the lubricating properties of rh-lubricin to a known cartilage boundary lubricant[162]. In this experiment, rh-lubricin was present in the bulk solution and permitted to localize at the tissue surface.

Experiment II: To investigate the role of rh-lubricin when it is localized at the tissue surface, extracted (n = 5) and non-extracted cartilage (n = 5) was articulated against glass with PBS as a lubricant. Additional extracted (n = 5) and non-extracted (n = 5) tissues were incubated in either ESF or 50 μg/ml rh-lubricin for one hour at 4˚C. Following incubation, the samples were rinsed with PBS to remove any non-bound material, and subjected to friction testing with PBS as a lubricant. The incubation with ESF or rh-lubricin was conducted to determine if exposure subsequent to rh-lubricin extraction would functionally recover boundary lubrication to μ values equal to or better than native cartilage explants.

Experiment III: To investigate the effective lubricating ability of rh-lubricin localized only in the bulk solution or both in the bulk solution and the tissue surface, 50 and 150 μg/ml adjusted ionic strength rh-lubricin solutions were used as lubricants. Cartilage explants were incubated in the 1.5M NaCl lubricin extraction solution and friction tested with 50 and 150 μg/ml rh-lubricin solutions in either 0.14M (PBS), 0.5M, or 1.5M NaCl (n = 8) to determine μ_{eq} and μ_0. The 50 and 150 mg/ml rh-lubricin solutions were chosen as they exhibited maximal lubricating effect. The range in ionic strength was selected as lubricin is found to be localized at the surface

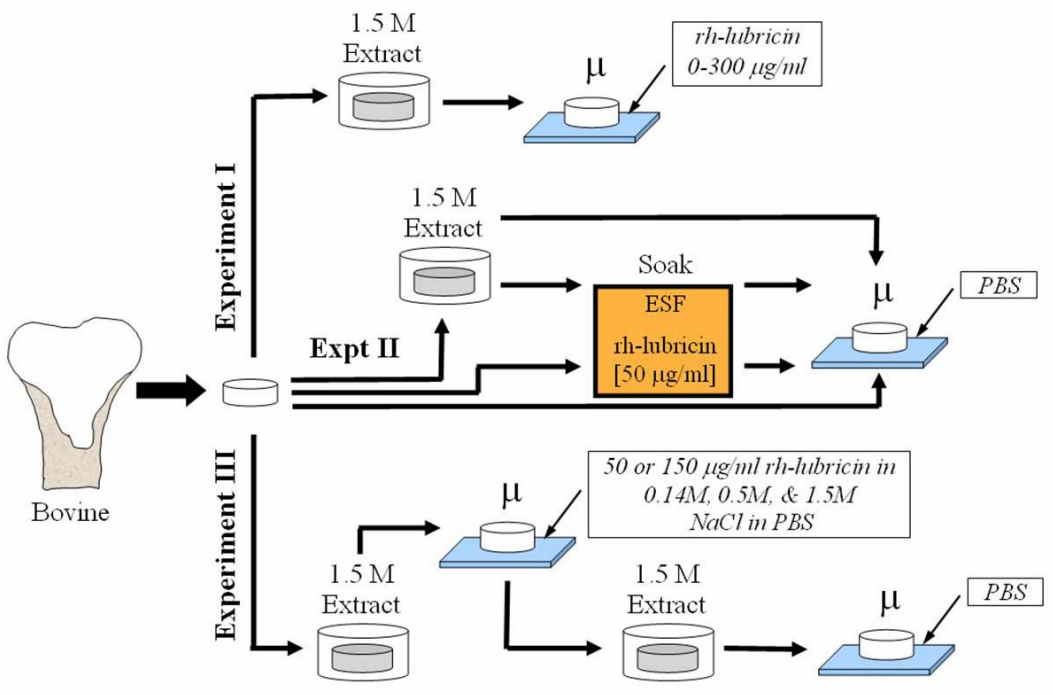

Figure 3.1: Cartilage explants were harvested from bovine stifle joints and used in one of three separate experiments. (Experiment I) Explants were incubated in 1.5M NaCl to extract bound lubricin and friction tested using 0 – 300 μg/ml rh-lubricin as a lubricant to determine the rh-lubricin concentration-reaction with rh-lubricin localized in the bulk solution and at the tissue surface. (Experiment II) Explants and explants with lubricin extracted with 1.5M NaCl were either friction tested or soaked in either ESF or 50 μg/ml rh-lubricin prior to friction testing with PBS as a lubricant to determine the role of rh-lubricin when it is localized at the cartilage surface. (Experiment III) Explants were extracted and friction tested with either 50 or 150 μg/ml rh-lubricin solutions at different ionic strengths (0.14M, 0.5M, or 1.5M), to determine the ability of rh-lubricin to lubricate when localized at the tissue surface or in the bulk lubricant solution. Subsequently, lubricin was extracted with 1.5M NaCl and friction tested to ensure the frictional properties were due to the lubricant solutions rather than alterations of the bulk tissue properties.

of young bovine articular cartilage for ionic strengths less than 1.5M[89]. Immediately following friction testing, explants underwent a rinse with and soak/vortex in PBS at room temperature for 5 minutes prior to an additional friction test. The secondary friction test served as a control to ensure that alterations in μ_{eq} and μ_0 were the result of the lubricating solution and not due to changes in the mechanical properties such as Young's modulus (E_Y), which are modulated by the ionic environment within the tissue[3].

Concentration-Response Model

A generalized variable slope concentration-response (VSCR) model[158] was fit to the experimental μ_{eq} – rh-lubricin concentration data in the first experiment to determine if a first-order lubricin binding mechanism explained the observed decrease in μ_{eq}. The four-parameter model of the form:

$$\mu_{eq} = B + \frac{A - B}{1 + 10^{(\log EC50 - [\mathrm{rh-lubricin}])*D}} \tag{3.1}$$

consisted of the baseline (A) and maximal effect (B) parameters, the EC50, which is the concentration of the agonist required to provoke a response of (B-A)/2, and the Hillslope (D) which characterizes the steepness of the curve. The VSCR model is a general form of an agonist binding model that does not assume that the observed effect is linearly proportional to the agonist binding ratio. If the effect is first-order, then the value for Hillslope is 1 and the equation reduces to the classic Langmuir binding/chemisorption isotherm:

$$\mu_{eq} = B + \frac{(A - B)[\mathrm{rh-lubricin}]}{EC50 + [\mathrm{rh-lubricin}]} \tag{3.2}$$

Statistical Analysis

A t-test was used to analyze μ_{eq}, μ_0, and τ_μ data to determine the effect of lubricant type (PBS, ESF, rh-lubricin). The effect of rh-lubricin incubation time on μ_{eq} was assessed using a one factor analysis of variance (ANOVA). The effect of rh-lubricin concentration and applied strain on μ_0 and μ_{eq} was determined using a two factor ANOVA with Tukey's HSD post hoc test. Similarly, effects of lubricant type and extraction state as well as rh-lubricin concentration and ionic strength on μ_{eq} were also calculated with a 2 factor ANOVA and Tukey's HSD post hoc test. The VSCR model was fit with a nonlinear regression using R^2 and root mean square error (RMSE) to evaluate the fit to experimental data. All data are presented as mean +/- SD and all analyses were carried out using SigmaStat [SPSS Inc, Chicago, IL] with calculated p values being considered significant for $p<0.05$.

3.4 RESULTS

The instantaneous friction coefficient, $\mu(t)$, monotonically increased to an equilibrium value for all lubricants tested, including rh-lubricin solutions (Figure 3.2). Trends in the data are presented for all applied ε_N (20 – 40%) with specific data given based upon Figure 3.1 for PBS, ESF, and 50 μg/ml rh-lubricin solution, the rh-lubricin concentration found to minimize μ_{eq} most significantly. Upon application of strain, μ_0 was similar for rh-lubricin, ESF, and PBS with μ_0 = 0.019 +/- 0.004, 0.018 +/- 0.006, and 0.020 +/- 0.005 respectively at ε_N = 30%. While the τ_μ was very similar for all lubricants tested ($\tau_{\mu ESF}$ = 695 +/- 15 seconds, $\tau_{\mu PBS}$ = 688 +/- 40 seconds, $\tau_{\mu 50\mu g/ml\ rh\text{-}lubricin}$ = 700 +/- 22 seconds), the μ_{eq} achieved by the lubricants were different ($p<0.002$) with ESF (0.115 +/- 0.013) and 50 μg/ml rh-lubricin (0.093+/- 0.011) both lower than PBS (0.281 +/- 0.014).

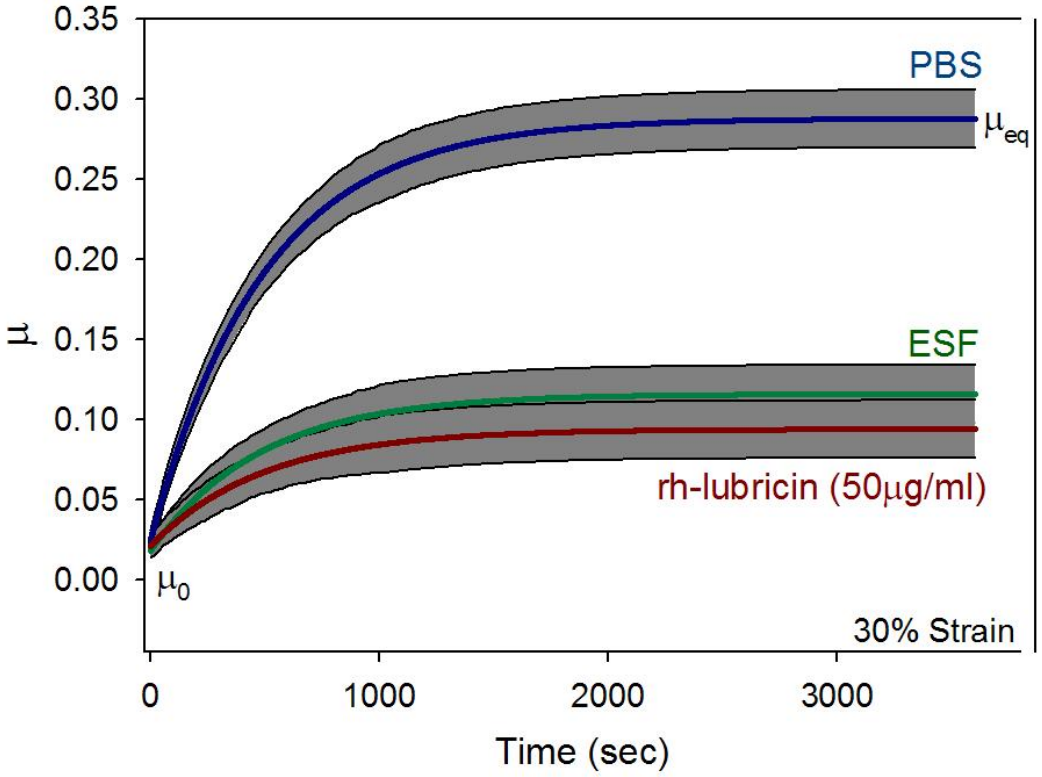

Figure 3.2: Poroelastic model fit to an example μ(t) data set (n = 6) for a cartilage-glass bearing lubricated with either PBS, ESF, or 50 μg/ml rh-lubricin at v = 0.33 mm/s and 30% normal strain. For clarity, model fits are shown with grey shaded regions representing one standard deviation of the data.

Experiment I: Concentration-response of rh-lubricin

The addition of rh-lubricin to the cartilage-glass interface lowered the μ_{eq} in a concentration dependent manner (Figure 3.3A); however, minimal changes ($p = 0.62$) in μ_0 were observed (Figure 3.3B) due to applied ε_N. The concentration dependent response of μ_{eq} was well described by a single VSCR model over all ε_N tested, with $R^2 > 0.98$ and RMS error < 0.036 and model parameters of: baseline $\mu_{eq} = 0.317$, maximal effect $\mu_{eq} = 0.097$, EC50 = 11.49 μg/ml, and Hillslope = 0.1022 (Figure 3A). A Langmuir isotherm was also calculated for comparison to the VSCR model with $R^2 < 0.90$ and RMS error > 0.124 and a baseline $\mu_{eq} = 0.325$, maximal effect $\mu_{eq} = 0.072$, and EC50 = 11.62 μg/ml calculated (Figure 3.3A).

Overall, rh-lubricin solutions greater than 50 μg/ml lubricated similarly to ESF with μ_{eq} on the order of 0.09, representing 3 fold better lubrication than PBS with an μ_{eq} of 0.29 +/- 0.045 (Figure 3.3A). At $\varepsilon_N = 20\%$, a 50 μg/ml rh-lubricin solution produced a minimum μ_{eq} (0.082 +/-0.009) and a significant increase in μ_{eq} ($p = 0.042$) was seen from 50 to 100 μg/ml ($\mu_{eq} = 0.114$ +/- 0.012); however, neither solution was different from rh-lubricin concentrations greater than 100 μg /ml. While 50 and 100 μg /ml rh-lubricin solutions produced different μ_{eq} at $\varepsilon_N = 20\%$, this difference was absent as ε_N increased to 30 and 40% (Figure 3.3A inset for $\varepsilon_N = 40\%$). The μ_0 remained constant over the tested rh-lubricin concentrations (0.021 +/- 0.008), and similar in magnitude to values for ESF (0.019 +/- 0.009) and PBS (0.022 +/- 0.006) (Figure 3.3B).

Experiment II: Localizing rh-lubricin at the tissue surface

Extraction of endogenous surface rh-lubricin significantly increased ($p < 0.001$) μ_{eq} (0.325 +/- 0.034) approximately 15% compared to non-extracted tissue

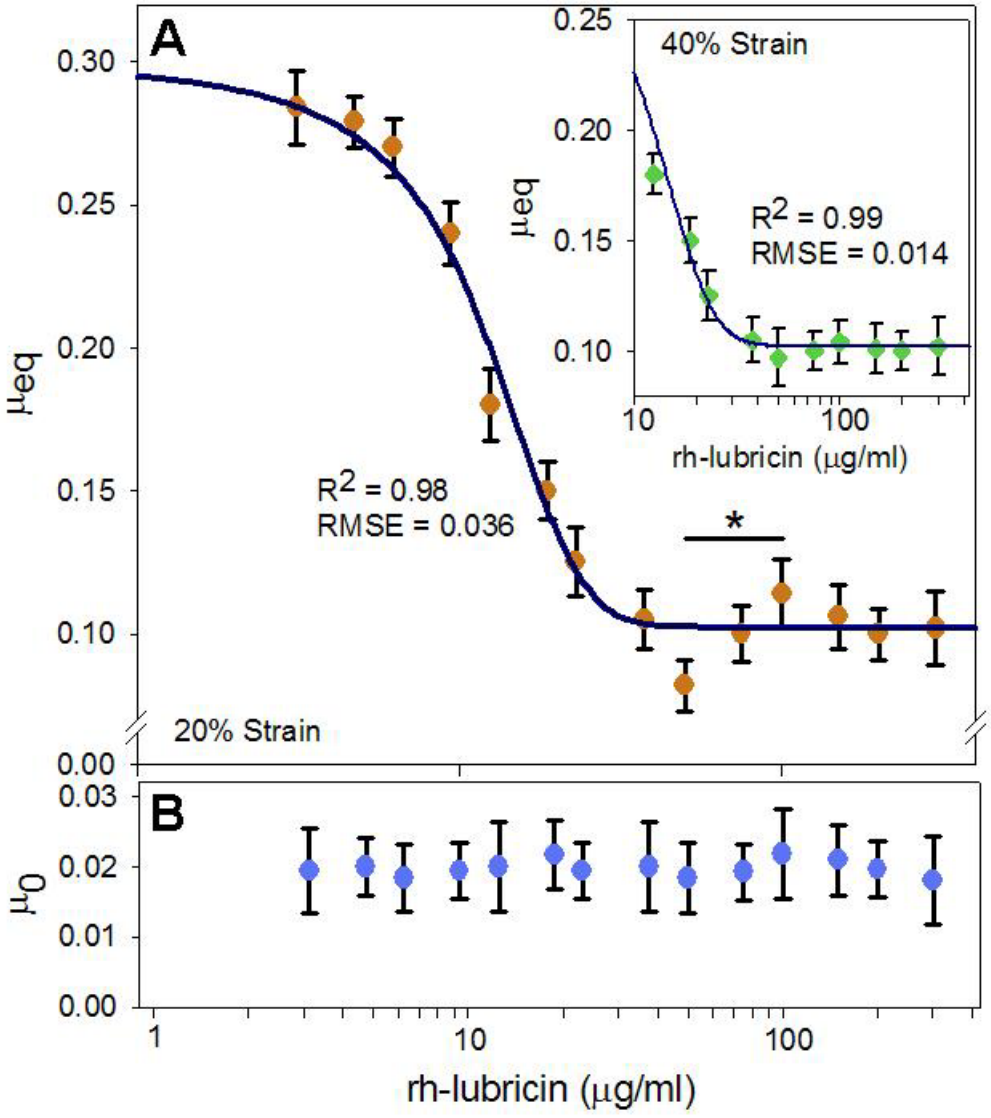

Figure 3.3: Concentration-dependent response on μ_{eq} (A) and μ_0 (B) for a range of rh-lubricin concentrations at v = 0.33 mm/s and 20% normal strain. VSCR model fit to data +/- SD for 20% strain (A) and 40% strain (A, inset). Data represented as mean +/- SD with n = 6 per rh-lubricin concentration (* = $p < 0.05$).

(0.284 +/- 0.042) with PBS as a lubricant (Figure 3.4A). Incubation in and removal of excess ESF and 50 μg/ml rh-lubricin did not alter μ_{eq} for non-extracted tissue; however, recovery of lubrication subsequent to a soak decreased μ_{eq} to values (μ_{eqESF} = 0.280 +/- 0.014, $\mu_{eqrh\text{-}lubricin}$ = 0.277 +/- 0.009) not significantly different than non-extracted tissue. Additionally, incubation time in 50 μg/ml rh-lubricin modulated the equilibrium friction properties with the maximum reduction in μ_{eq} observed after a 15 minute incubation period (Figure 3.4B). Trends seen in μ_{eq} for rh-lubricin extraction and lubrication recovery in addition to rh-lubricin incubation time were consistent over the 20 - 40% ε_N conditions tested.

Experiment III: Partitioning rh-lubricin in bulk solution and at tissue surface

Changes in ionic strength of the lubricin solution significantly altered the equilibrium lubricating properties of lubricin at both applied doses (Figure 3.5A), but minimal changes were noted in μ_0 (Figure 3.5B). In PBS (0.14M NaCl), application of 50 μg/ml rh-lubricin decreased μ_{eq} by 71%, while application 150 μg/ml rh-lubricin lubricated only 63% as well. The lubricating effect of 50 μg/ml rh-lubricin was completely removed by testing in 1.5M NaCl (μ_{eq} = 0.310 +/- 0.042), but only partially inhibited by testing in 0.5M NaCl (μ_{eq} = 0.131 +/- 0.036, $p < 0.03$). In contrast, at a concentration of 150 μg/ml, rh-lubricin in 1.5M NaCl retained some lubricating action, lowering μ_{eq} by 15% (0.267 +/- 0.032, $p<0.05$), but was not as effective as in PBS (0.124 +/- 0.028, $p < 0.001$). Delivery of 150 μg/ml rh-lubricin in 0.5M NaCl did not affect the lubricating ability of rh-lubricin, lowering μ_{eq} by 53%, similar to that observed in PBS. For samples tested in both 50 and 150 μg/ml 1.5M NaCl rh-lubricin solutions, E_Y was not significantly different ($p = 0.54$) compared to extracted cartilage controls (0.46 +/- 0.11). In addition, μ_{eq} values returned to those of

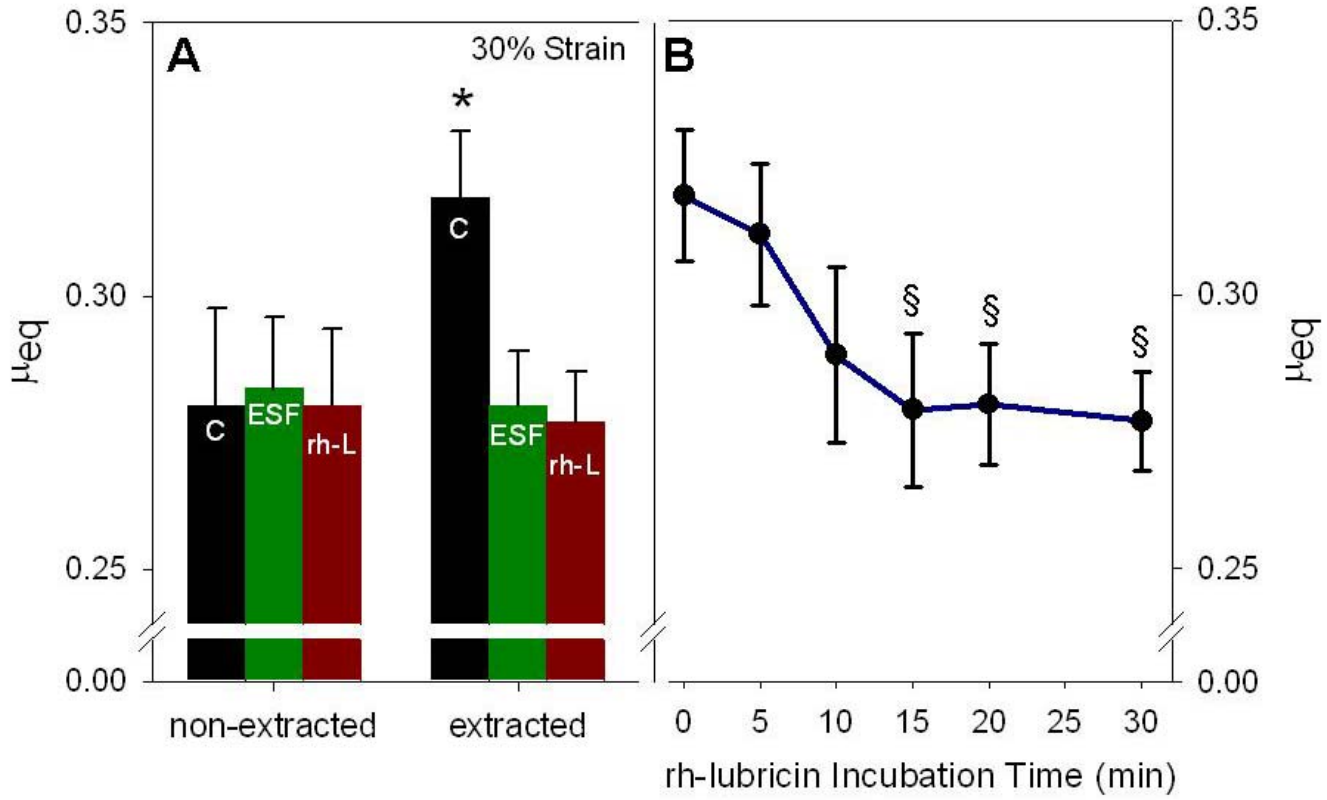

Figure 3.4: μ_{eq} for extracted and non-extracted cartilage explants prior and subsequent to a soak in either ESF or 50 μg/ml rh-lubricin at v = 0.33 mm/s and 30% normal strain (A). μ_{eq} for explants incubated at various times in 50 μg/ml rh-lubricin solution (B). Data represented as mean +/- SD with n = 5 per condition (* = $p < 0.001$ compared to all others, § = $p < 0.05$ compared to μ_{eq} at t = 0 minutes).

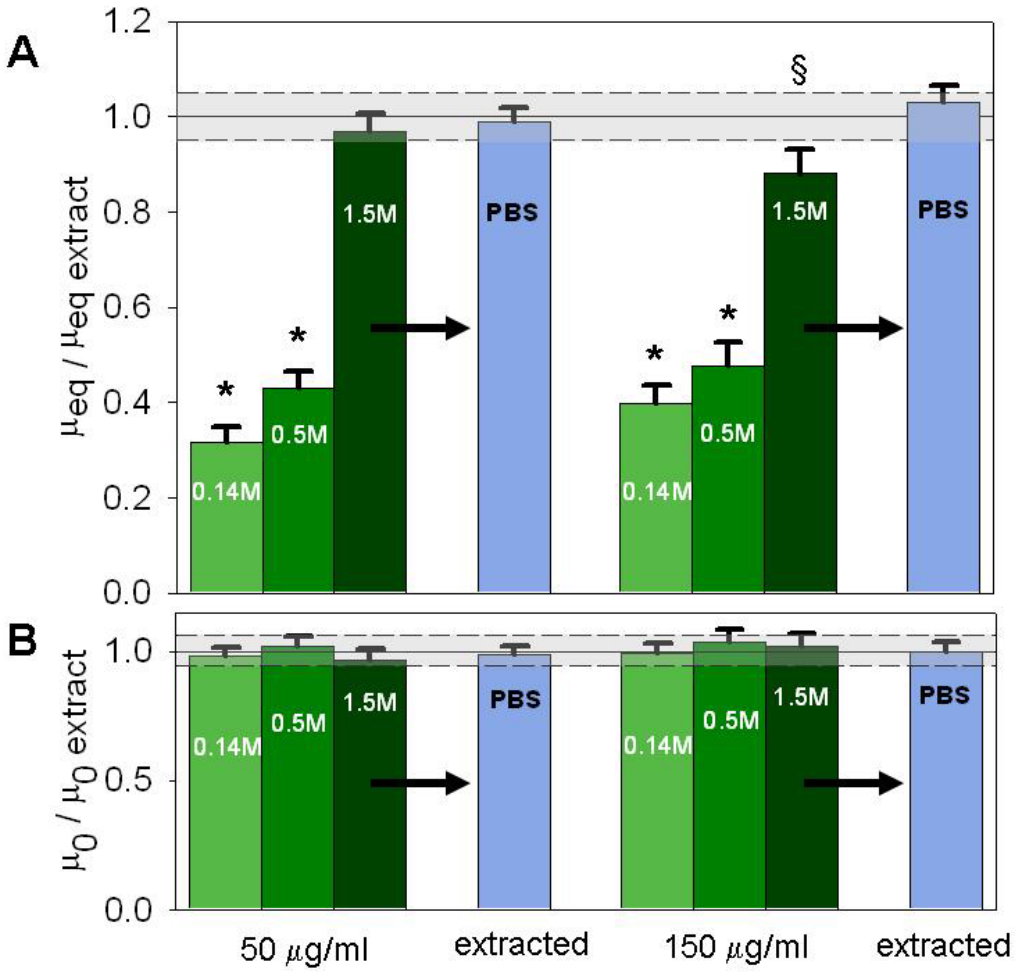

Figure 3.5: Effects of ionic strength and lubricin concentration on μ_{eq} (A) and μ_0 (B) normalized to μ_{eq} and μ_0 of extracted cartilage respectively. Experiment performed at v = 0.33 mm/s and 30% normal strain. Overlaid gray box represents mean (solid line) and SD for cartilage explants tested under the same conditions with PBS as a lubricant. Data represented as mean +/- SD with n = 8 per rh-lubricin concentration and ionic strength (* = $p < 0.01$ compared to PBS, § = $p < 0.01$ compared to extracted controls).

extracted cartilage following subsequent rinsing and testing in PBS (Figure 3.5A). In addition, μ_{eq} values returned to those of extracted cartilage following subsequent rinsing and testing in PBS (Figure 3.5A). Under all experimental conditions, μ_0 was not significantly different from extracted cartilage controls with μ_0 remaining approximately 0.018 +/- 0.008 (Figure 3.5B).

3.5 DISCUSSION

These studies demonstrated that rh-lubricin lowers cartilage μ_{eq} in a dose-dependent manner. Further, soluble and bound rh-lubricin were shown to make distinct contributions to the lubrication process as indicated by alterations in μ_{eq} in different electrostatic environments. A significant lubricating effect of rh-lubricin was observed, with a time-dependent behavior and a maximal effect that is similar to synovial fluid. μ_{eq} exhibited a concentration-response relationship where a decrease in μ_{eq} was observed with increasing rh-lubricin concentration, which was well described with a VSCR model with slope of <1. If the response relationship were due to a first order binding phenomena, the Hillslope would equal 1 and the model would be simplified to a standard Langmuir isotherm, which describes chemisorption of a monolayer. The results of this model indicate a likely role of multimerization[48,89] and/or steric arrangement[14] of rh-lubricin in producing low μ_{eq}; however, mechanistic relationships and information about adsorption kinetics cannot be inferred from a VSCR model with a non-unity slope.

The lubricating ability of rh-lubricin in this cartilage-glass system was different than in other systems, with an effective lubricating concentration equivalent to ESF. A cartilage-cartilage interface lubricated with purified lubricin (450 μg/ml) from bovine synovial fluid was unable to achieve the low μ observed when the bearing

is lubricated with synovial fluid[162]. Conversely, a latex-glass bearing was able to demonstrate similar μ when lubricated with purified bovine lubricin but required 200-260 μg/ml[76] to achieve this level of lubrication. In the current study, maximum lubrication occurred at concentrations equal to or greater than 50 μg/ml rh-lubricin, but a cartilage-cartilage bearing was able to achieve overall significantly lower friction coefficients compared to the cartilage-glass and latex-glass systems[162]. This suggests that lubricin may interact differently in a cartilage-cartilage interface, enabling lower μ_{eq} than those observed in a cartilage-glass bearing. Additionally, taken together these data indicate that chemisorption of lubricin at the tissue surface enables lubrication at lower effective concentrations than physisorption. This enhanced efficiency of chemisorped lubricin may be due to localization at the interface that is independent of fluid flow and pressure.

The addition of 50 μg/ml of rh-lubricin produced the maximal lubricating ability, and in fact, an increase in μ_{eq} from 50 to 100 μg/ml was noted under ε_N = 30%. While this pattern subsided with increasing strain, the fact that this phenomenon is less pronounced at higher loads/strains may indicate that rh-lubricin aggregation, localization, or arrangement on the cartilage surface is affected by the amount of normal load. Additionally, the observation that 50 μg/ml is the lowest concentration of rh-lubricin to achieve maximal lubrication is consistent with other studies. A full layer of purified lubricin was found to be physisorbed on a sheet of mica at 50 μg/ml as identified by atomic force microscopy (AFM)[179].

This study demonstrates that the ability of rh-lubricin to lubricate cartilage is dependent on the ionic environment, suggesting that electrostatic interactions play a significant role in rh-lubricin-mediated boundary lubrication of cartilage. Electrostatic interactions are known to regulate the binding of lubricin to cartilage[89] and may also influence aggregation of the molecule in solution. Both binding and aggregation of

lubricin might be expected to affect the ability of the molecule to lubricate cartilage. In the presence of 0.5 M NaCl, there was a small, but significant loss of lubrication observed for both 50 and 150 μg/ml. Since this ionic strength does not remove lubricin from cartilage, the increase in μ_{eq} observed in this case may be related to other phenomena such as steric arrangement[195], multimerization[48,89], or the possibility of rh-lubricin to structure water at the tissue surface. The lubricating effect of 50 μg/ml was completely abolished in 1.5M NaCl, a condition that removes bound lubricin from cartilage[89]. These data suggest that at doses at or below 50 μg/ml, localization of rh-lubricin at the surface of the tissue plays an integral role in the lubricating action of the molecule. At 150 μg/ml, the presence of 1.5 M NaCl inhibited the lubricating ability of rh-lubricin only partially. This suggests that at a higher dose, rh-lubricin acts via a mechanism that does not require binding to the cartilage surface. This is consistent with previous studies of lubrication of synthetic bearings, in which the concentration of purified lubricin required to lower μ_{eq} were 200 to 260 μg/ml[76].

For all conditions tested, μ_{eq} was independent of applied axial strain, confirming that μ_{eq} reflects the behavior of the tissue in boundary mode lubrication. Additionally, the Young's modulus was invariant for the explants tested in high ionic strength rh-lubricin solutions, and μ_{eq} subsequent to rinsing with PBS produced values similar to extracted cartilage. As such, alterations in μ_{eq} are not the result of changes in mechanical properties of the tissue due to ionic environment as seen when cartilage is soaked in various ionic strength solutions[3].

The studies documented herein collectively point to two distinct mechanisms by which rh-lubricin lubricates. The first mechanism involves rh-lubricin that is bound to the surface of the tissue and the second involves rh-lubricin in solution, with greatest lubrication noted when rh-lubricin is localized both at the tissue surface and in solution. Further investigations are needed to determine the manner of rh-lubricin

localization at the surface of cartilage in normal and pathologic states in order to develop potential therapeutic interventions to recapitulate or maintain the low friction properties of articular cartilage.

CHAPTER 4

BOUNDARY MODE FRICTIONAL PROPERTIES OF ENGINEERED CARTILAGINOUS TISSUES[†]

4.1 ABSTRACT

Despite the fact that lubrication is a primary function of articular cartilage, there is little information on the frictional properties of cartilaginous engineered tissues. A biochemical mediator of cartilage frictional properties in boundary lubrication, lubricin, has been shown to be secreted from chondrocyte-hydrogel constructs. In the current studies we utilized articular chondrocytes (CON), meniscal fibrochondrocytes (MEN), and mesenchymal stem cells (MSC) in alginate cultures to determine lubricin localization and the inherent boundary lubrication friction coefficient. Additionally, we investigated the ability of these tissues to be lubricated by synovial fluid and the reversibility of this lubrication. Cell-alginate constructs were cultured over six weeks, culture medium assayed for lubricin release by ELISA and constructs analyzed with immunohistochemical (IHC) methods to investigate the localization of lubricin. Engineered tissues were tested in a custom friction instrument to determine the equilibrium friction coefficient μ_{eq} in boundary lubrication mode, following incubation with equine synovial fluid (SF), and subsequent extraction in l.5M NaCl. MSCs released 10 fold more lubricin than CON or MEN cultures. IHC analysis showed no localization of lubricin to alginate, minimal focal staining of engineered constructs at six weeks in culture, and the ability of all engineered tissues to localize lubricin when exogenously treated with SF. Frictional characterization

[†] Gleghorn, J.P., Jones, A.R.C., Flannery, C.R., and Bonassar, L.J. (2007) "Boundary Mode Frictional Properties of Engineered Cartilaginous Tissues," Eur Cell Mat J, 14: 20-8 discussion 28-9.

showed no difference in μ_{eq} over culture for all engineered tissues, while incubation in SF decreased μ_{eq} for all tissues over culture duration, and extraction of lubricin resulted in a loss of lubrication of all engineered tissues.

4.2 INTRODUCTION

Articular cartilage, an avascular, aneural tissue found at the ends of articulating bones, is responsible for providing a load-bearing, low friction interface for diarthrodial joints. In joints, the primary source of lubricant is synovial fluid, which contains a variety of macromolecules synthesized by joint tissues. Components of synovial fluid contribute to joint lubrication across a variety of mechanical mechanisms from hydrodynamic to boundary modes. Boundary lubrication occurs through molecules localized at the tissue surface under conditions of high compressive loads and low entraining speeds. Under such conditions the asperities of the two cartilage surfaces interact and surface chemistry dominates the lubrication properties. This interaction produces the highest friction coefficients μ of any mode of lubrication[27,156,191], and thus the maximum potential to cause wear and transfer high shear stresses to the articular cartilage. While the structure of cartilage in part accomplishes the low friction function of cartilage[103], biochemical interactions at the surface of the tissue have been shown to reduce the μ under boundary mode conditions[162].

One such biochemical mediator of frictional properties is lubricin, a glycoprotein found to lubricate load bearing surfaces that localize the molecule, including articular cartilage[164], meniscus[166,171], and tendon[153,155,171]. Lubricin, also referred to as proteoglycan 4 (PRG4)[75], megakaryocyte stimulating factor (MSF) precursor[48,78], superficial zone protein (SZP)[164] and CACP protein[119] is found in

synovial fluid[175] and is secreted by superficial zone chondrocytes[98,164], select cells in the meniscus[166] and synoviocytes[84,165]. Localization of lubricin in the tissue is limited primarily to the surface of the tissues lining the joint with little accumulation within joint tissue extracellular matrix[164,166]. Previous studies have demonstrated that lubricin is removed from the surface of articular cartilage by extraction with 1.5M NaCl[89], indicating that tissue localization in cartilage is not the result of covalent attachment. The efficacy of lubricin in boundary mode has been shown in material-material interfaces including latex-glass[76,81,83], in cartilage-cartilage interfaces[162], and in preliminary studies of cartilage-glass interfaces[57]. While boundary lubrication in a dose dependant manner is evident by purified lubricin[162], the specific mechanism is unknown.

Efforts to regenerate or engineer joint tissues have typically focused on producing tissues with proper compressive or tensile properties[74,96,106,168,176,181]. Despite the fact that lubrication is a primary function of articular cartilage, there is little documentation of efforts to engineer tissues with proper frictional properties. Current in vitro efforts with engineered cartilage focus on evaluating the expression[58,59] and secretion[58,96,98,163] of lubricin from chondrocytes under various culture conditions and medium supplements. These studies have focused primarily on production of lubricin by articular chondrocytes, but little is known about the ability of other types of chondrocytes, such as meniscal fibrochondrocytes, to generate lubricin in 3D culture. Further, there has been great interest in the use of mesenchymal stem cells (MSCs) as a cell source for cartilage tissue engineering, but little is known about the ability of these cells to generate lubricin after chondrogenic differentiation. Regardless of cell source, there is little information on the frictional properties of cartilaginous engineered tissues.

Toward this end, the objectives of this study were to utilize three distinct cell types, articular chondrocytes, meniscal fibrochondrocytes, and bone marrow derived mesenchymal stem cells in three dimensional alginate cultures to determine: 1) the production and localization of lubricin; 2) the inherent boundary lubricated friction coefficient of these engineered tissues; 3) the ability of these tissues to be lubricated by lubricin from synovial fluid; and 4) the reversibility of synovial fluid lubrication by removal of lubricin via extraction with salt solutions.

4.3 METHODS

Cell / lubricant preparation

Equine sternal bone marrow mesenchymal stem cells (MSC) and stifle joint synovial fluid (ESF) were aspirated from three geldings (22-24 months old) within 15 minutes of euthanasia following protocols approved by the Cornell University Institutional Animal Care and Use Committee. Bone marrow aspirates were pooled and plated using standard protocols[190] to isolate MSCs. Briefly, aspirates were washed and plated in tissue culture flasks with growth medium in an incubator at 37°C and 5% CO_2 environment, resulting in a population of adherent cells, taken to be MSCs, from the bone marrow aspirate after 24 hours. The medium was changed, removing non-adherent cells, and the flasks were washed with sterile phosphate buffered saline (PBS) [Mediatech, Herndon VA], prior to the removal of MSCs from the culture flasks with trypsin [Sigma, St. Louis MO] for 4 minutes. ESF aspirates were visually inspected to ensure blood and contaminate free, pooled, and frozen at -20°C until use in friction testing.

Primary bovine chondrocytes (CON) and meniscal fibrochondrocytes (MEN) were sterilely isolated from harvested patellofemoral groove cartilage and both lateral

and medial menisci from four 1-3 day old calves. The tissue was pooled and underwent similar cell isolation protocols by digestion for 18 hours with 0.3% collagenase digest followed by a series of washing and centrifugation steps[10,53]. All tissues collected were from animals with no musculoskeletal pathologies.

Creation of engineered tissues

Cell-alginate constructs were created at a seeding density of $2.5x10^7$ cells/mL and cultured in an incubator at 37°C and 5% CO_2 environment for 0, 2, 4, and 6 weeks. MSC, CON, and MEN were encapsulated in 20 mg/mL of Protanal LF 10/60, a low viscosity alginate with a mean guluronate/mannuronate ratio of 70/30 [FMC Biopolymer, Drammen Norway] in PBS. Cell-alginate suspensions were mixed with 20 mg/mL calcium sulfate [Mallinckrodt Baker, Phillipsburg NJ] in PBS in a 2:1 ratio via a 3-way stopcock[23]. The resulting mixture was injected between two parallel plates separated by a 1mm spacer to produce a sheet of cell-seeded gel. From this sheet, 6 mm disks were cut using a dermal biopsy punch, resulting in 48 disks (12 disks/time point) for each of the cell-alginate conditions. The disks were placed in culture with standard culture media supplemented with 10% fetal bovine serum (FBS) [Gemi Bio-Products, Woodland CA], 100 U/mL penicillin [Mediatech, Herndon VA], and 100 μg/mL streptomycin [Mediatech, Herndon VA]. In addition, MSC media was supplemented with 5 ng/mL TGF-β1 [Peprotech, Rocky Hill NJ] to enhance chondrogenic differentiation[189,190]. For all conditions, media was changed every three days, with spent media stored at -20°C for biochemical analysis.

Following culture at the respective time points, samples were stored for subsequent mechanical and biochemical characterization. Cell-alginate constructs for confined compression testing followed by biochemical characterization (n=5) and

friction testing (n=5) were removed from culture and frozen at -20°C for later testing. Histological cell-alginate samples (n=2) were removed from culture and placed in 10% neutral buffered formalin [Fisher Diagnostics, Middletown VA] supplemented with 1mM $CaCl_2$ [Sigma, St. Louis MO] to prevent gel dissolution[136]. Acellular controls were created utilizing the same protocols for cellular constructs and were frozen at -20°C for later confined compression (n=5) and friction testing (n=5).

Characterization of engineered tissues

Cell-alginate samples and acellular controls for mechanical testing were thawed in PBS with an EDTA-free protease inhibitor cocktail [Roche Diagnostics, Mannheim Germany] to prevent dissolution of the alginate gel due to calcium chelation by EDTA. The protease inhibitor cocktail focuses on inhibiting serine and cysteine proteases while MMP protease activity was limited by minimizing the time from thawing to mechanical testing. Samples were thawed, equilibrated in PBS, and mechanically tested within 1 hour.

Confined compression testing (n=5 samples/time point/cell type, n=5 acellular controls) was performed for comparison of compressive properties to values obtained in the literature for CON-, MEN-, and MSC-alginate generated tissue. Cell-alginate constructs were tested using an ELF-3200 test system [Bose EnduraTEC, Minnetonka, MN] in confined compression with the application of 50μm displacement steps applying 5-45% strain. Each displacement step was held for 12 minutes which was determined as a minimum of three times the time constant for 6 week constructs (τ_{CON} = 2.8, τ_{MEN} = 2.7, τ_{MSC} = 2.3 minutes) from preliminary data (not shown) ensuring full relaxation of the sample. The resulting compressive loads were fit to a poroelastic model[150] allowing for the calculation of an equilibrium modulus H_A and permeability

k from the equilibrium stress-strain curve (Figure 4.2c inset figure, example 6 week data).

Immediately following confined compression testing the samples were papain [Sigma, St. Louis MO] digested at 60°C for 14 hours and standard biochemical assays were utilized for biochemical characterization of proteoglycan and collagen localization. Glycosoaminoglycan (GAG) content was assayed with a modified DMMB dye assay[44] at low pH, and a DMAB assay[137] was utilized to measure the hydroxyproline content of the engineered tissues.

Analysis of lubricin synthesis and localization

Media from the CON, MEN, and MSC constructs was thawed and assayed to determine quantities of lubricin released to the media from the cell-alginate constructs over culture time (n=10 samples/cell type). A direct ELISA using rabbit polyclonal antibody 06A10[193] was developed to assay the lubricin concentration in the conditioned media from the respective samples, using recombinant human lubricin as a standard.

Following fixation in formalin, the tissue was embedded and sectioned into 5 μm thick sections using standard histological procedures to investigate tissue localization of lubricin. Sections underwent immunohistochemical (IHC) staining for lubricin using monoclonal antibody 3-A-4 as previously described (Schumacher et al, 1999). To assess the ability of lubricin to bind to engineered tissues, sections were incubated with bovine synovial fluid (BSF) for one hour at 20°C. BSF treated sections were washed twice with tris buffered saline (TBS)/0.1% Tween at 20°C and once with TBS at 20°C before IHC staining for lubricin.

Friction testing

The engineered tissue and acellular controls were tested in a custom friction apparatus[56] using PBS as a lubricant (Figure 4.1). Briefly, the friction apparatus linearly oscillates each sample against a glass counterface (RMS roughness 5nm +/- 0.17nm) at a controlled speed with imposed normal strains on the tissue. A servo motor driven linear slide oscillates glass under a tissue sample while a custom biaxial load cell [normal direction: 2.5 kg max load, resolution = 1 g; shear direction: 250 g max load, resolution = 10 mg] applies a normal strain and simultaneously measures the resulting normal and frictional shear loads on the sample. The tissue samples are submerged in a lubricant bath of PBS throughout the duration of testing. Custom Matlab code [The Mathworks, Natick MA] is utilized to calculate the equilibrium frictional coefficient μ_{eq} , which is the ratio of the normal load to the shear load when the engineered sample has fully relaxed from the applied normal strain.

Prior to testing, a Stribeck curve[67] was created to determine appropriate entraining speeds and normal strains to produce boundary mode lubrication for engineered samples lubricated with PBS (data not shown). In this Stribeck analysis, μ_{eq} was measured over a range of entraining speeds from 0.25 mm/sec to 5 mm/sec and normal strains from 10% to 50%. The region of the speed-strain space that yielded constant μ_{eq} was considered boundary lubrication. As such, for these boundary lubrication studies, the instrument linearly oscillated each sample at 0.32 mm/sec against glass with an imposed normal strain of 30% for 40 minutes to allow full relaxation of the sample. The application of 30% normal strain results in an approximate normal stress of 3, 8, and 10 kPa for MSC, CON, and MEN respectively. PBS was utilized as a lubricant for all friction tests.

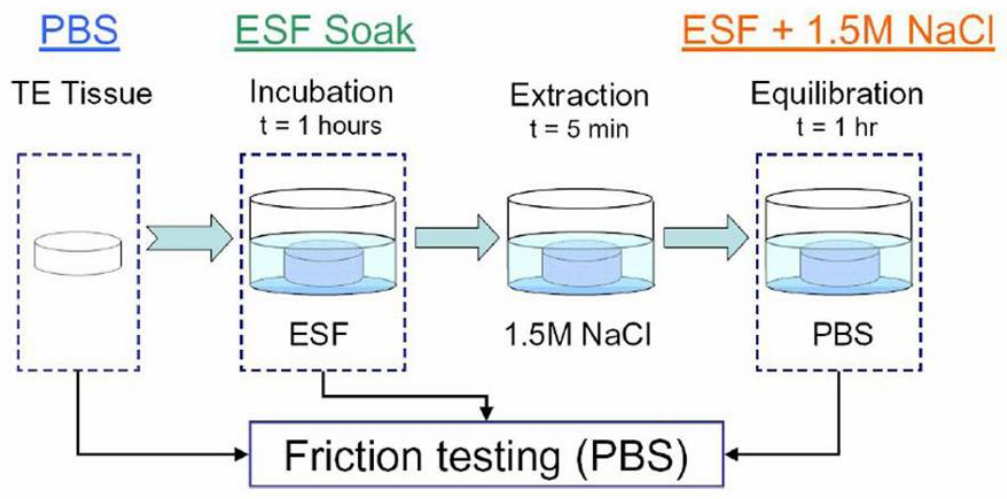

Figure 4.1: Schematic of steps used to test frictional properties of engineered tissue. Cultured tissues at each time point were tested in PBS (PBS). Following testing, the tissue was incubated for 1 hr in ESF, rinsed, and tested for a second time in PBS (ESF Soak). The tissue was then extracted with 1.5M NaCl for 5 minutes and then equilibrated in PBS. Following an hour equilibration, the tissue was tested for a third time (ESF + 1.5M NaCl).

A friction testing protocol (Figure 4.1) was developed to determine the frictional properties of the engineered cartilaginous tissues with endogenous or exogenous lubricin localization. An initial friction test was run (PBS) to determine μ_{eq} for the thawed samples (n=5 samples/time point/cell type, n=5 acellular controls). After testing, each sample was then incubated in ESF at 20°C for 1 hour and rinsed with PBS, to remove any excess unbound synovial fluid constituents, then friction tested in PBS (ESF Soak). Following the second friction test, the samples were incubated in 1.5M NaCl [Sigma, St. Louis MO] in PBS at 4°C for 5 min and then equilibrated in PBS at 20°C for 1 hour. Exposure to 1.5M NaCl has been shown to extract lubricin from the surface of cartilage with minimal proteoglycan loss[89]. Friction coefficients were then measured for a third time (ESF + 1.5M Extract).

Statistical Analysis

All data are presented as mean +/- standard deviation. The effect of treatment on normalized GAG and hydroxyproline content, H_A, and k was determined using a one factor analysis of variance (ANOVA) with a Tukey's HSD post hoc test to determine the effect of culture duration. A one way repeated measures ANOVA was performed on lubricin ELISA data to determine the effect of culture duration on lubricin concentration in the conditioned media. A two factor linear mixed mode ANOVA model was used to determine the effects of culture duration and the repeated measure of lubrication treatment on μ_{eq}. All statistical analysis was carried out using SPSS [SPSS Inc, Chicago IL] with calculated p values being considered significant for $p<0.05$.

4.4 RESULTS

Characterization of engineered tissues

Biochemical analysis of all engineered tissues showed an increase in GAG (Figure 4.2a) and hydroxyproline (Figure 4.2b) content, corresponding to localization of ECM molecules within the constructs over culture time. GAG content (Figure 4.2a) was similar in CON (5.76 +/- 0.40 μg GAG/mg tissue ww) and MEN (5.01 +/- 0.29 μg GAG/mg tissue ww) seeded alginate constructs; however over six weeks in culture, MSC seeded constructs only reached approximately 25 to 30% of GAG accumulation (1.60 +/- 0.16 μg GAG/mg tissue ww) achieved by the other engineered tissue. MSC generated tissue increased in GAG content over 2 and 4 weeks ($p<0.03$) but had lower GAG content than CON and MEN ($p<0.001$) at all time points. Hydroxyproline content (Figure 4.2b), an indicator of collagen content, similarly increased in all constructs at all points in culture (CON = $p<0.001$, MEN = $p<0.001$, MSC = $p<0.03$). Throughout culture CON consistently localized more hydroxyproline than MSC but less than MEN with MEN localizing 2.5 times more (3.34 +/- 0.17 μg hydroxyproline/mg ww) than CON (1.42 +/- 0.07 μg hydroxyproline/mg ww) and 6.5 times that of MSC constructs (0.55 +/- 0.11 μg hydroxyproline/mg tissue ww) at six weeks.

Confined compression testing revealed differences in equilibrium moduli and permeability between cell types over the time in culture (Figure 4.2c). H_A for CON (31 kPa) and MEN (40 kPa) seeded alginate disks similarly increased by three to four times over six weeks in culture (each, $p<0.001$) with MEN possessing a higher H_A than CON after 2 weeks. Additionally, MEN and CON disks had a higher H_A than both MSC and acellular control disks after 2 weeks. MSC seeded constructs showed no change in equilibrium modulus over six weeks in culture (11 kPa) or compared to

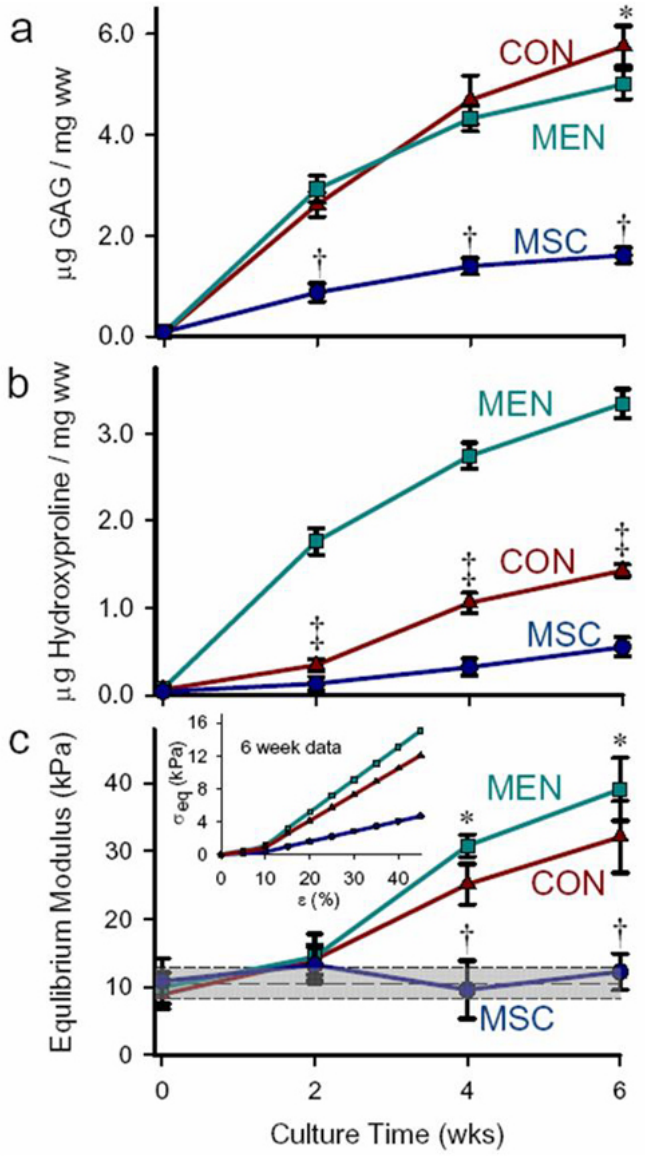

Figure 4.2: Characterization of biochemical and mechanical properties of the engineered cartilaginous tissues including: (**a**) GAG content normalized to tissue wet weight (* = $p<0.001$ vs. all other CON, § = $p<0.002$ vs. all other MEN, † = $p<0.017$ different than MSC 0 & 2), (**b**) hydroxyproline content normalized to tissue wet weight (‡ = $p<0.027$ vs. all other MSC, * = $p<0.001$ vs. all other CON, § = $p<0.001$ vs. all other MEN), and (**c**) equilibrium modulus († = $p<0.009$ vs. all other CON, * = $p<0.001$ vs all other MEN). Overlaid gray box represents mean +/- SD of acellular controls ($p<0.001$ for controls compared to CON and MEN after 2 weeks). All data are presented as mean +/- SD with n=5. Inset: Representative equilibrium stress (σ_{eq}) – strain (ε) curves for 6 week samples.

acellular controls. Permeability decreased over culture (data not shown) from an initial value of $5.5x10^{-12}$ m^2 Pa^{-1} s^{-1} to $1.3x10^{-12}$ ($p<0.001$), $1.0x10^{-12}$ ($p<0.001$), and 3.8 $x10^{-12}$ m^2 Pa^{-1} s^{-1} ($p<0.05$) for CON, MEN, and MSC respectively.

Analysis of lubricin synthesis and localization

Analysis of culture medium (Figure 4.3) showed production and loss of lubricin to the media by all cell-alginate constructs over time. MSC constructs released approximately ten-fold more lubricin (25 mg) to media at 42 days compared to CON (2.7 mg) or MEN (0.9 mg) samples. The rate of release of lubricin from MSC seeded constructs was similar to CON and MEN seeded constructs over the first ten days, after which the rate of release from MSC-alginate constructs increased dramatically.

Lubricin IHC staining revealed no reactivity to lubricin for any cell-alginate construct at zero weeks, as illustrated by CON samples (Figure 4.4a – 3A4 column). Minimal immunoreactivity was observed at two weeks (data not shown) and six weeks (Figure 4.4b – 3A4 column), with some focal staining noted, particularly on the surface of meniscal samples (Figure 4.4b – 3A4 column, bottom). However, it may be noted that comparisons of lubricin release and localization between the constructs could, at least in part, reflect potential differences in antibody immunoreactivity between species. Incubation with BSF preceding IHC staining showed no immunoreactivity to lubricin at zero weeks for any tissue, CON samples shown (Figure 4.4a – BSF+3A4 column). However, significant immunoreactivity was noticed in four week (data not shown) and six week samples (Figure 4.4b – BSF+3A4 column), particularly at the surface of CON seeded samples (Figure 4.4b – BSF+3A4

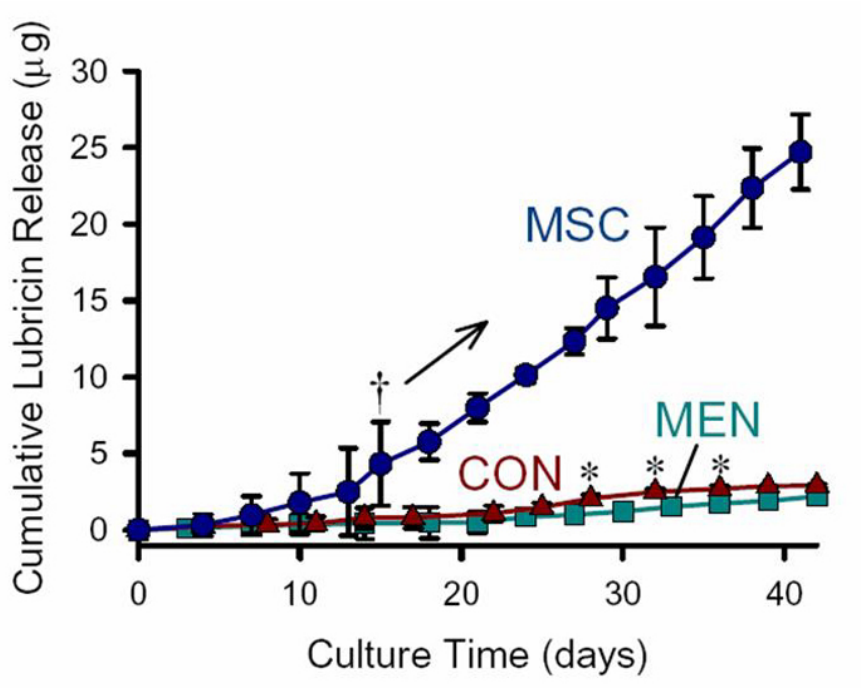

Figure 4.3: Cumulative release of lubricin to the media over six weeks in culture. Data is presented as mean +/- SD with n=6.

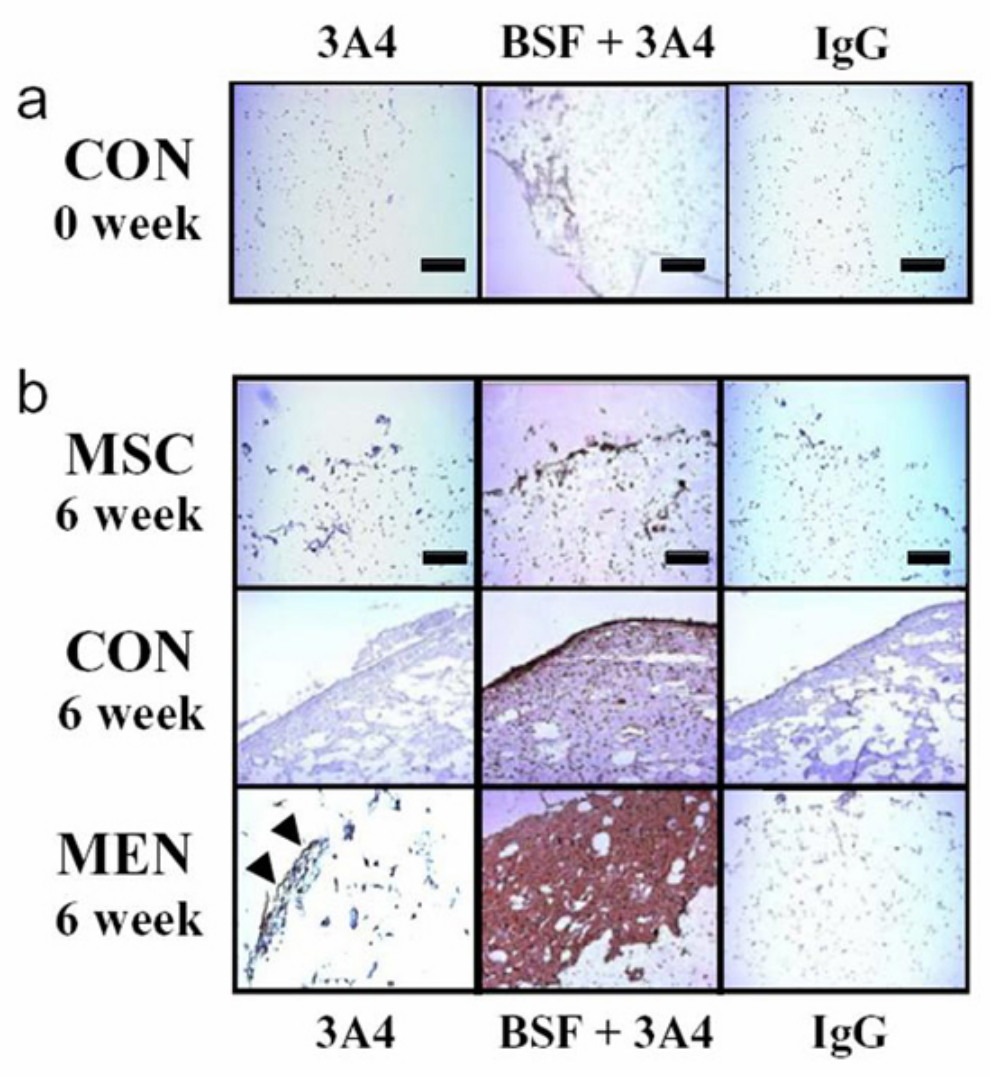

Figure 4.4: IHC staining of zero week alginate-CON constructs (**a**) and six week alginate-cell tissues (**b**) investigating localization of lubricin from endogenous production of lubricin over culture [3-A-4] and exogenous incubation with BSF [BSF + 3-A-4]. Lubricin noted at surface of MEN constructs after 6 weeks in culture. (Scale bar = 100 μm).

column, middle) and throughout the bulk of MEN seeded samples (Figure 4.4b – BSF+3A4 column, bottom).

Friction testing

Friction testing revealed differences in μ_{eq} with cell type, culture duration, and synovial fluid exposure (Figure 4.5). For all cell types over all culture times μ_{eq} was similar (~0.45) for engineered constructs and acellular controls (0.458 +/- 0.021). Incubation of the engineered tissues in ESF had no effect on zero week samples, however CON and MEN samples produced lower μ_{eq} over culture duration (μ_{eqCON} = 0.231 +/- 0.022, μ_{eqMEN} = 0.218 +/- 0.027) compared to MSC (μ_{eqMSC} = 0.372 +/- 0.009). The friction coefficient of ESF-soaked MSC constructs decreased by 10% at four weeks ($p<0.03$) and 20% at six weeks ($p<0.001$) (Figure4.5a) while μ_{eq} of ESF-soaked CON (Figure 4.5b) and MEN (Figure 4.5c) samples decreased by 20% at 2 weeks and 50% at four and six weeks ($p<0.001$). Following the extraction protocol with 1.5M NaCl in PBS, μ_{eq} for all engineered tissues at 2, 4, and 6 weeks increased and returned to values similar to those obtained prior to ESF incubation. No statistical difference is noted between ESF + 1.5M Extract samples and either PBS or acellular controls for all cell types and culture times tested.

4.5 DISCUSSION

This study demonstrates that articular chondrocytes, meniscal fibrochondrocytes, and chondrogenically differentiated MSCs all produce lubricin in 3D alginate culture. The retention of lubricin in these constructs was limited, with only meniscal constructs showing some focal surface localization of endogenously

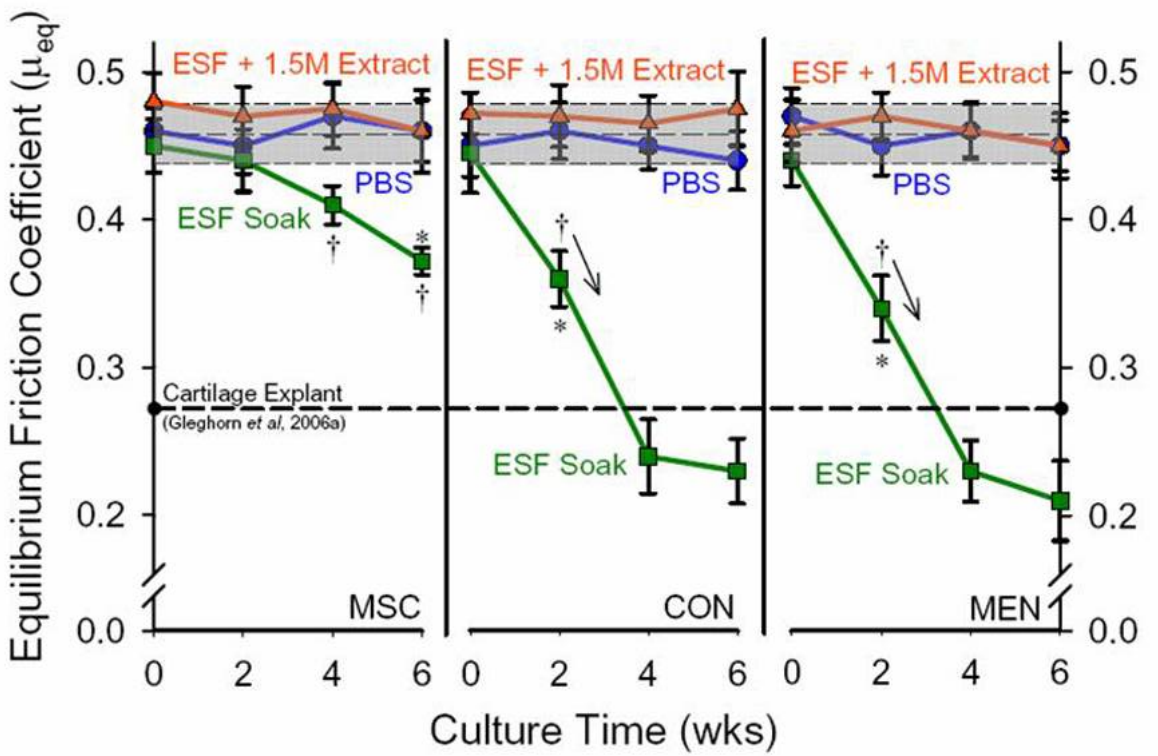

Figure 4.5: Temporal profile of equilibrium friction coefficient of engineered tissues tested in PBS (PBS), following incubation in ESF (ESF Soak), and following lubricin extraction (ESF + 1.5M NaCl) († = $p<0.001$ for ESF Soak compared to PBS and ESF + 1.5M NaCl, * = $p<0.05$ for ESF Soak compared to ESF soak at all other time points for a given cell type). Overlaid gray box represents mean +/- SD of acellular controls ($p<0.001$ for controls compared to ESF Soak at 2, 4 and 6 weeks for CON and MEN and 4 and 6 weeks for MSC). Reference value (mean) of a cartilage explant tested in the same system (μ_{eq}=0.278 +/- 0.018) is indicated overlaid on the plot (- - -). Data is presented as mean +/- SD with n=5.

produced material. The engineered tissues varied in ability to localize lubricin when exposed to BSF, with meniscal constructs retaining material throughout the bulk of the sample, articular cartilage constructs localizing material at the surface, and MSC constructs showing little localization.

The limited localization of endogenous lubricin in engineered constructs was not sufficient to lower friction coefficient. However, the ability to localize lubricin upon BSF exposure appeared to correlate with changes in friction coefficient, with CON and MEN constructs being significantly more lubricated than MSC constructs. Together, these data suggest that the production of matrix that is capable of localizing lubricin may be just as or more important than lubricin production in the lubrication of engineered tissues.

Differences in lubricin release patterns were present based upon cell type, with higher amounts released from MSC cultures, particularly after 12 days. This may represent a distinct phase of chondrogenic differentiation of MSCs. In native cartilage and meniscus, it is well established that only cells from the surface zone express lubricin[98,164,166]. The relatively low release from CON and MEN alginate disks may be due to a limited population of lubricin expressing cells in the seeded constructs, as cells from all areas of the tissue were utilized rather than harvesting cells from superficial tissue areas. The high lubricin release from MSC constructs may be due to a larger population of MSCs differentiating into a lubricin expressing phenotype. Alternatively, media constituents may also play a role in increased lubricin release in MSC seeded constructs. TGF-β was used to promote chondrogenic differentiation of MSCs in this study. However, TGF-β has also been implicated in upregulation of lubricin biosynthesis in cartilage explant cultures[48], and as such, likely contributed to the high level of lubricin release by MSCs seen here.

This study utilized three common cell sources for engineering cartilaginous tissue resulting in engineered tissue with similar ECM composition and mechanical properties to previous studies[23,124] of these engineered tissues. Over all culture times, MSC-, CON- and MEN-seeded alginate constructs had the same frictional properties as unseeded alginate disks. The inherent boundary lubricated equilibrium friction coefficient of the engineered tissues ($\mu_{eq} \sim 0.45$) is greater than that reported in preliminary studies of patellofemoral groove cartilage explants tested under the same conditions with μ_{eq}=0.278 +/- 0.018 and the same cartilage following lubricin extraction with 1.5M NaCl having a μ_{eq}=0.347 +/- 0.022[57]. While no change in lubrication was evident, MSCs, CON, and MEN in alginate all produced lubricin in static culture as evidenced by lubricin release to media. Immunohistochemical analysis revealed low levels of lubricin at the surface of engineered tissue for six week cultured tissues even though incubation with BSF demonstrates the ability of lubricin to significantly bind to the tissue. Taken together these data suggest insufficient localization of lubricin at the surface of these engineered tissues while in culture.

IHC revealed the absence of lubricin localized on zero week alginate constructs after incubation with BSF. These data suggests that localization of lubricin on the surfaces of joint tissues such as articular cartilage[98,164] and meniscus[166] may not be a simple adsorption mechanism. Together, these data suggest that controlling localization of lubricin in engineered tissues may be critical for proper lubricating function.

Constructs from all cell types were lubricated by ESF at later culture times with CON and MEN disks able to achieve a μ_{eq} similar to that of a cartilage explant after 4 weeks. Further lubrication was reversed with 1.5M NaCl, a protocol known to

extract lubricin from the surface of articular cartilage[89]. For intact articular cartilage this extraction removes minimal amounts of proteoglycan; however the possibility of proteoglycan loss due to extraction of tissue engineered constructs cannot be completely discounted. This reversible lubrication in tandem with IHC data showing an increase in lubricin localization over culture time with incubation in ESF suggests production of ECM components capable of localizing lubricin. The ability to localize lubricin seen by a decrease in μ_{eq} is cell type dependant with CON and MEN similar but greater than MSC generated tissues. The localization of lubricin at the tissue surface plays a role in cartilage tissue lubrication.

The mechanism of boundary lubrication of cartilaginous tissues has not been fully elucidated. This study demonstrates that molecular modification of the tissue surface by localization and subsequent removal of lubricin altered the frictional properties of the tissue. Further investigations are needed to identify which ECM molecules localize lubricin at the tissue surface. Understanding the mechanical implications of the surface localization of lubricin is an important consideration for creating functional tissue engineered cartilage with appropriate low friction, low wear properties.

CHAPTER 5

FRICTIONAL PROPERTIES OF ARTICULAR CARTILAGE MODULATED BY TGF-β, IL-1β, AND ONCOSTATIN M*

5.1 INTRODUCTION

Articular cartilage is a heterogeneous tissue responsible for endowing diarthrodial joints with a low friction bearing. The remarkable frictional properties of the tissue are achieved, at least in part, by lubricin, a mucin-like glycoprotein localized in synovial fluid[173] and at the surface of joint tissues[164-166]. Lubricin is synthesized by several tissues including cartilage, meniscus, and tendon[153,164-166], and is expressed by the PRG4 gene[75]. There are numerous post-translational products of the PRG4 gene[48,75,78,84,105,112,119,129] including megakaryocyte stimulating factor (MSF) precursor and superficial zone protein (SZP), which have significant homology to lubricin[48,84] and as such, we will refer to them collectively as lubricin.

Lubricin has been identified to play several important roles in the maintenance of joint metabolism including boundary lubrication of cartilage, chondroprotection, and inhibition of synovial cell overgrowth[85,155,162]. Lubricin has been observed to boundary lubricate a range of bearings including latex-glass, tissue-glass, and cartilage-cartilage[55,76,161,162,175] although the mechanism is not fully understood. From a biomechanical perspective, the importance of lubricin is evident; however, lubricin's role in the prevention of synovial overgrowth and cell adhesion and infiltration[155] is equally important. This role is made evident by CACP syndrome patients who cannot synthesize lubricin[119]. Overgrowth of the synovium and pannus formation is abundant

* Gleghorn, J.P., Jones, A.R.C., Flannery, C.R., and Bonassar, L.J. "Frictional Properties of Articular Cartilage Modulated by TGF-β, IL-1β, and Oncostatin M," in preparation.

in these patients, and their synovial fluid aspirates do not lubricate a latex-glass bearing as effectively as non-pathologic human synovial fluid[77]. Additionally in rheumatoid arthritis (RA), where pannus on the cartilage surface is profuse, loss of boundary lubricating ability is also noted, due to the proteolytic degradation of lubricin by cathepsin B, a cysteine protease abundant in RA synovial fluid[43]. Therefore, lubricin is a key synovial molecule and, as such, alterations in its metabolism may significantly impact proper joint homeostasis.

Recent studies have documented modulation of lubricin expression, synthesis, and surface localization by cytokines found to be up regulated in joint injury and disease[88,161]. Bovine cartilage explants exposed in vitro to transforming growth factor β1 (TGF-β1) demonstrate an up regulation of lubricin synthesis and surface localization[32,48,88,94,142,161], while insulin-like growth factor 1 (IGF-1), another potent anabolic signaling molecule in cartilage, reveals no effect on lubricin metabolism and localization[161]. Conversely, bovine explants treated with catabolic soluble factors such as interleukin 1α (IL-1α), interleukin 1β (IL-1β), and tumor necrosis factor α (TNF-α) a down-regulate lubricin synthesis and tissue surface localization[32,48,88,94,142,161]. While modulation of lubricin metabolism is achieved by these cytokines, concomitant alterations in cartilage composition occur. IL-1β is a potent mediator of proteoglycan loss and long term IL-1β exposure is associated with the disruption of collagen structure[188]. Conversely TGF-β upregulates proteoglycan synthesis[131,132]. The role of proteoglycan content on the frictional properties of articular cartilage remains uncertain, with studies reporting both a dependence and independence of the equilibrium friction coefficient on proteoglycan content[12,147].

Since the turnover of lubricin and proteoglycan are co-regulated in the cases of IL-1β and TGF-β treatments, it is difficult to evaluate the molecular origins of changes in frictional behavior induced by these agents. However, this conflict may be

resolved with the recent finding that oncostatin M (OSM), a member of the chondrodisruptive IL-6 cytokine family, increases lubricin synthesis and tissue surface localization of lubricin in bovine explant cultures[89]. OSM is associated with joint inflammation[143] and stimulates resorption, inhibits synthesis, and demonstrates aggressive release of aggrecan from cartilage[22,73] via depolymerization of hyaluronic acid[40]. The apparent stimulation of endogenous lubricin and concomitant extraction of cartilage proteoglycans induced by OSM may provide a platform to probe the specific contributions of lubricin and proteoglycan metabolism on the frictional properties of articular cartilage. Therefore, the objectives of this study were to (1) evaluate the functional effects of TGF-β1, IL-1β, and OSM treatment over 24 and 48 hours on the friction properties of cartilage explants and (2) determine the ability of cartilage exposed to these molecules to be lubricated by synovial fluid following extraction of endogenous lubricin.

5.2 METHODS

Cartilage Explant Harvest and Culture

Full thickness bovine patellofemoral groove cartilage disks (n = 96) were harvested from ten stifle joints of 1-10 day old calves using a biopsy punch and a scalpel[55] (Figure 5.1). The resulting 6mm diameter by 2mm thick explants were cultured in spinner flasks for 96 hours, in serum free culture medium (DMEM/F12 [Invitrogen, Carlsbad, CA] supplemented with 100 U/ml penicillin [Mediatech, Herndon, VA], 100 μg/ml streptomycin [Mediatech], and 50 μg/ml ascorbic acid (Asc) [Sigma, St. Louis, MO]). The entire media volume was changed once at 48 hours. Explants were then transferred to 24 well plates and cultured in 1 ml of serum

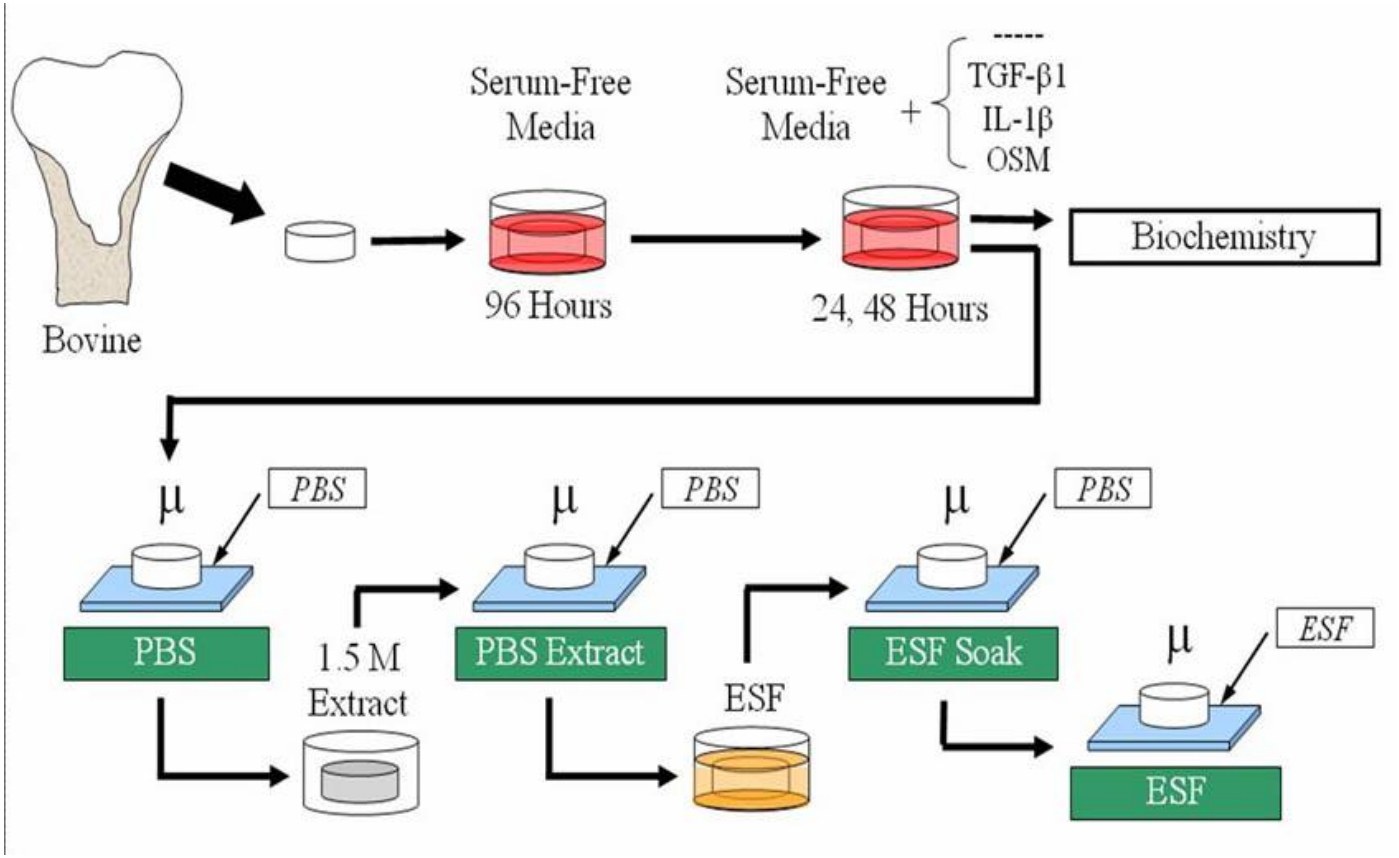

Figure 5.1: Cartilage explants were harvested from bovine stifle joints, tissue cultured, and incubated with a cytokine for 24 or 48 hours. Following cytokine exposure, explants were removed from culture and either biochemical analyzed for proteoglycan content or friction tested. Samples were friction tested serially under four different conditions. Samples were tested with PBS as a lubricant (PBS), followed by lubricin extraction with 1.5M NaCl and friction tested again using PBS (PBS Extract). Explants were then soaked in ESF for 1 hour, friction tested with PBS as a lubricant (ESF Soak), and subsequently friction tested using ESF as a lubricant.

free culture medium supplemented with either no cytokine for controls or 10 ng/ml of either TGF-β1 [Peprotech, Rocky Hill, NJ], IL-1β [R&D Systems, Minneapolis, MN], or Oncostatin M (OSM) [R&D Systems]. Following either 24 or 48 hours of culture, samples (n = 12/supplement/time) were frozen and stored at -20˚C prior to friction testing and biochemical analysis[55]. At the time of testing samples were thawed and equilibrated for 1 hour in phosphate buffered saline (PBS) [Invitrogen] supplemented with a protease inhibitor cocktail [complete protease inhibitor cocktail, Roche Applied Science, Indianapolis, IN] in a water bath at 38˚C.

Friction Testing

A custom friction testing apparatus[55] linearly oscillated cartilage explants against glass (n = 6-7/supplement/time) to determine the initial (μ_0) and equilibrium (μ_{eq}) friction coefficients. The operating conditions for the friction test (sliding speed (v) and normal axial strain (ε_N)) were chosen to produce boundary mode lubrication using the lubricants described below[54]. Boundary mode is the lubrication regime where friction between two surfaces is determined by the properties of the surfaces and of the lubricant other than bulk viscosity[177]. An operational manifestation of boundary mode lubrication is invariance in μ_{eq} over a range of v, ε_N, or lubricant dynamic viscosity (η)[55,177]. Due to alterations in the structure and composition of the cartilage ECM and concomitant changes in mechanical properties from cytokine exposure, the cartilage explants were friction tested over a range of applied ε_N. This range in ε_N acted as a control within the experiment to confirm independence of μ_{eq} on ε_N and thereby validate the test was conducted in boundary mode for all samples.

Each friction test consisted of oscillating cartilage against glass at v = 0.33 mm/s and three different ε_N (20, 30, and 40%) to measure the time dependent normal

($L_N(t)$) and shear ($L_S(t)$) loads. The ε_N was initially applied through a step displacement of 20%, and subsequently increased in 10% increments following a relaxation period of three times the previously determined stress relaxation time constant (τ_N). The instantaneous friction coefficient ($\mu(t) = L_S(t)/L_N(t)$) was calculated producing a monotonically increasing temporal friction profile, and a poroelastic model was fit to the $\mu(t)$ data to determine μ_0, μ_{eq}, and τ_μ (Figure 5.2). Likewise, a poroelastic model was fit the stress relaxation data, calculated from the sample geometry and the $L_N(t)$ data, to determine an equilibrium stress and time constant of the relaxation in order to calculate a Young's modulus (E_Y)[55,95].

Lubricants used in this study included PBS and equine synovial fluid (ESF). Utilizing guidelines approved by the Cornell University Institutional Animal Care and Use Committee, ESF was sterilely aspirated from the stifle joints of animals [College of Veterinary Medicine, Cornell University, Ithaca, NY] being euthanized for pathologies unrelated to the selected joint. The aspirates were pooled (7 joints from 9 animals aged 7 months to 9 years), aliquoted, and stored at -20ºC as described previously[55]. On the day of friction testing, ESF aliquots were thawed at 38 ºC in a water bath, vortexed, and used as a lubricant.

Biochemical Analysis

Samples (n = 4-5/supplement/time) were digested in a 0.125 mg/ml papain [Sigma, St. Louis, MO] solution at 60˚C for 14 hours. The sulfated GAG content of the digested explants was assayed with the dimethylmethylene blue (DMMB) colorimetric assay[44] with chondroitin-6-sulfate from shark cartilage [Sigma] as a standard. GAG content of the samples was used as a measure to determine changes in proteoglycan content as a result of cytokine exposure.

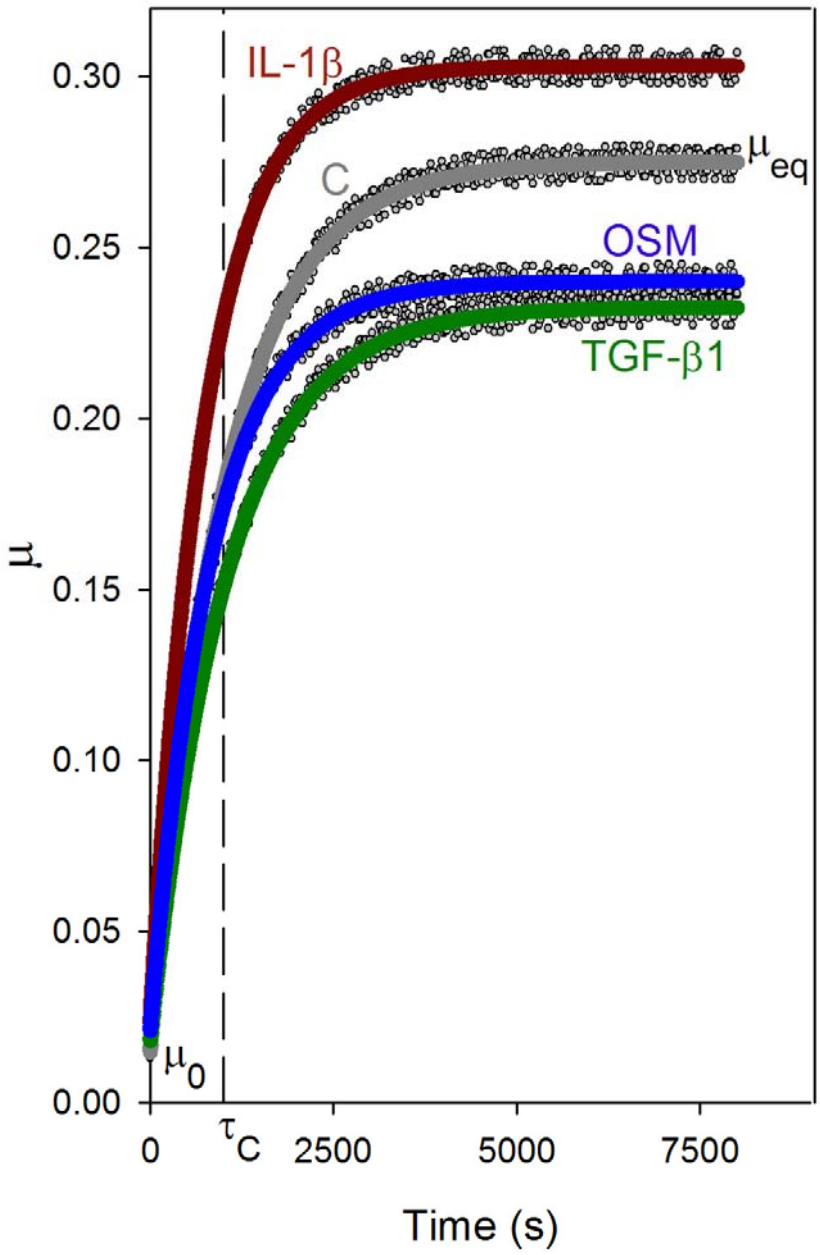

Figure 5.2: Representative μ(t) data (ε_N = 30% and v = 0.33 mm/s) for control, TGF-β, IL-1β, and OSM exposed cartilage explants (data points) with resulting poroelastic model fit overlaid (line). From the poroelastic model, the initial (μ_0) and equilibrium (μ_{eq}) friction coefficients as well as the time constant of the response (τ) were determined.

Experimental Design

A friction testing protocol was developed to determine the functional implications of cytokine mediated lubricin synthesis and localization (Figure 5.1). Treated explants were tested using PBS as a lubricant to determine the effects of endogenously localized lubricin on μ_0, μ_{eq}, and τ_μ (labeled "PBS"). Subsequently, samples underwent an established lubricin extraction protocol[89] with 1.5M NaCl in PBS at 4˚C for 1 hour followed by another friction test with PBS as a lubricant (labeled "PBS extract"). Friction testing of samples under an extracted condition permitted the determination of relative contributions of endogenously localized lubricin on the frictional properties of the tissue. In addition, extracted conditions established a baseline relative to controls to determine alterations in μ due to changes in tissue structure or composition, as a result of cytokine exposure. Following the second friction test, samples were then soaked in ESF at 20˚C for 1 hour, rinsed with PBS to remove any unbound synovial fluid constituents, and subsequently friction tested with PBS as a lubricant (labeled "ESF Soak"). Lastly, PBS was removed from the lubricant bath and replaced with ESF and samples were friction tested a fourth time (labeled "ESF"). The last steps of the protocol enabled investigation of the ability for lubricin, found in the ESF, to lubricate the treated explants after localizing at the tissue surface (ESF Soak) or when surface localized and in the bulk lubricating solution (ESF).

Statistical Analysis

The effect of cytokine treatment and culture duration on E_Y, τ_μ, and normalized tissue GAG content was determined with a two factor analysis of variance (ANOVA) with Tukey's HSD post hoc test. A three factor linear mixed mode ANOVA model

was used to determine the effects of culture duration, cytokine/growth factor type and the repeated measure of lubricant treatment on μ_{eq} and μ_0. All data were presented as mean +/- standard deviation. Statistical analysis was carried out using SPSS [SPSS Inc, Chicago, IL] with calculated p values being considered significant for $p<0.05$.

5.3 RESULTS

Cartilage explants treated with TGF-β, IL-1β, and OSM exhibited a monotonically increasing $\mu(t)$ from an initial to equilibrium value (Figure 5.2) following 24 and 48 hours of culture. While the $\mu(t)$ response of treated samples was similar in profile to that of controls, the μ_0 and μ_{eq} values were different and dependent on which cytokine the tissue was exposed to. Additionally, the rate at which $\mu(t)$ achieved equilibrium, denoted by the time constant of the response (τ_μ), was significantly different at 48 hours, with explants exposed to IL-1β (750 +/- 48 s, $p<0.005$) and OSM (830 +/- 42 s, $p<0.05$) achieving equilibrium faster than those cultured with TGF-β (1033 +/- 36 s) or the controls (1002 +/- 30 s). A similar trend was noted for all samples at 24 hours, however no significant differences were observed.

Cartilage exposed to TGF-β for 24 and 48 hours retained a μ_0 similar to that of control tissue (0.019 +/- 0.005) (Figure 5.3). Tissue treated with IL-1β (0.031 +/- 0.007, $p<0.01$) and OSM (0.030 +/- 0.008, $p<0.01$) demonstrated a significant increase in μ_0 after 24 hours and increased further at 48 hours (IL-1β = 0.054 +/- 0.009, $p<0.001$; OSM = 0.050 +/- 0.007). Similar trends in μ_0 were noted following endogenous lubricin extraction, a soak in ESF, and testing in ESF. No significant differences were observed in μ_0 as a result of treatments to alter lubricin localization at the tissue surface or in the bulk lubricating solution.

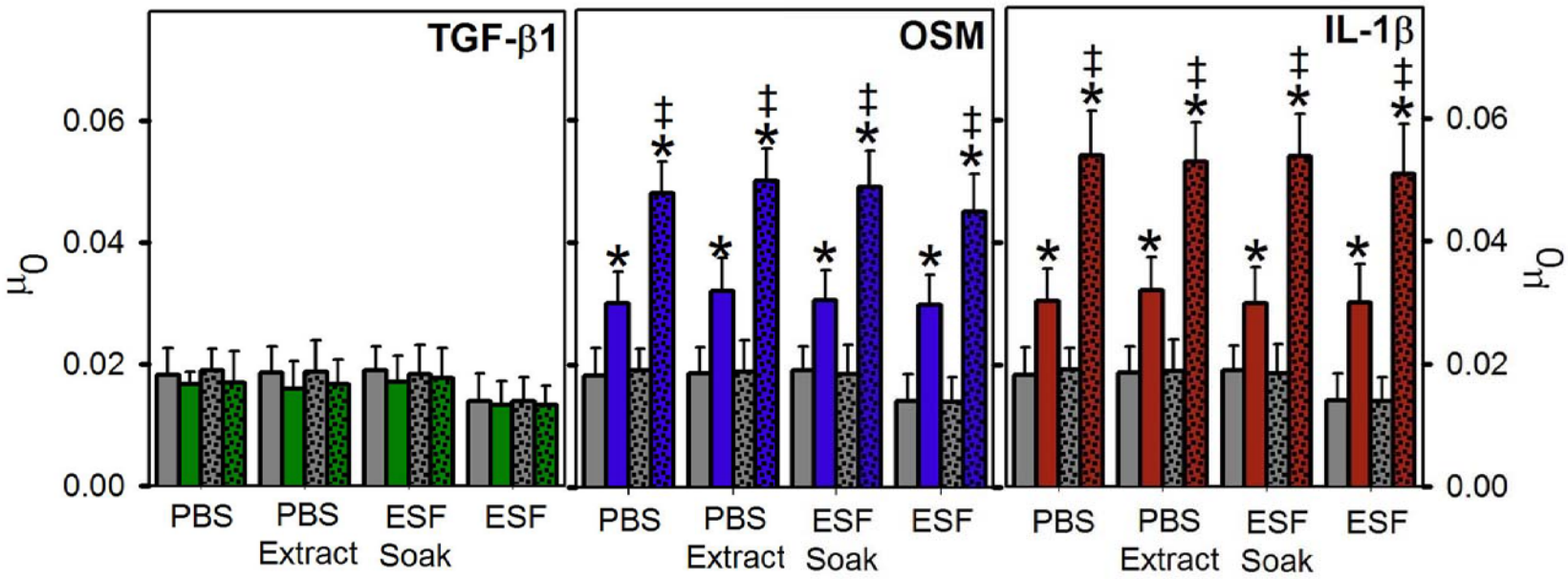

Figure 5.3: μ_0 for cartilage explants following 24 (open bars) and 48 hours (shaded bars) exposure to TGF-β, IL-1β, and OSM compared to controls (gray bars) at ε_N = 30% and v = 0.33 mm/s. Data represented as mean +/- SD with n = 6-7/supplement/time (* = $p<0.05$ compared to control, ‡ = $p<0.05$ compared to 24 hours).

In contrast, μ_{eq} of cartilage exposed to TGF-β, IL-1β, and OSM was significantly modified with alterations in lubricin localization (Figure 5.4). Treatment with cytokines for both 24 and 48 hours of culture potentiated μ_{eq} compared to controls. In TGF-β and OSM treated samples a μ_{eq} decreased after 24 hours (TGF-β = 0.232 +/- 0.013, $p<0.01$; OSM = 0.225 +/- 0.010, $p<0.01$) with a further reduction at 48 hours (TGF-β = 0.215 +/- 0.017, $p<0.005$; OSM = 0.210 +/- 0.015, $p<0.005$). Conversely, the opposite effect was noted in samples exposed to IL-1β, with an increase in μ_{eq} at 24 hours (0.303 +/- 0.021, $p<0.01$) followed by a further increase at 48 hours (0.357 +/- 0.028, $p<0.001$). Extraction of endogenous lubricin from TGF-β and OSM treated explants at both 24 and 48 hours achieved μ_{eq} similar to extracted controls (0.325 +/- 0.011), thereby eradicating any modulation of μ_{eq} from endogenous lubricin. For IL-1β treated samples, the lubricin extraction procedure did not significantly alter the μ_{eq} values achieved on initial friction testing after 24 hours, but following 48 hours μ_{eq} was significantly greater than ($p<0.01$) 24 hour treated samples and 48 hour extracted controls. A soak in ESF enhanced lubrication for all cytokines tested over 24 and 48 hours. Lubrication was further increased with the use of ESF as a lubricant, with samples achieving μ_{eq} equal to or less than (TGF-β1 & OSM) that of controls (0.092 +/- 0.009). IL-1β incubated explants similarly demonstrated a decrease in μ_{eq} using ESF as a lubricant but samples at 24 (0.136 +/- 0.039, $p<0.05$) and 48 hours (0.196 +/- 0.044, $p<0.001$) had μ_{eq} values 1.5 to 2 fold higher than controls.

Young's modulus and GAG content were determined for all samples at both culture durations. GAG content remained constant over 48 hours (Figure 5.5A) for explants treated with TGF-β1, however significant loss in GAG content was noted for samples cultured with OSM and IL-1β. Tissue GAG content dropped to 92% and 88% of controls after 24 hours for OSM ($p<0.05$) and IL-1β ($p<0.05$) exposed

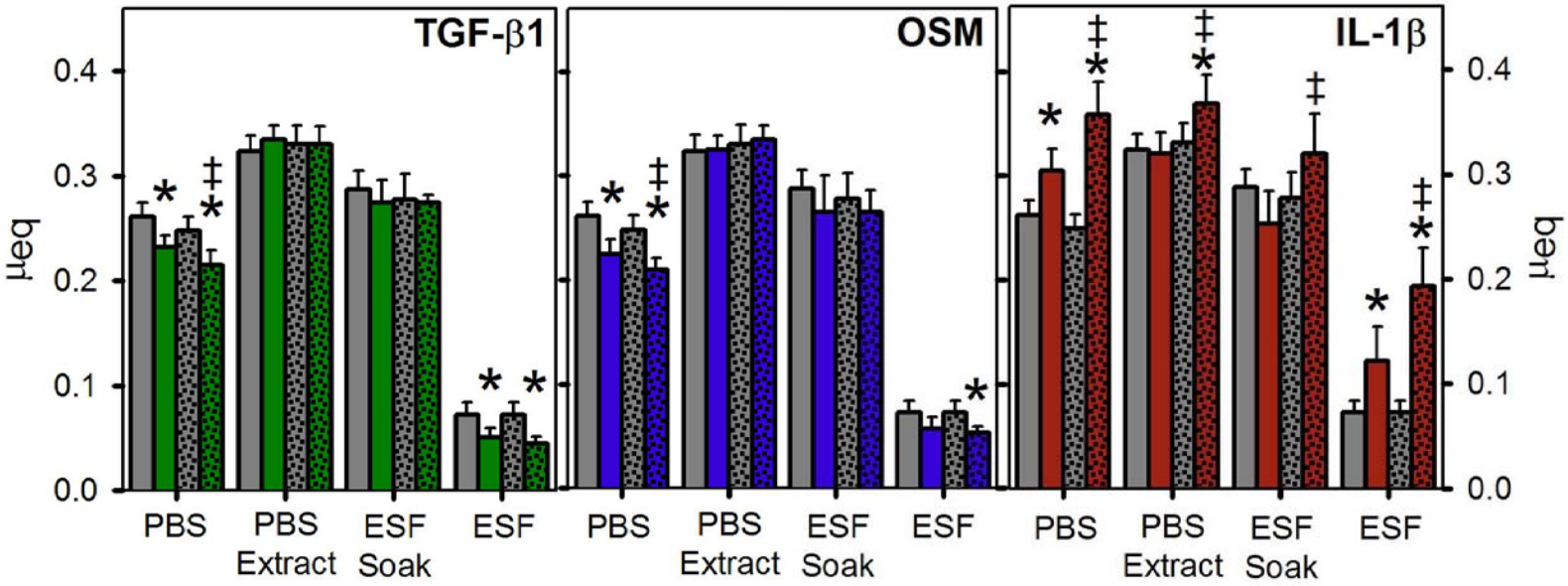

Figure 5.4: μ_{eq} for cartilage explants following 24 (open bars) and 48 hours (shaded bars) exposure to TGF-β, IL-1β, and OSM compared to controls (gray bars) at ε_N = 30% and v = 0.33 mm/s. Data represented as mean +/- SD with n = 6-7/supplement/time (* = $p<0.05$ compared to control, ‡ = $p<0.05$ compared to 24 hours).

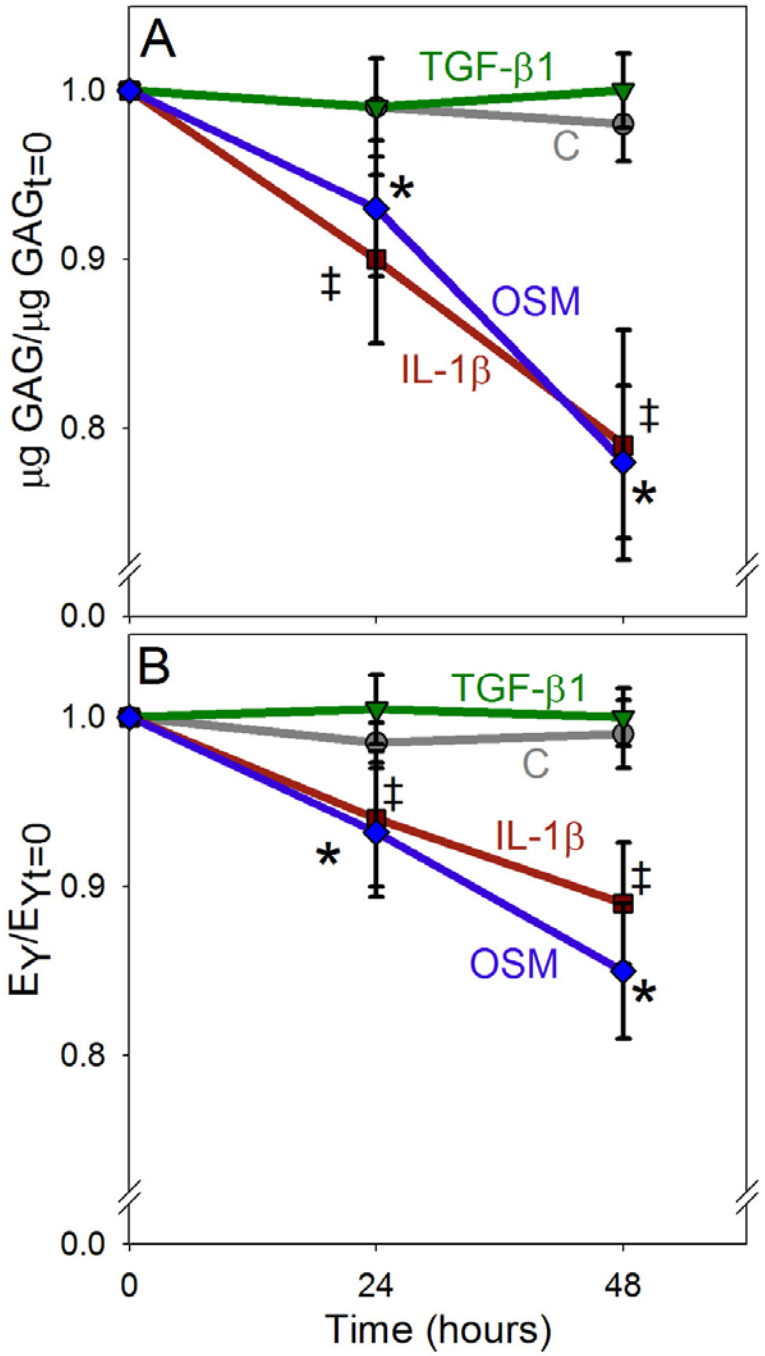

Figure 5.5: Normalized GAG concentration (A) and Young's modulus (B) for explants treated with TGF-β, IL-1β, and OSM over 48 hours of culture. Data represented as mean +/- SD with n = 4-5/supplement/time (GAG) and n = 6-7/supplement/time (E_Y) (* = $p<0.05$ compared to all other OSM, ‡ = $p<0.05$ compared to all other IL-1β, § = $p<0.05$ compared to C and TGF-β).

explants respectively, with a continued loss noted after 48 hours (~80%) for both cytokines ($p<0.001$). A corresponding trend was seen for E_Y (Figure 5.5B), with a significant decrease in modulus noted for IL-1β ($E_Y = 0.418$ +/- 0.021 MPa, $p<0.001$) and OSM ($E_Y = 0.396$ +/- 0.024 MPa, $p<0.001$) treated explants and no noted changes with TGF-β1 ($E_Y = 0.474$ +/- 0.009 MPa) or controls ($E_Y = 0.452$ +/- 0.011 MPa) over 48 hours of culture. Trends seen in μ_0, μ_{eq}, and temporal properties were consistent over all applied strains tested, which validated that the tests were performed in boundary lubrication mode.

5.4 DISCUSSION

The present study demonstrates that cartilage boundary mode friction coefficient, μ_{eq}, was mediated by short exposure to cytokines commonly found in arthritis and injury. These results demonstrate modulation of μ_{eq} consistent with endogenous lubricin surface localization by TGF-β, IL-1β, and OSM[89], and indicate μ_{eq} was independent of cartilage proteoglycan content. Additionally, localization of lubricin had minimal effect on μ_0, with treatments that caused either loss (IL-1β) or accumulation (OSM) of lubricin both increasing μ_0. Together, the current data point to distinct biochemical origins of boundary and biphasic lubrication mechanisms in cartilage, with boundary lubrication regulated by accumulation of lubricants on the tissue surface and biphasic lubrication controlled by factors that affect water movement through the bulk of the tissue.

This study assessed the friction properties of cartilage to determine functional implications of differentially regulated lubricin metabolism and localization by TGF-β, IL-1β, and OSM. All explants treated with cytokines started at a minimum μ and monotonically increased to an equilibrium μ (Figure 5.2) similar to controls and consistent with biphasic lubrication[49,103]. Boundary mode lubrication was achieved

upon equilibrium, as evidenced by invariance in μ_{eq} over a range (20-40%) of applied normal strains[54,177]. In boundary mode lubrication, bovine explants exposed to TGF-β and OSM produced lower μ_{eq} and IL-1β treated produced higher μ_{eq} values than controls, which is consistent with an increase (TGF-β & OSM) and decrease (IL-1β) in the amount of surface bound lubricin as analyzed by Western blotting[89]. These results demonstrate the functional ability of differentially regulated endogenous lubricin by TGF-β, IL-1β and OSM localized at the tissue surface to lubricate cartilage.

The boundary lubricating effect of surface bound lubricin appears to be independent of compositional ECM changes resulting from short time exposure to TGF-β, IL-1β and OSM. Significant alterations to the proteoglycan content and compressive properties were observed over 48 hours of treatment with IL-1β and OSM (Figure 5.5A), but lubrication of OSM treated explants occurred, as evidenced by significantly lower μ_{eq} than controls. Furthermore, extraction of endogenous lubricin with 1.5M NaCl produced μ_{eq} values similar to extracted controls, demonstrating that alterations to proteoglycan content do not affect boundary mode μ_{eq} in this cartilage-glass system and supports the findings of Pickard et al[147]. One interesting result is a significantly increased μ_{eq} with IL-1β treated explants after 48 hours that does not change following lubricin extraction. As this increased μ_{eq} is not noted in OSM treated explants, these data suggest that potential compositional changes, independent of proteoglycan concentration, play a role in mediating μ_{eq}. Further studies should be conducted to examine the role of surface structure and properties (e.g. surface roughness, collagen loss and/or disruption, etc.) induced by these cytokines on friction and lubrication of cartilage.

Consistent with biphasic lubrication, alterations to proteoglycan content from IL-1β and OSM significantly increased μ_0 with time in culture. Removal of

proteoglycans increases the tissue permeability and decreases the hydration of the tissue, resulting in a decreased ability to pressurize fluid within the tissue. The hydrostatic pressurization of cartilage endows the tissue with the very low μ_0 observed in this study and others[49,55,103]. Alterations in μ_0 due to lubricin localization at the tissue surface were not observed, and in fact, were not expected. Initial compressive loading of cartilage while sliding results in a mixed lubrication mode and lubricin, a boundary lubricant, acts via biochemical modification of the tissue surface, which plays a minimal role in mixed mode lubrication[54,177].

Another major finding from this study was the ability of ESF, at the surface (ESF Soak) and as a lubricant (ESF), to recover and enhance boundary lubrication in explants exposed to TGF-β, IL-1β, and OSM. Following lubricin extraction, the ESF soak localized lubricin at the catabolically exposed cartilage surface. Interestingly, ESF localization produced μ_{eq} values for the TGF-β and OSM treated cartilage similar to controls, but a reduction in μ_{eq} similar to values as low as those obtained with the endogenous lubricin was not achieved. This result may be due to differences in concentration and/or arrangement of the lubricin molecules at the tissue surface, or alterations to a lubricin binding molecule. In addition, after ESF soak, IL-1β treated explants produced lower a μ_{eq} at both 24 and 48 hours than those immediately following cytokine exposure, indicating that IL-1β exposure did not affect the lubricin localization mechanism. In fact IL-1β treatment may have enhanced binding of lubricin to cartilage by removing ECM molecules that block binding sites. When ESF was used as a lubricant, μ_{eq} for all treated explants and controls significantly decreased, with TGF-β and OSM treated tissue lubricated more effectively than controls. IL-1β exposed tissue likewise produced a marked decrease in μ_{eq}; however, the tissue was not able to achieve the low friction coefficients observed in controls. This inability of ESF to fully restore optimal lubrication suggests that IL-1β treatment

alters additional physical and chemical characteristics of cartilage that regulate frictional properties. As a result, the recovery of lubrication for catabolically exposed tissue by exogenous lubricin in ESF may be therapeutically important to combat high tissue friction found in injury and disease.

CHAPTER 6

CONCLUSIONS

Boundary lubrication of articular cartilage is critical to the protection and maintenance of the articular cartilage surface[128]. This dissertation presents investigations on the role of lubricin in mediating cartilage boundary mode friction coefficient. Chapter 2 details a friction testing apparatus to enable measurement of friction coefficients and maps cartilage lubrication modes. Chapter 3 investigates the role of exogenous rh-lubricin and its localization at the tissue surface and in the bulk fluid, while Chapters 4 and 5 examine the ability of endogenous lubricin, with synthesis altered by cell type or cytokine exposure, to lubricate tissue in the context of engineered cartilage and early disease. This chapter discusses some of the major findings as well as potential future studies.

The studies presented in Chapter 2 document the development and validation of a novel device to study the frictional behavior of articular cartilage. The most significant outcome of these studies was the creation of a Stribeck surface for cartilage, an extension of previous work[110], which enabled the visualization and determination of lubrication mode. An important experimental finding was the inability of cartilage to achieve full film lubrication following tissue depressurization. Cartilage lubrication occurred in either boundary or mixed modes, potentially due to the tissue's permeability allowing efflux of fluid from the cartilage glass interface into the tissue, which is consistent with other theoretical and experimental studies[4,72,110,127,169]. As a result of the dependence of operating parameters on μ_{eq}, it is apparent that fluid equilibrium within the tissue is necessary but not sufficient for true boundary mode lubrication to occur. These data, pointing to the need for control over

experimental variables, offer a potential suggestion as to why friction coefficients of cartilage reported in the literature range broadly (μ = 0.002-0.4) not only from system to system but within systems utilizing the same operating conditions[11,25,26,49,90,91,102,103,109,111,115,126,180,182]. The creation of the Stribeck surface analysis paradigm, coupled with the simultaneous control of ε_N, v, and interface congruity, allows for the control of lubrication mode enabling mechanistic and screening investigations of putative biolubricants for normal and diseased tissue.

The studies in Chapter 3 demonstrated that rh-lubricin lowers cartilage μ_{eq} in a dose-dependent manner, with an effective lubricating concentration (50 μg/ml) similar to the lubricin content of ESF. Further, soluble and bound rh-lubricin were shown to make distinct contributions to the lubrication process as indicated by alterations in μ_{eq} in different electrostatic environments. These new findings point to two distinct mechanisms by which rh-lubricin lubricates, one mechanism involving lubricin bound to the tissue surface and the other involving lubricin in solution. With doses at or below 50 μg/ml, localization of rh-lubricin at the surface of the tissue plays an integral role in the lubricating action of the molecule. At 150 μg/ml, high ionic strength inhibited the lubricating ability of rh-lubricin only partially suggesting that at a higher dose, rh-lubricin acts via a mechanism that does not require binding to the cartilage surface. This finding is consistent with previous studies of lubrication of synthetic bearings, in which the concentration of purified lubricin required to lower μ_{eq} were 200 to 260 μg/ml[76]. Taken together, these data indicate that chemisorption of lubricin at the tissue surface enables lubrication at lower effective concentrations than physisorption. This enhanced efficiency of chemisorped lubricin may be due to localization at the interface that is independent of fluid flow and pressure.

Articular chondrocytes, and for the first time, meniscal fibrochondrocytes and chondrogenically differentiated MSCs were shown in Chapter 4 to endogenously

produce lubricin in 3D alginate culture. Over all culture times, cell-seeded alginate constructs had the same frictional properties as unseeded alginate disks with immunohistochemical analysis revealing low levels of lubricin at the surface of engineered tissue. The limited localization of endogenous lubricin in engineered constructs was not sufficient to lower friction coefficient. However, the ability to localize lubricin upon BSF exposure appeared to correlate with changes in friction coefficient. These findings suggest 1) that controlling localization of lubricin in engineered tissues may be critical for proper lubricating function and 2) that the production of matrix that is capable of localizing lubricin may be just as or more important than lubricin production in the lubrication of engineered tissues.

Cartilage boundary mode friction coefficient, μ_{eq}, is mediated by short time exposure to cytokines commonly found in arthritis and injury. The studies in Chapter 5 demonstrate modulation of μ_{eq} consistent with endogenous lubricin surface localization by TGF-β, IL-1β, and OSM[88], and indicate an independence of μ_{eq} on the compositional ECM changes resulting from exposure to those cytokines. Together, the current data point to distinct biochemical origins of boundary and biphasic lubrication mechanisms in cartilage, with boundary lubrication regulated by accumulation of lubricants on the tissue surface and biphasic lubrication controlled by factors that affect water movement through the bulk of the tissue. Another major finding from this study is the ability of ESF, at the tissue surface and as a lubricant, to recover and enhance boundary lubrication in explants exposed to TGF-β, IL-1β, and OSM. As a result, the recovery of lubrication for catabolically exposed tissue by exogenous lubricin in ESF may be therapeutically important to combat high tissue friction found in injury and disease.

Many studies have investigated factors, both biochemical and biomechanical, which mediate the expression and synthesis of lubricin, with few investigating

functional implications of lubricin modulation and none investigating the functionality of localized lubricin. The studies documented within this dissertation confirm that molecular modification of the tissue surface by localization and subsequent removal of lubricin, either endogenous (Chapters 4 & 5), exogenous native (Chapter 4 & 5), or exogenous recombinant (Chapter3), altered the frictional properties of articular cartilage. In addition, the non-first order dose-response of rh-lubricin on the μ_{eq} (Chapter 3), in combination with the dependence on the ionic environment (Chapter 3) and lack of chemisorption to alginate gels (Chapter 4) indicate that lubricin-lubricin and/or lubricin-cartilage interactions play a significant role in rh-lubricin-mediated boundary lubrication of cartilage. Electrostatic interactions are known to regulate the binding of lubricin to cartilage[89] and in addition to steric conformation, may also influence aggregation of the molecule in solution. Understanding the mechanical implications of the surface localization of lubricin is an important consideration for both creating functional tissue engineered cartilage with appropriate low friction, low wear properties and to develop potential therapeutic interventions to recapitulate or maintain the low friction properties of articular cartilage.

6.1 FUTURE DIRECTIONS

This dissertation raises many more questions than it answers. Cartilage lubrication is complicated; and like many things in the human body, there are probably multiple components in a fine balance that contribute to the mechanism of lubrication enabling a dynamic, wear resistant, low friction interface. This section presents other areas of investigation (in no particular order) that should be investigated to understand lubricin's role in cartilage lubrication.

Utilize surface imaging/characterization tools to investigate lubricin localization.

Use of tools including imaging ellipsometry and atomic force microscopy (AFM) enables investigation into the formation of physiosobed layers on surfaces, as well as other phenomena such as steric arrangement[195], multimerization[48,89], or the possibility of lubricin to structure water at the tissue surface. As seen from the studies presented in this dissertation, lubricin-lubricin and lubricin-cartilage interactions play an important role in functional lubrication of cartilage.

Nanomechanics of aggrecan-aggrecan and aggrecan-substrate interactions have recently been carried out using AFM[35,62,63]. Modification and application of these techniques coupled with biochemical tools can be utilized to determine the structure function relationship of the lubricin. Utilization of Lub-N and Lub-C constructs[89], partial lubricin fragments consisting of the end domains of the amine and carboxyl termini respectively, can be utilized in combination with full-length rh-lubricin molecules to determine the role of aggregation, without the confounding electrostatic effects, in the boundary lubricating ability of lubricin. Additionally AFM can be used as a screening tool to identify which ECM molecules localize lubricin at the tissue surface and may also have the ability to experimentally determine binding constants of lubricin with the tissue, and bond strength of lubricin to the tissue surface. Characterization of these properties enables an understanding of the molecular mechanisms lubricin uses to boundary lubricate cartilage. To unlock the mechanisms of lubricin's boundary lubricating ability investigations at the micro scale must be conducted to put into context lubrication at the macro scale.

Utilize the friction apparatus as a hemiarthroplasty model.

The studies documented herein underscored the significance of control over operating variables for the investigation of cartilage frictional properties and defined

an operational variable space that produced boundary lubrication. The custom friction apparatus can serve as a hemiarthroplasty model to evaluate historic or novel materials for potential hemiarthroplasty. Investigations of multiple types of lubricated tissue and tissue engineered replacements, in addition to evaluation of materials for tissue replacement including hydrogels, foams, and commonly used hemiarthroplasty materials. Limited research has been performed investigating cellular, molecular, compositional, or structural changes to articular cartilage or cartilage replacements in a hemiarthroplasty. These changes could conceivably have significant impact on the design of such implants to enable longer functional life spans for these devices. In addition, with the ability to run multiple friction tests in parallel, control over the environment by placing the apparatus in an incubator would facilitate long term investigations of tissue wear, alterations to lubrication modes with tissue development, and potential lubricating biomolecules for these hemiarthroplasties.

Elucidate the role of potential co-mediators of cartilage boundary lubrication.

Few studies have noted that there are potential roles for different synovial molecules at different loading profiles[146,147]. Lipids, such as SAPL, have been strongly implicated in boundary lubrication[60,70] in addition to HA[13,147] and chondroitin sulfate[12]. Based upon the complexity of cartilage lubrication and the dynamic environment of the joint, it seems reasonable that other molecules found in the synovial fluid would play a role to enable, enhance, or inhibit lubricin in boundary lubrication. Further studies should be employed, along with the creation of Stribeck surfaces to map out the roles these molecules play in various modes of lubrication, independently or synergistically with lubricin.

Investigate the effects of aging, injury, and disease on frictional properties.

With all the research preformed to date in the literature, it is still not clear if loss of cartilage lubrication causes joint failure or joint failure causes loss of lubrication. While this chicken and egg debate will probably continue for at least the next decade, characterization of frictional properties for pathological tissue is an important step to answer this question. One severe limitation of the studies presented in this dissertation, as well as many other cartilage lubrication studies, is the use of immature bovine cartilage, which has a pristine surface and minimal (ab)use. While cytokines were used in one study presented herein (Chapter 5), the milieu of a diarthrodial joint is very complex with a wide range of mechanical and biochemical stimuli that is unable to be fully recapitulated in these models. The characterization of frictional properties in a range of tissue ages, and definable states of disease enables a more complete picture to evaluate biolubricants, such as lubricin, and their role in therapeutically altering pathophysiological states.

While the studies documented here have only directly investigated the μ_{eq} effects of ε_N (rate and magnitude), v, and co-planarity on lubrication mode by Stribeck surfaces, additional dependences on lubricant η[192] and tissue surface roughness[4,50,192] do exist. Alterations to the tissue and synovial fluid due to disease or injury can include changes in viscosity, composition, modulus, and surface features; all of which may influence the lubrication of the tissue due to differences in the manner fluid films are able to be developed and sustained, as well as changes in lubricant-cartilage interactions. Further studies should be undertaken to understand the importance of synovial fluid components and tissue structure in cartilage tribology as well as identify lubrication mechanisms of cartilage in various states of age, disease progression, and injury.

APPENDICIES

A. FRICITON INSTRUMENT ENGINEERING DRAWINGS

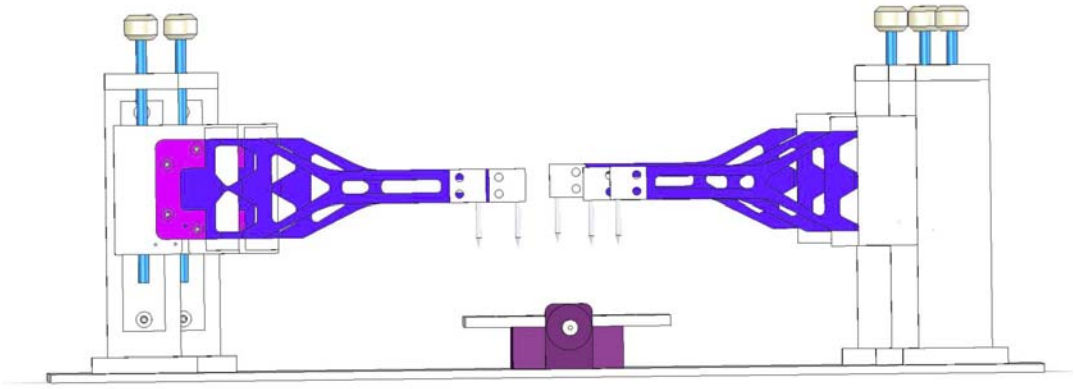

Figure A1: Custom friction instrument side view.

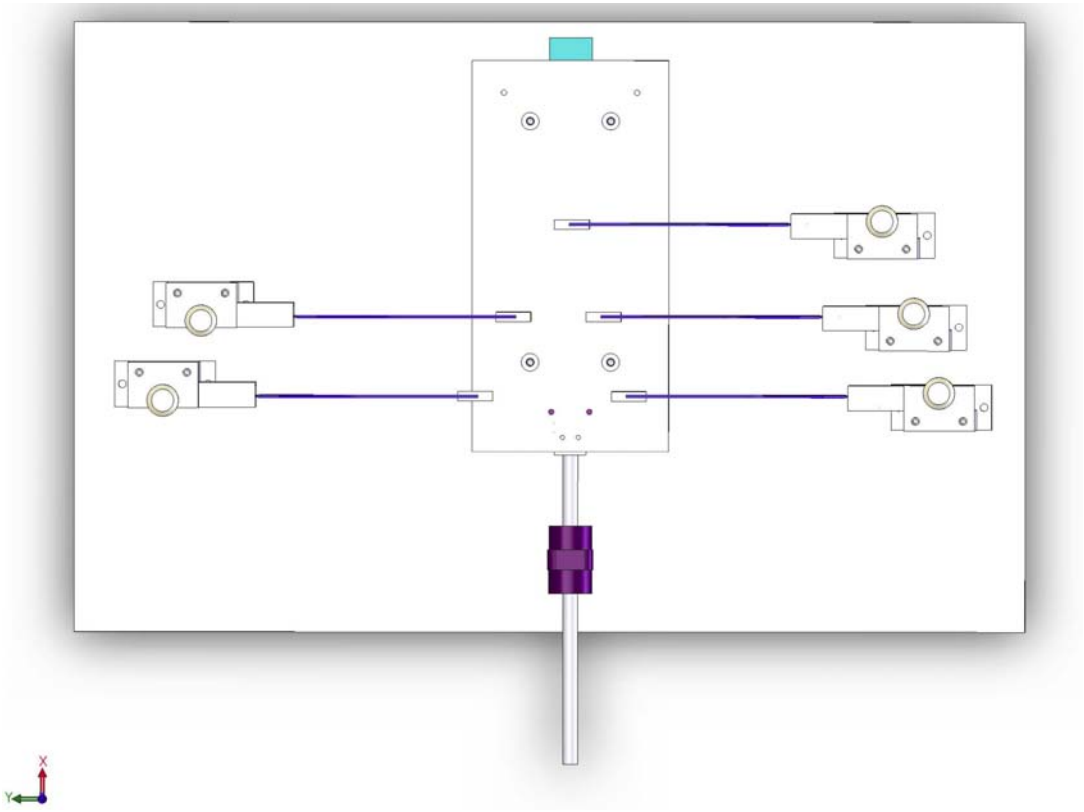

Figure A2: Custom friction instrument top view.

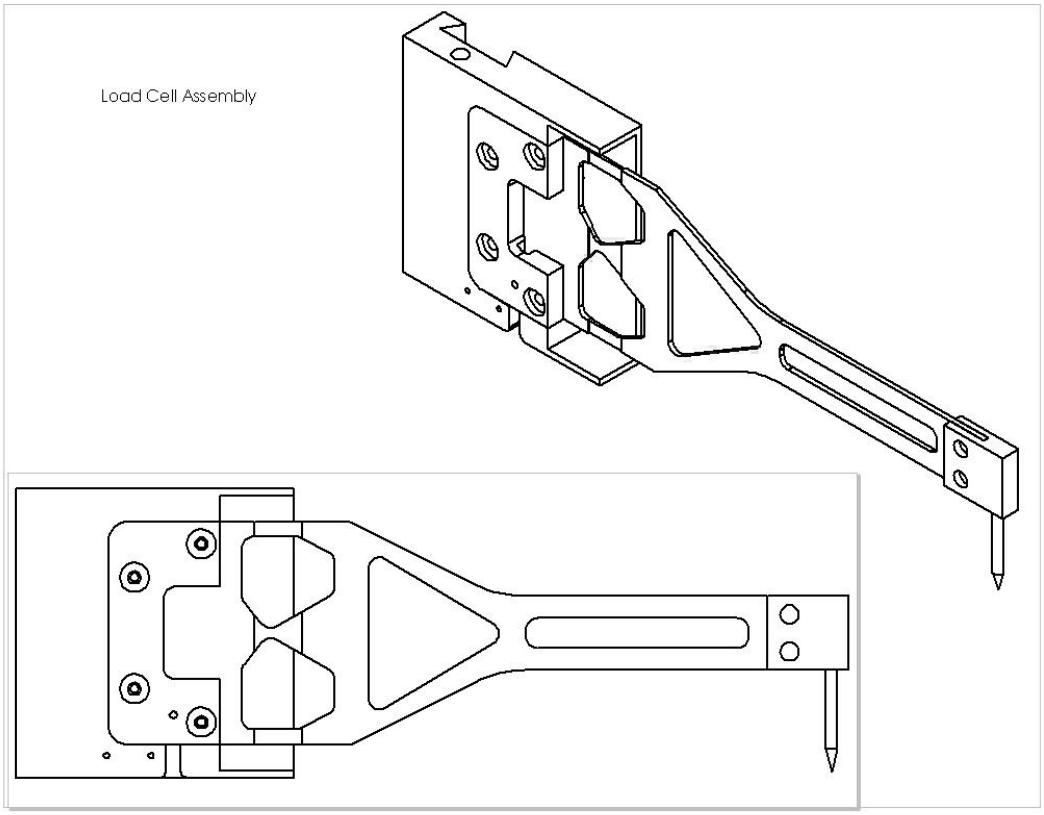

Figure A3: Load cell assembly.

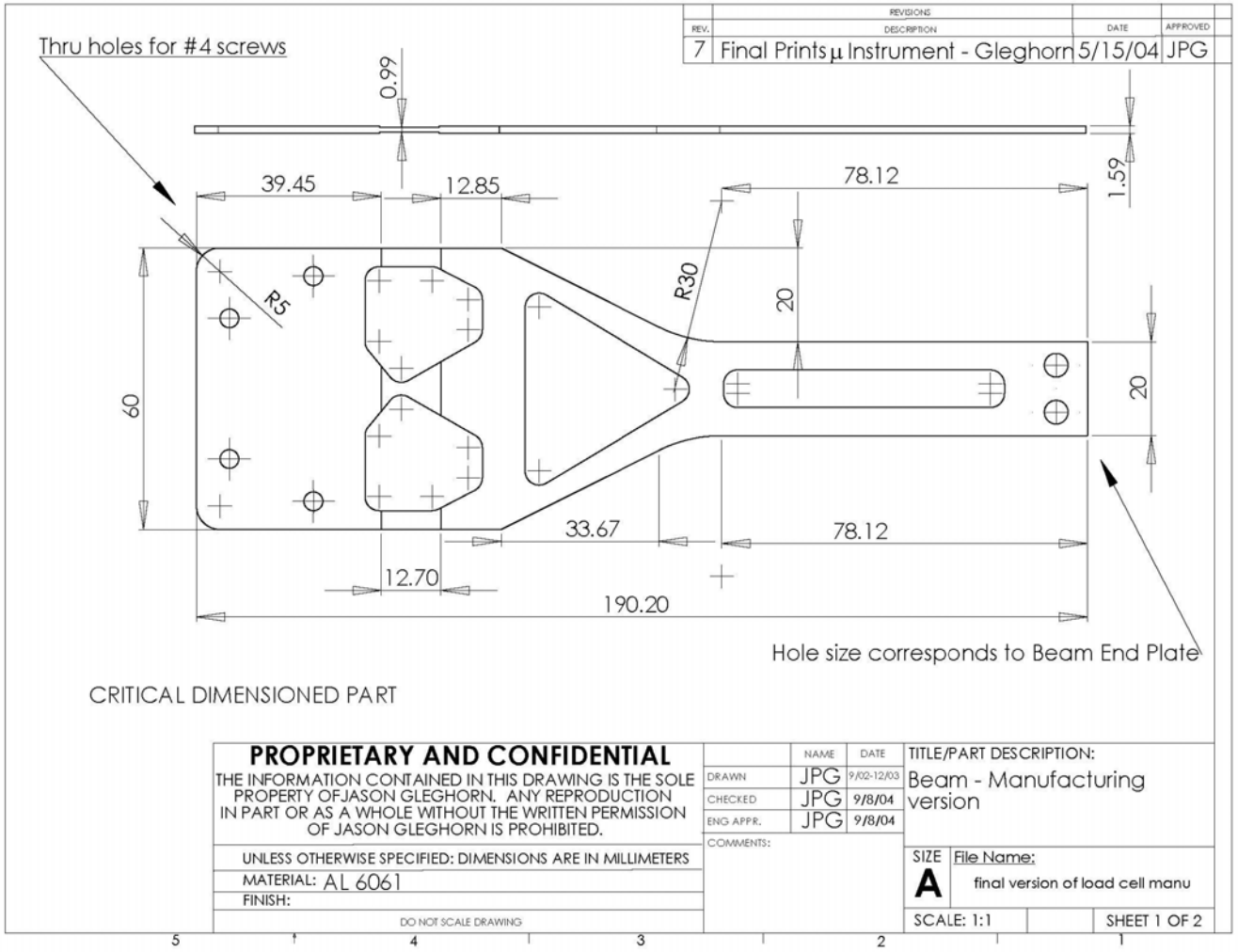

Figure A4: Dimensioned load cell part I.

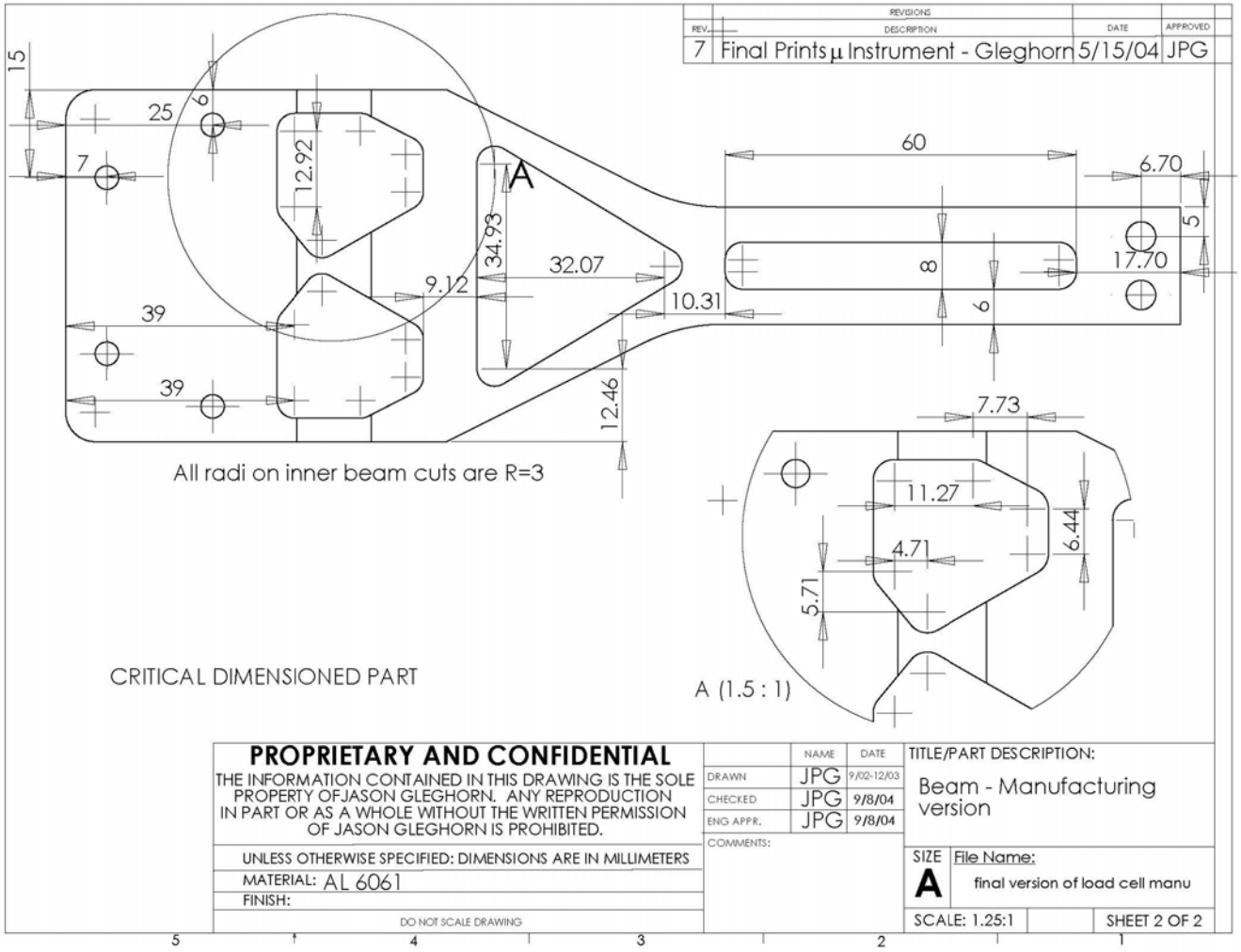

Figure A5: Dimensioned load cell part II.

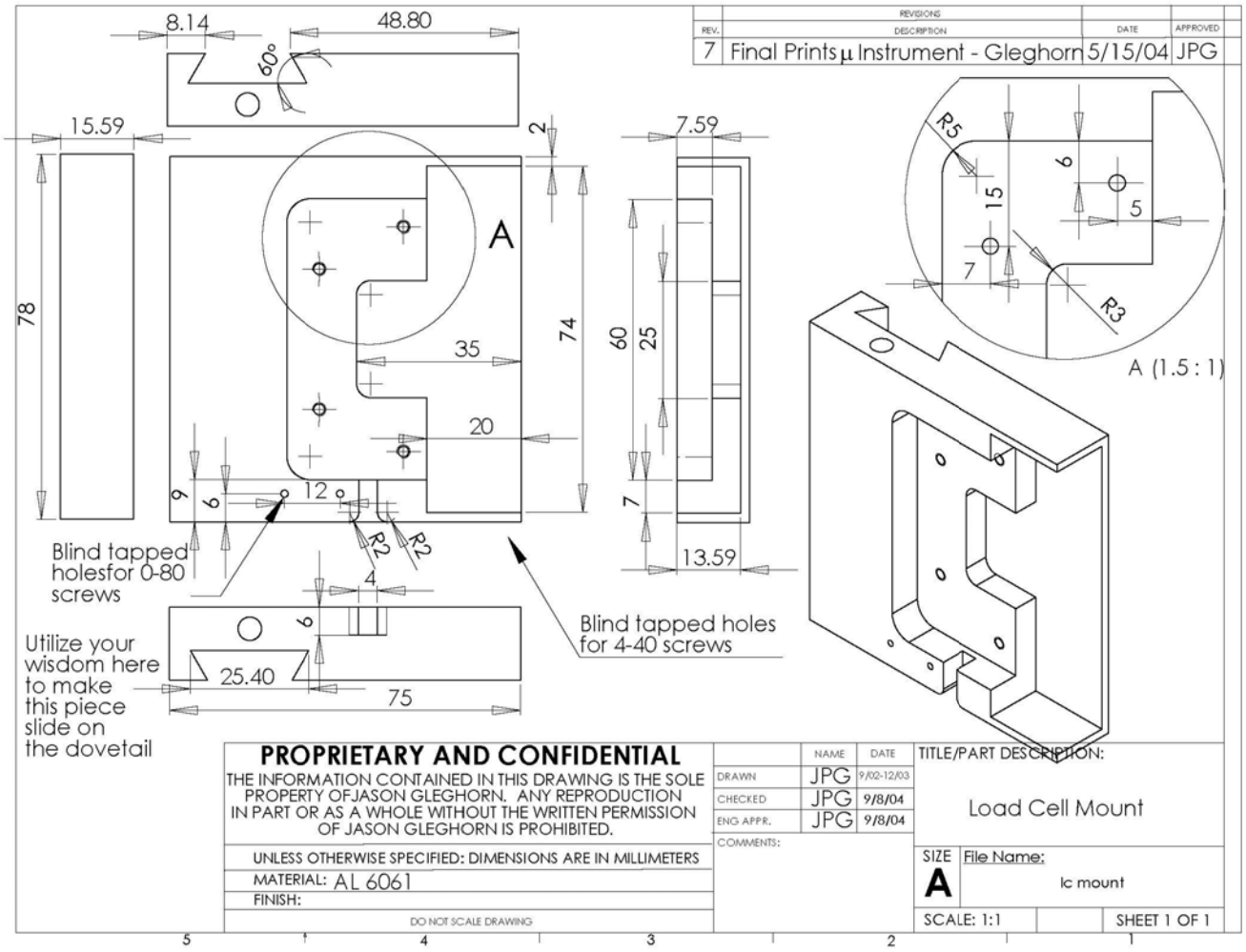

Figure A6: Dimensioned load cell mount.

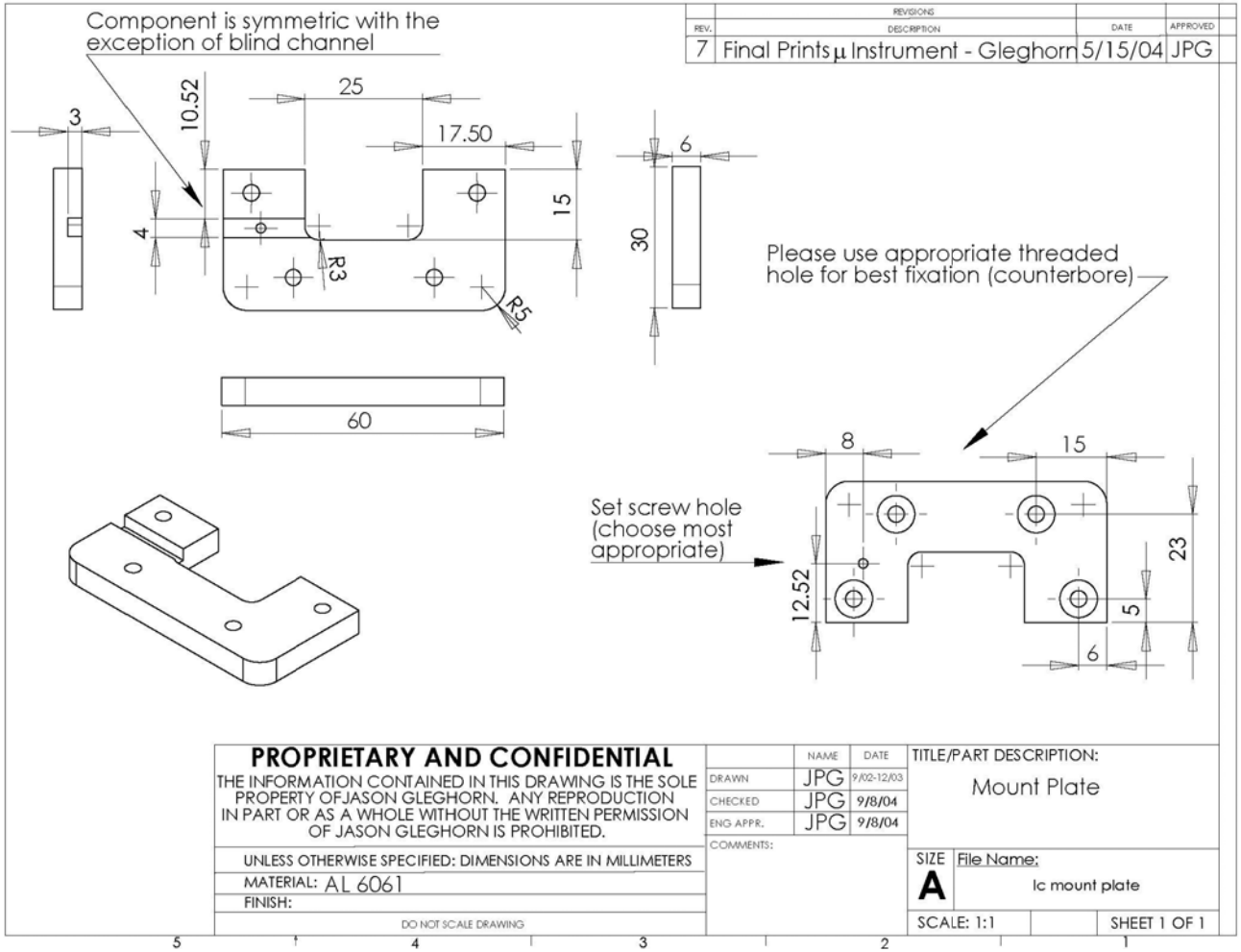

Figure A7: Dimensioned load cell mount plate.

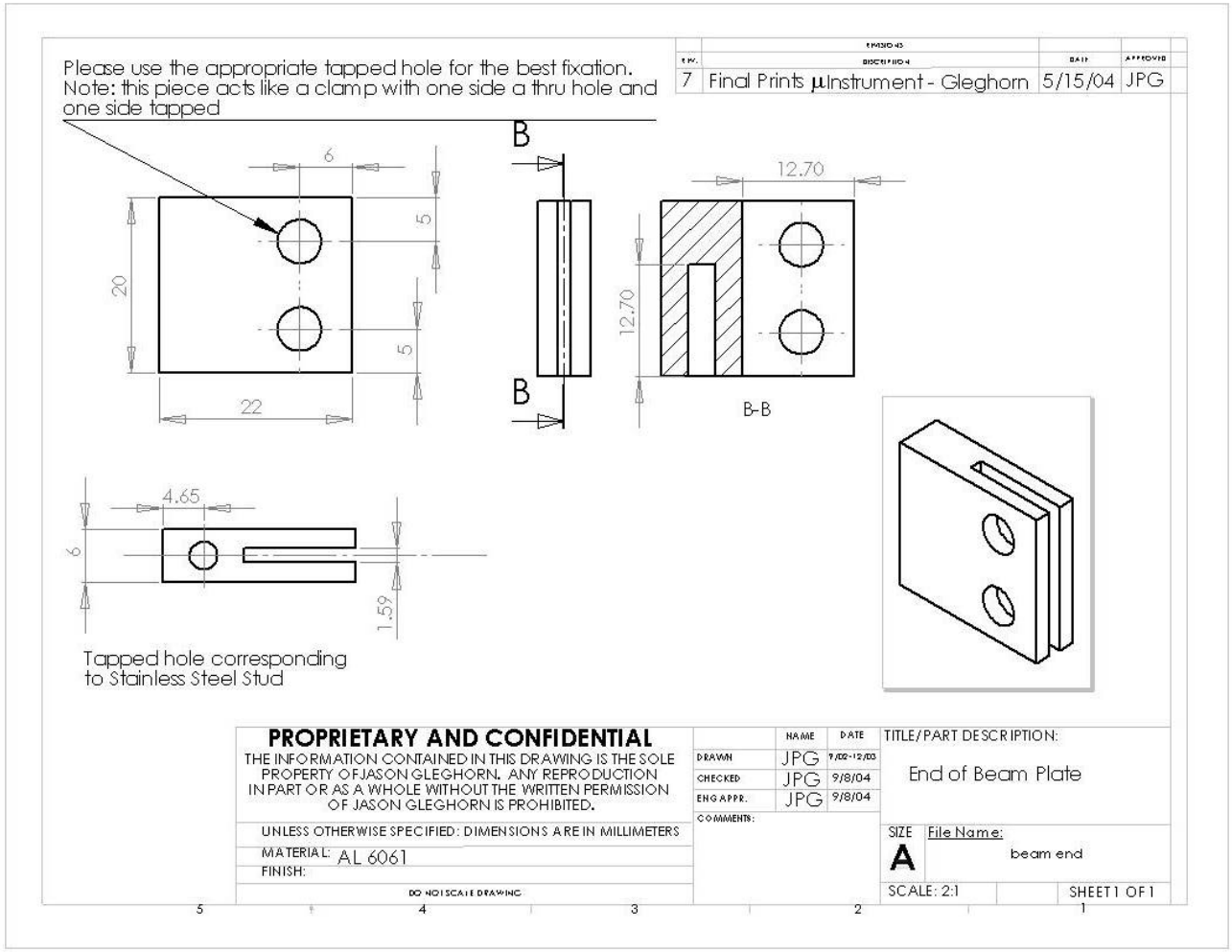

Figure A8: Dimensioned load cell beam end.

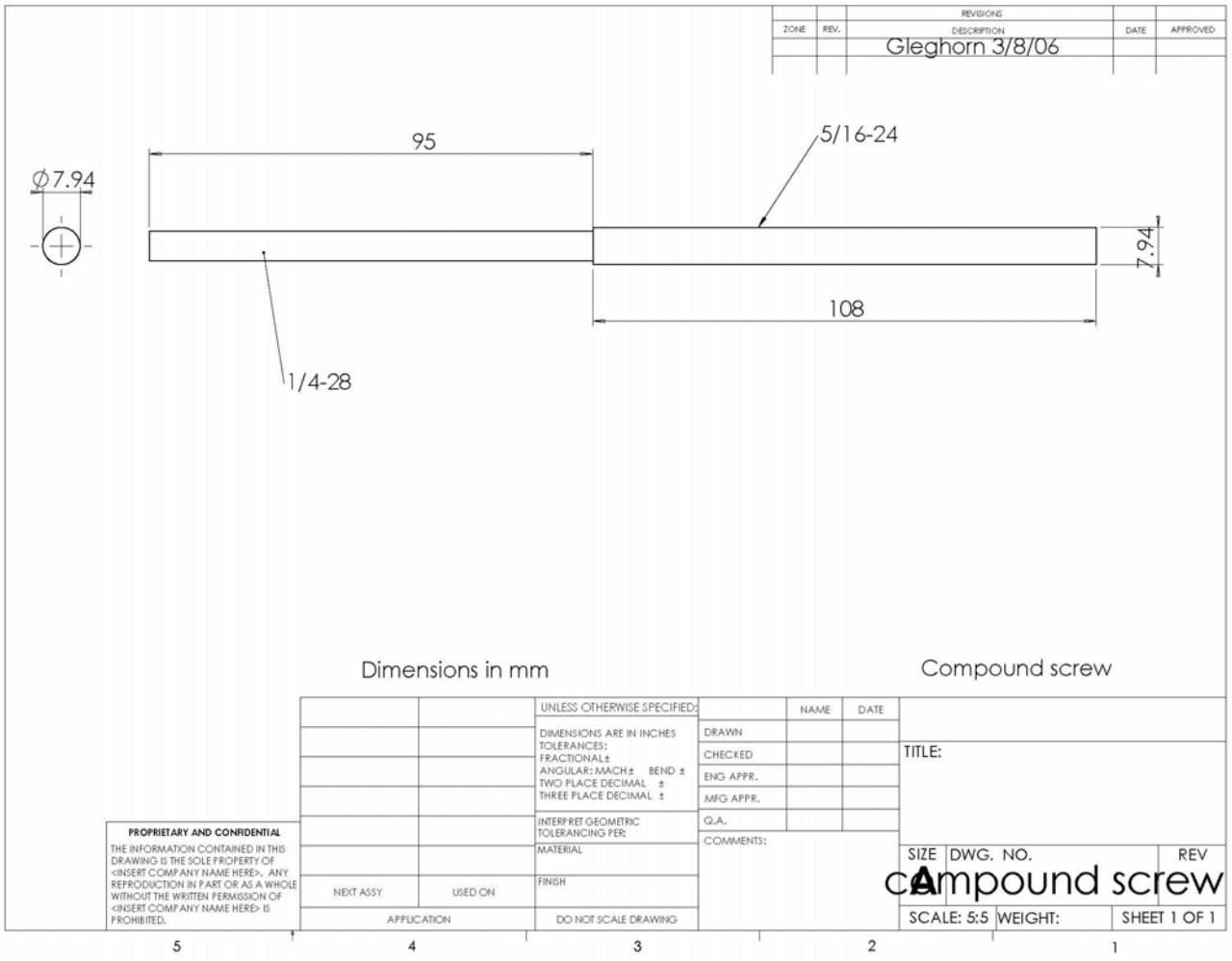

Figure A9: Dimensioned load compound screw.

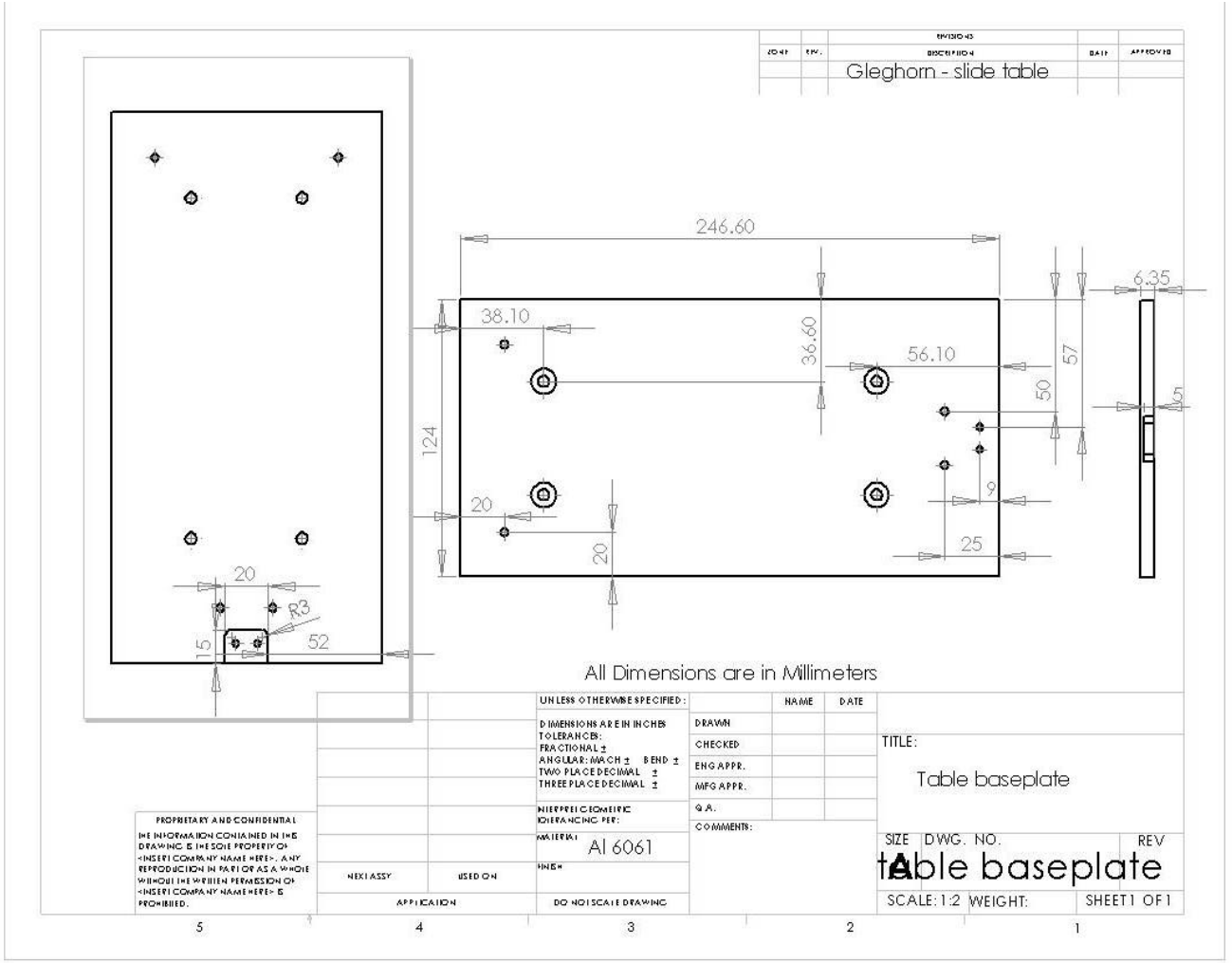

Figure A10: Dimensioned table baseplate.

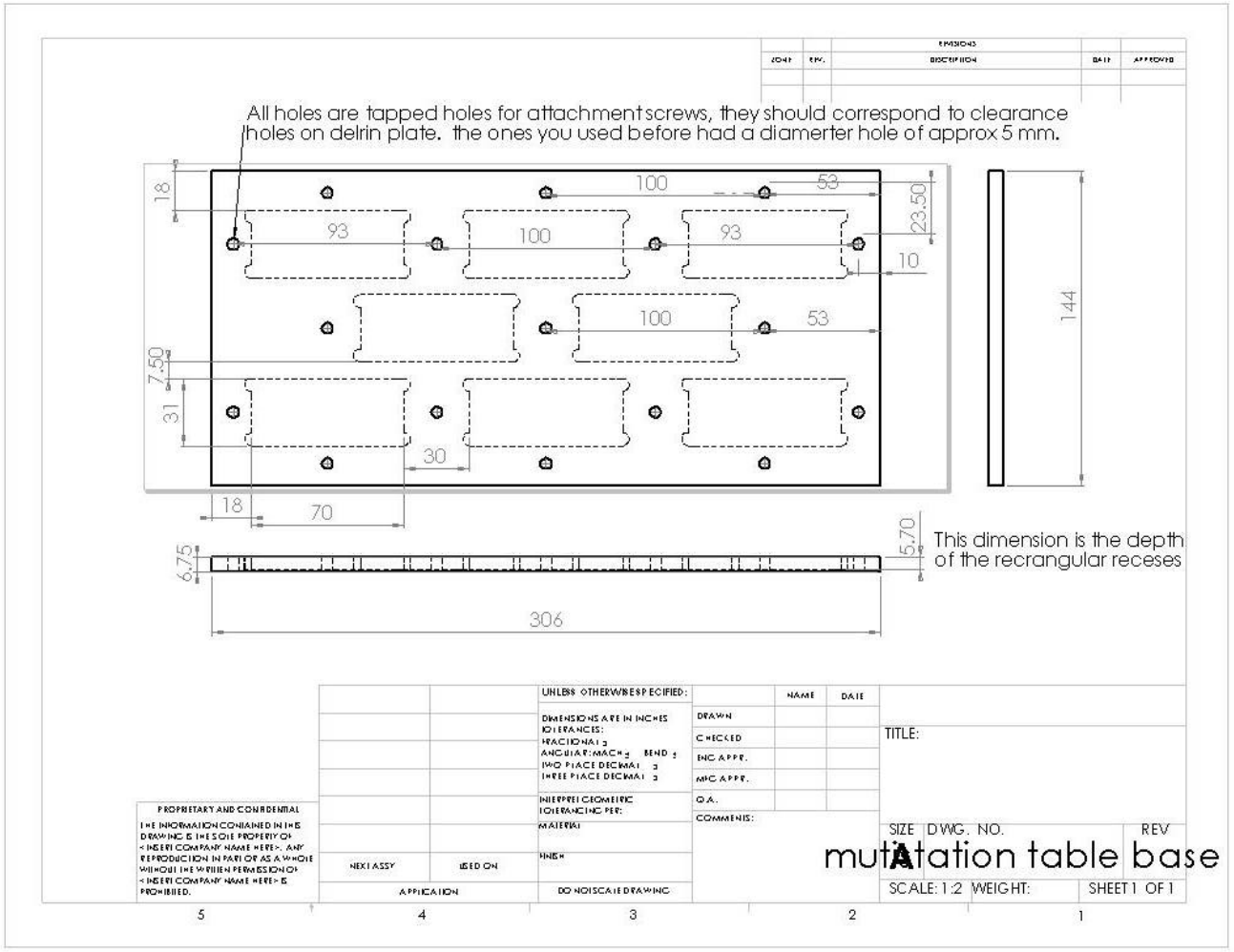

Figure A11: Dimensioned multistation table.

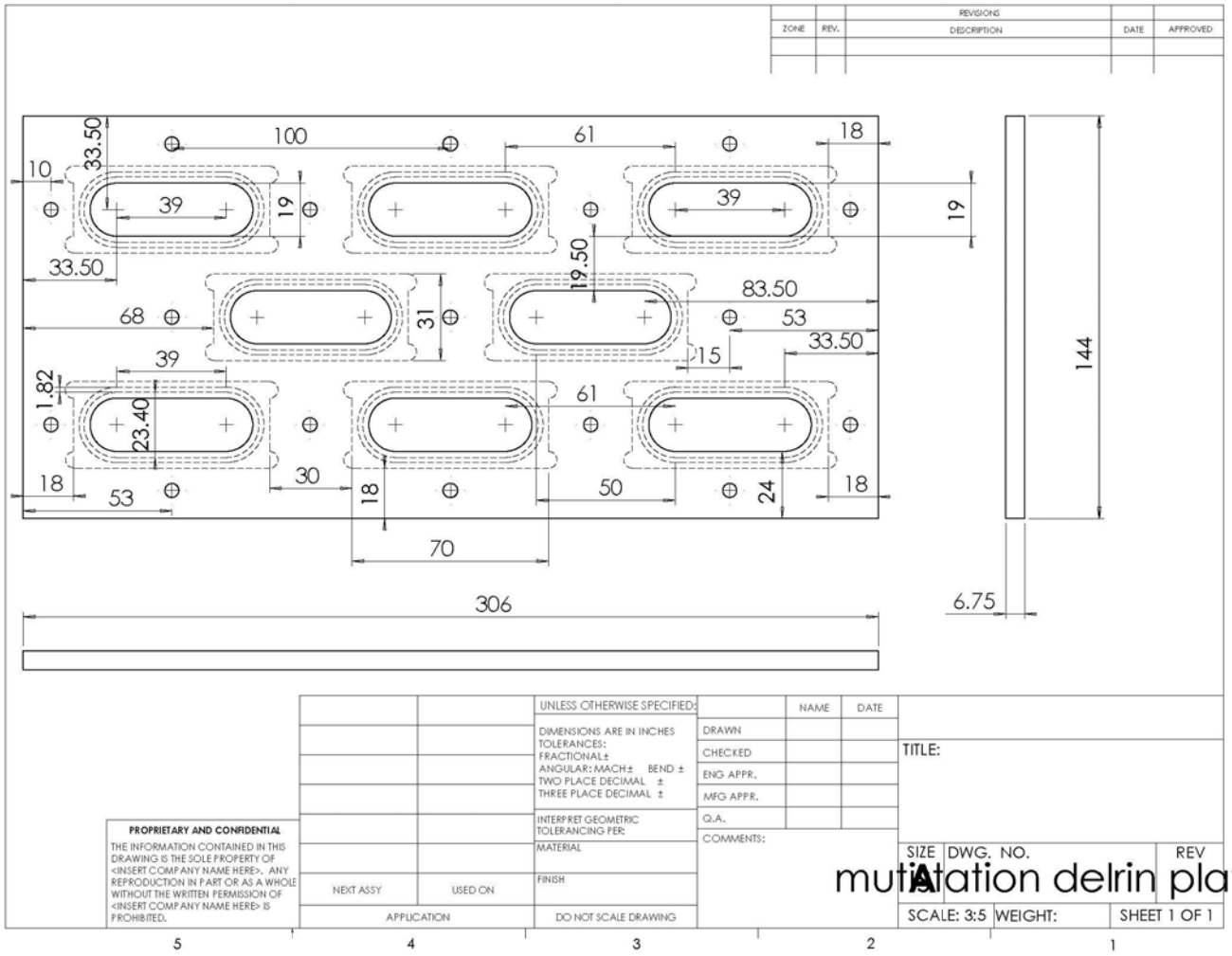

Figure A12: Dimensioned multistation table delrin plate.

B. FRICITON INSTRUMENT ELECTRONIC SCHEMATICS

Signal Conditioning

The schematics that follow are for the PCBs used in the “Signal Conditioning” Box.

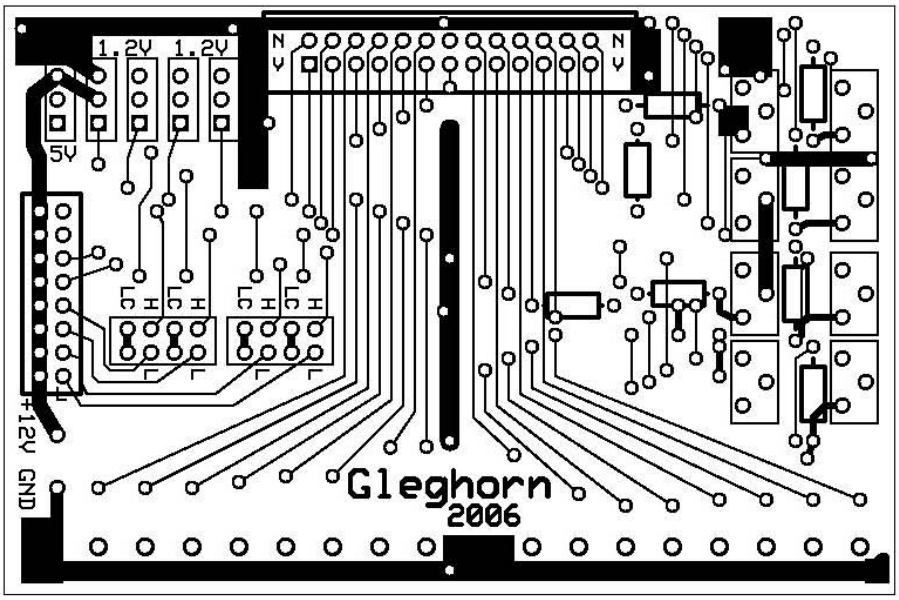

Figure B1: Signal conditioning motherboard PCB – Obverse.

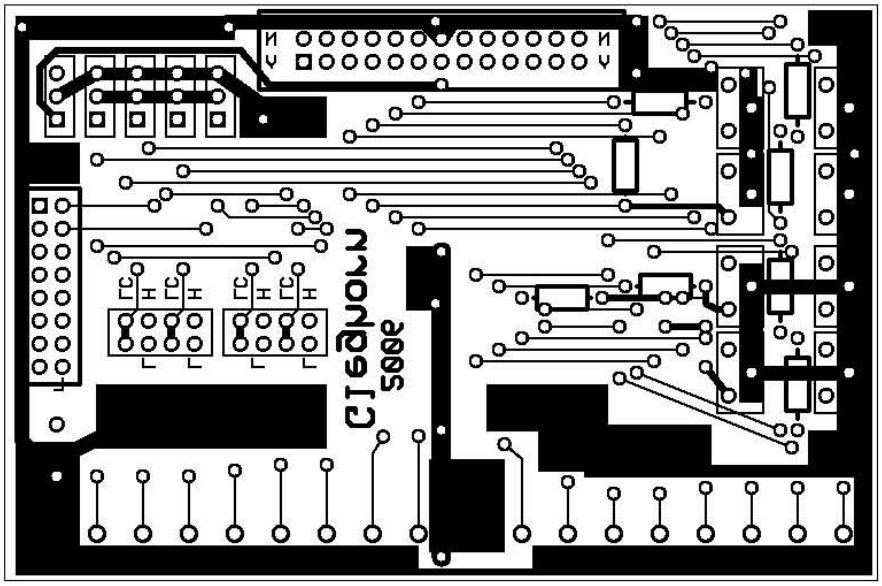

Figure B2: Signal conditioning motherboard PCB – Reverse.

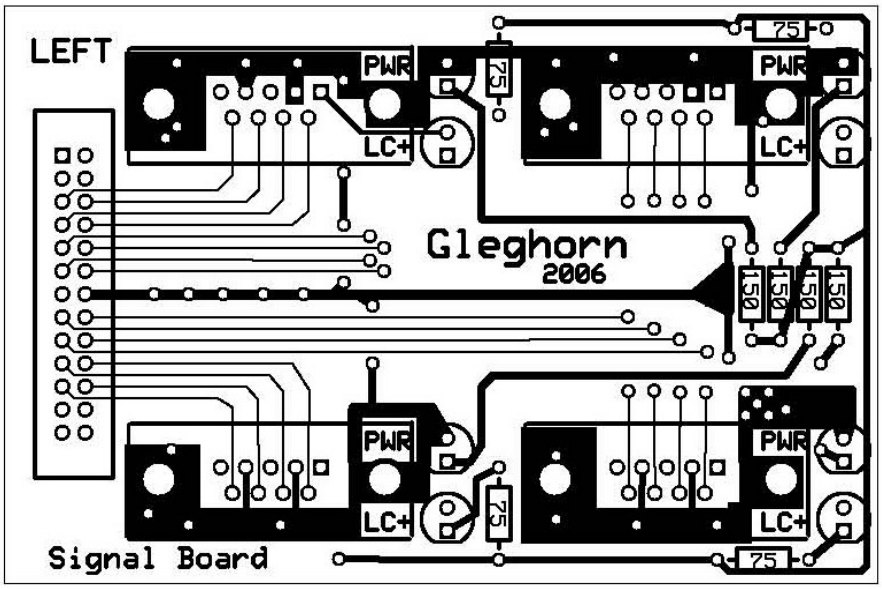

Figure B3: Signal conditioning throughput PCB – Obverse.

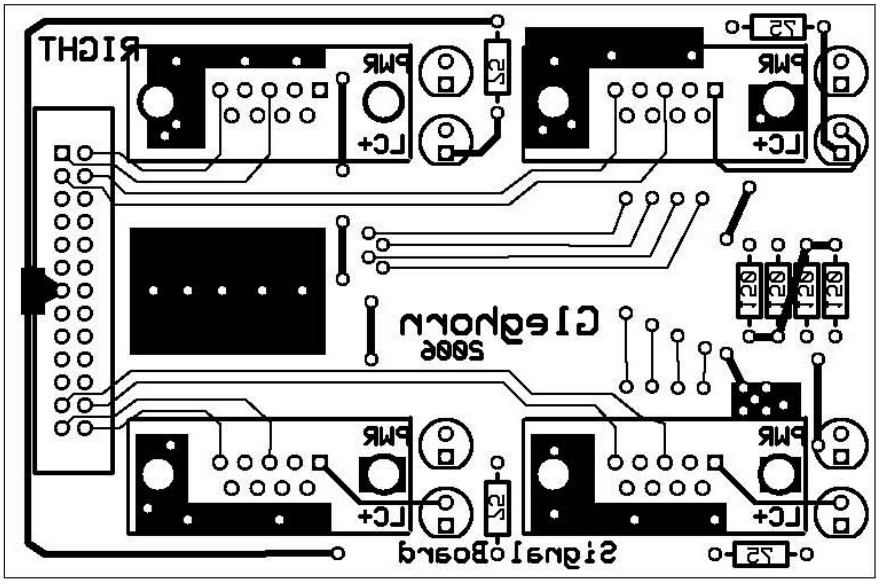

Figure B4: Signal conditioning throughput PCB – Reverse.

Motor Control

The schematics that follow are for the PCBs used in the "Motor Control" Box. These boards provide control for the motorized stage that controls the surface speed applied to the tissue. In addition, these boards control of individual motors located on each load cell to provide automatic positioning of the load cell for application of prescribed ε_N.

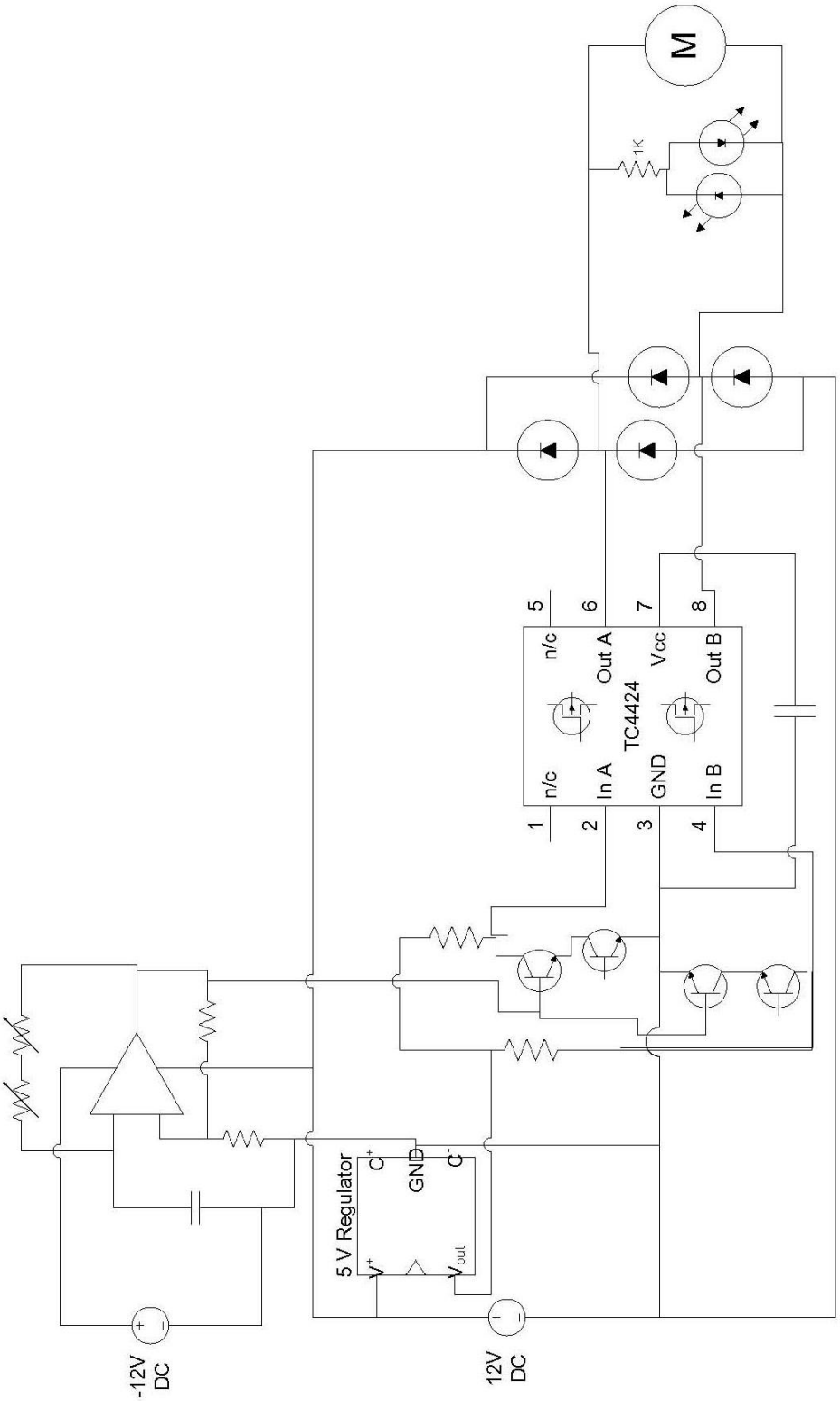

Figure B5: Generalized motor control circuit diagram.

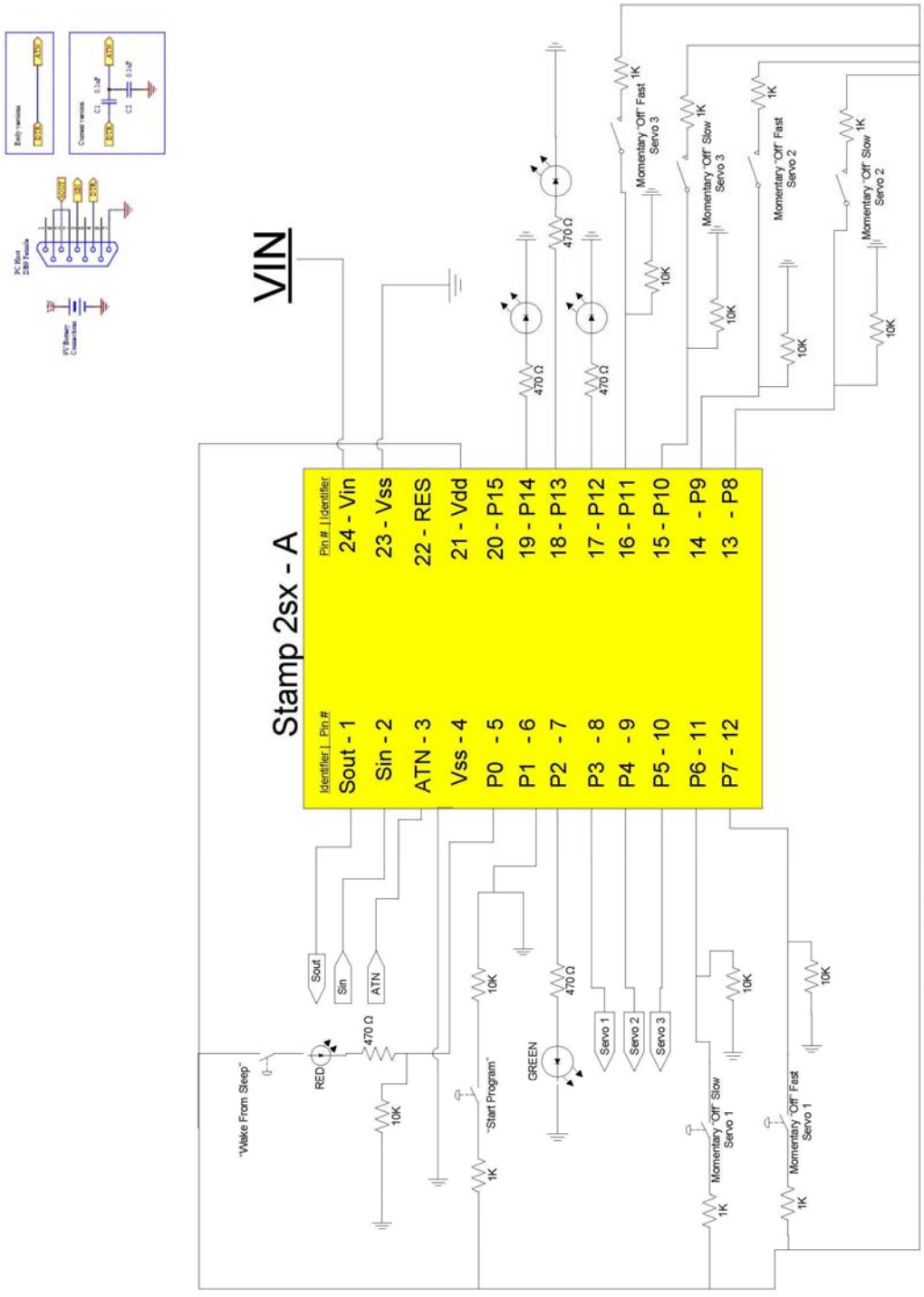

Figure B6: Schematic for BASIC stamp A.

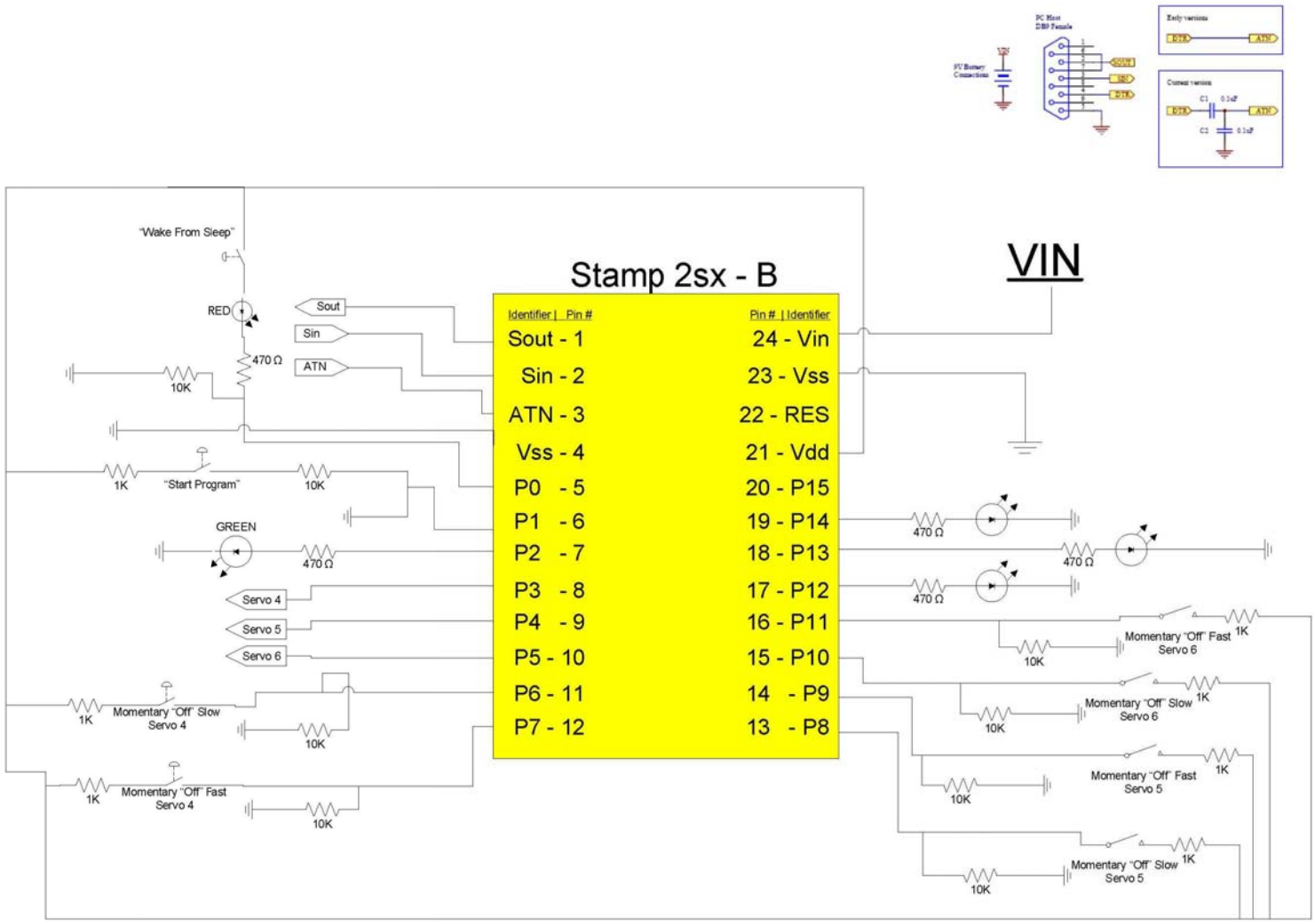

Figure B7: Schematic for BASIC stamp B.

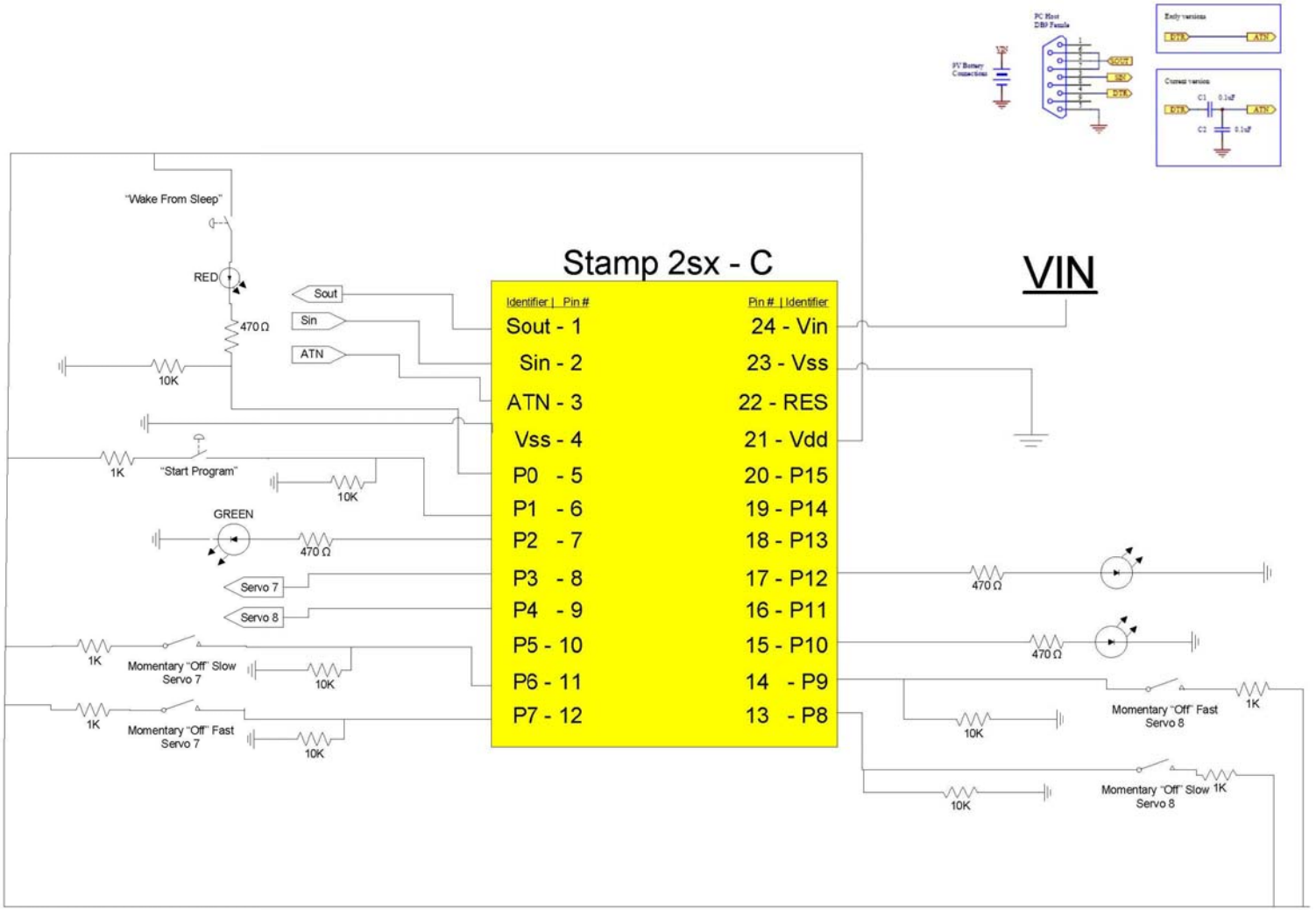

Figure B8: Schematic for BASIC stamp C.

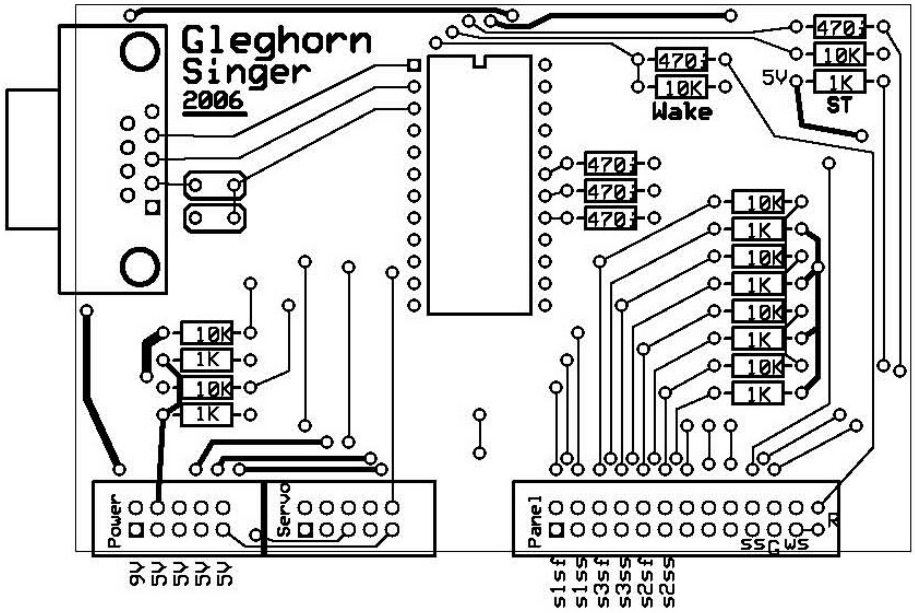

Figure B9: Motor control command PCB – Obverse.

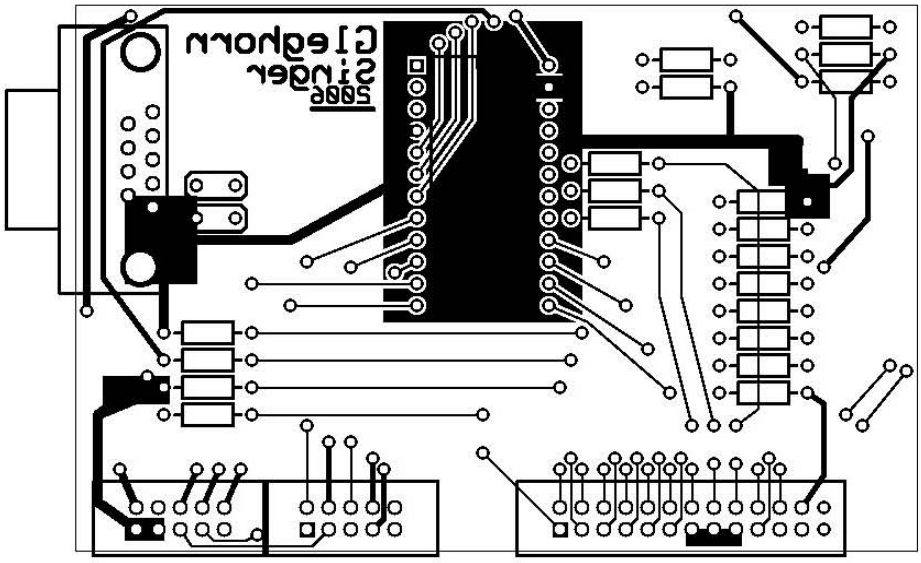

Figure B10: Motor control command PCB – Reverse.

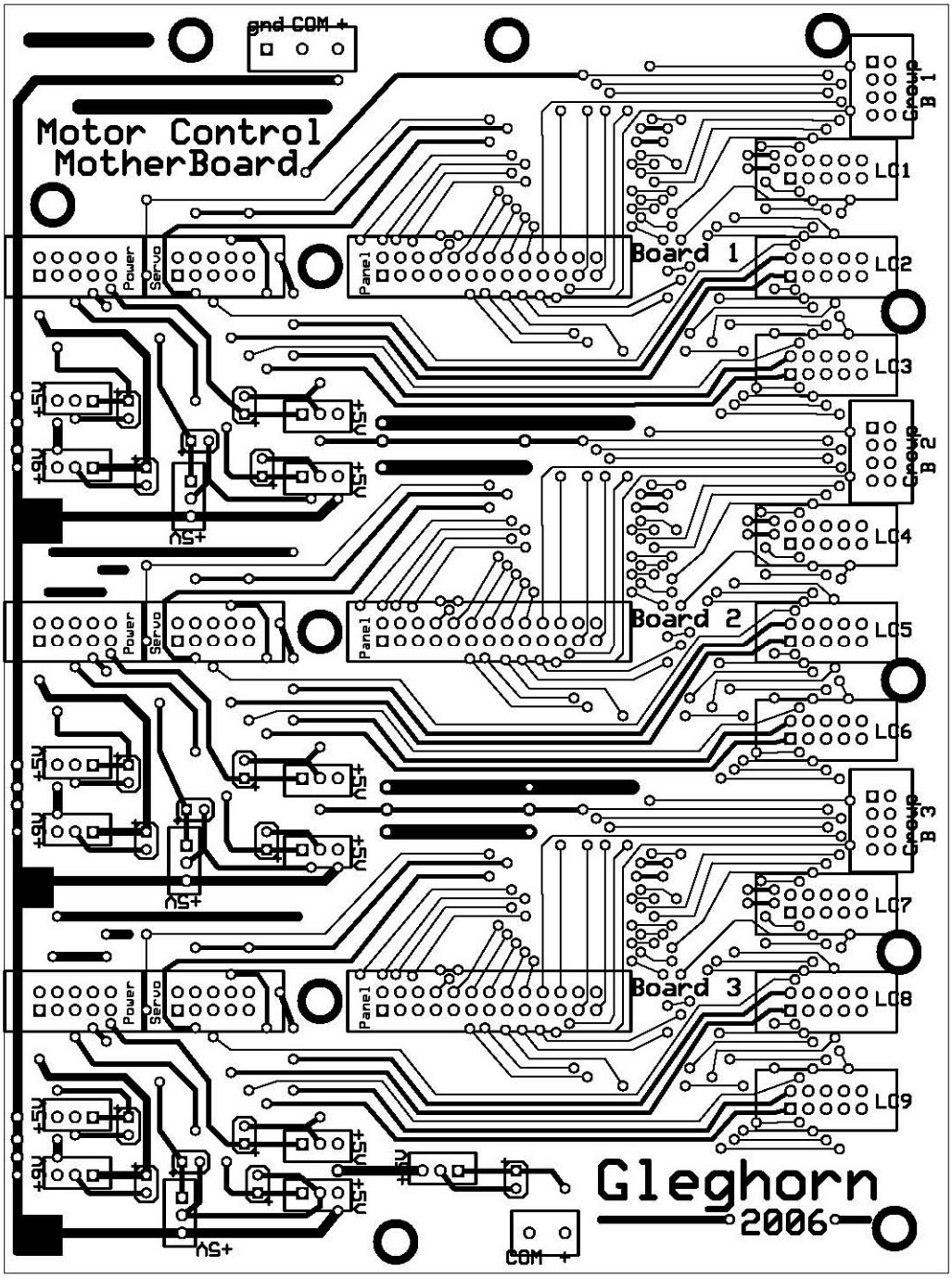

Figure B11: Motor control motherboard PCB – Obverse.

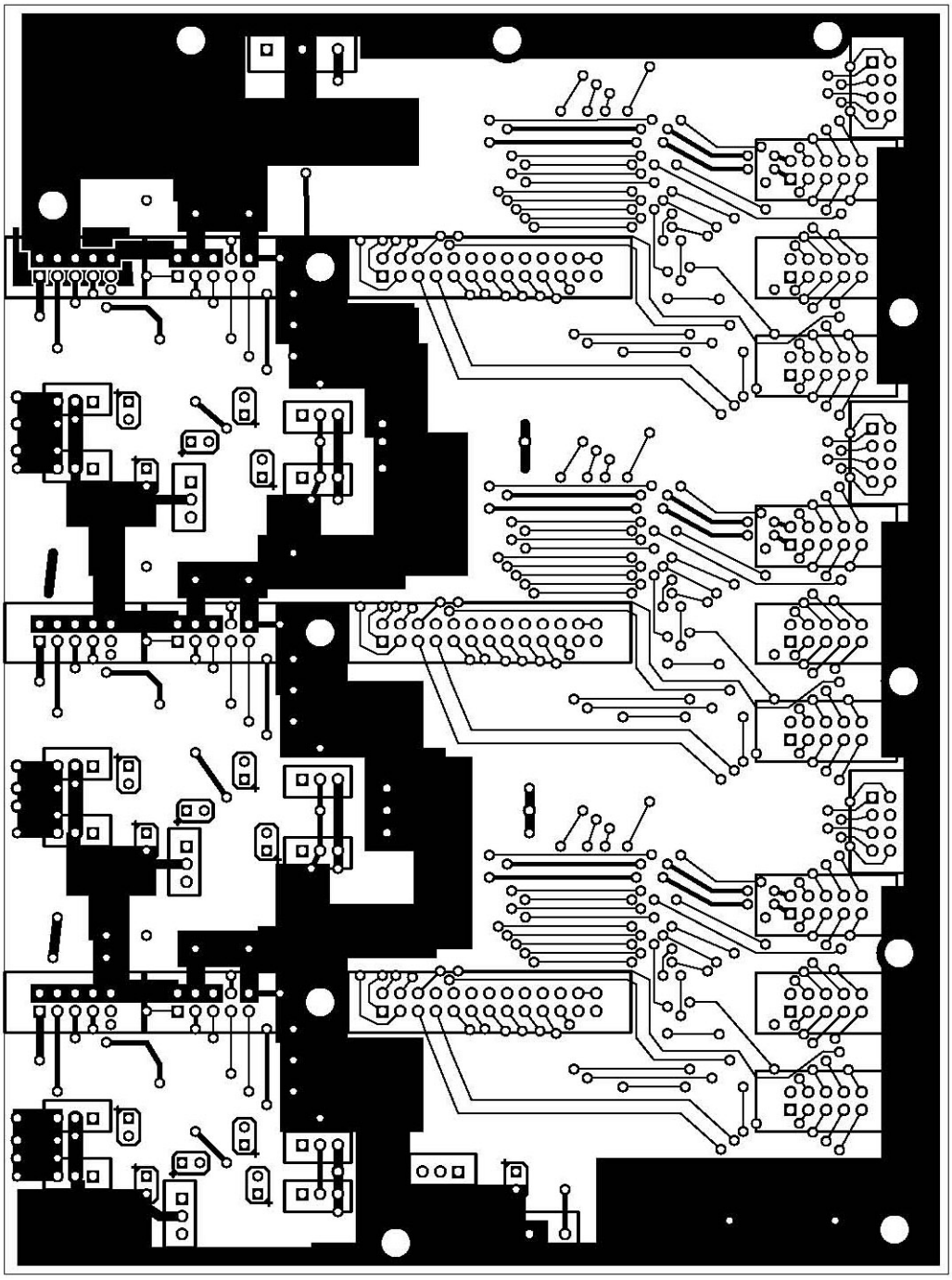

Figure B12: Motor control motherboard PCB – Reverse.

C. COMPUTER CODE

Acqusition Software

The acquisition software that collects, filters, and saves the data from the friction instrument is graphically written in LabView. As a result, "standard" linear scripts were not utilized but rather a graphical "wiring diagram" provides the code to Labview. What is contained on the following six pages represents images of the wiring diagram. In order to view the entire diagram, the following pages must be laid out in a 2x3 matrix. The figure captions contain the individual images' place in the matrix ($acqusition_{ij}$) using index notation as the naming convention.

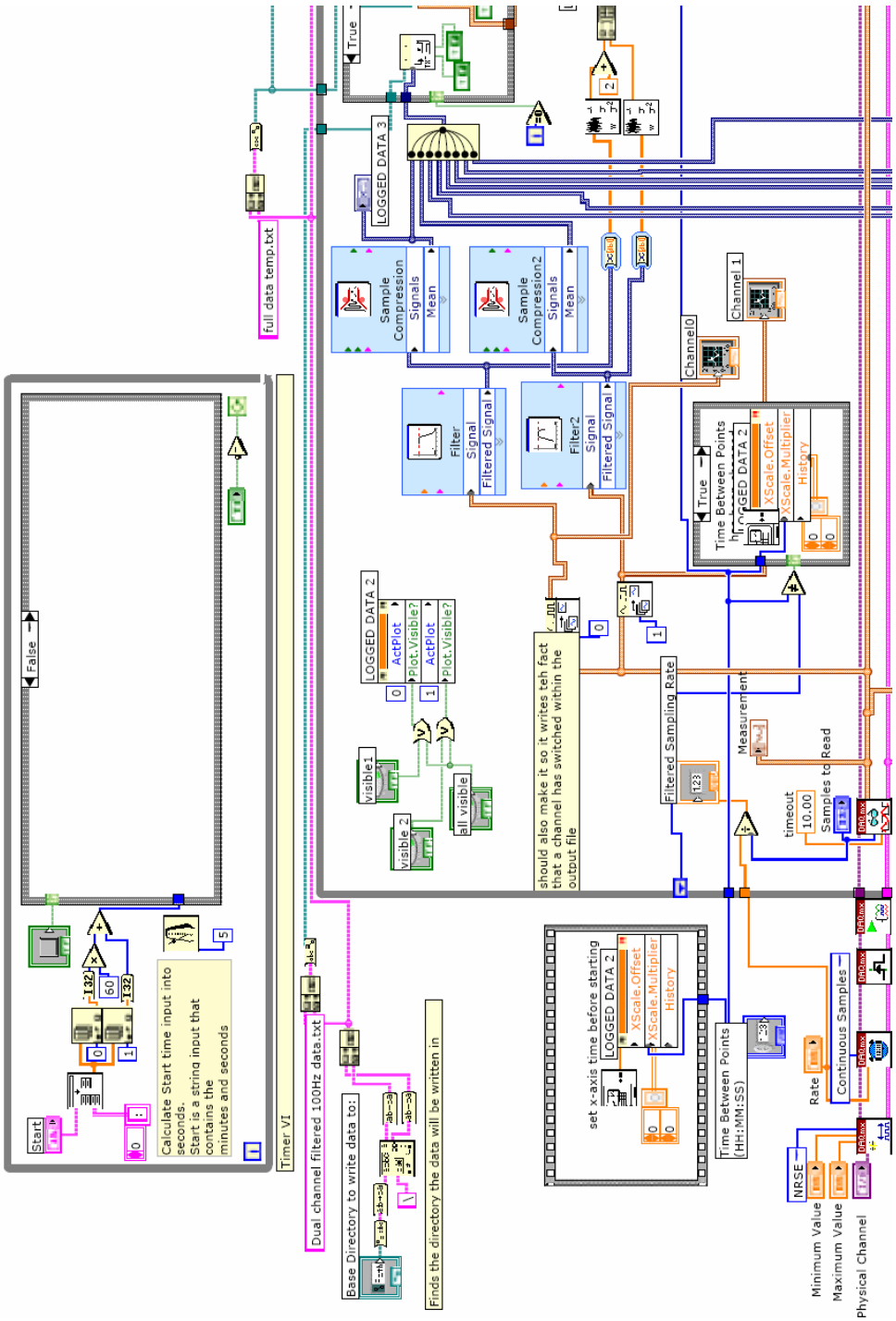

Figure C1: LabView code acquisition[11]

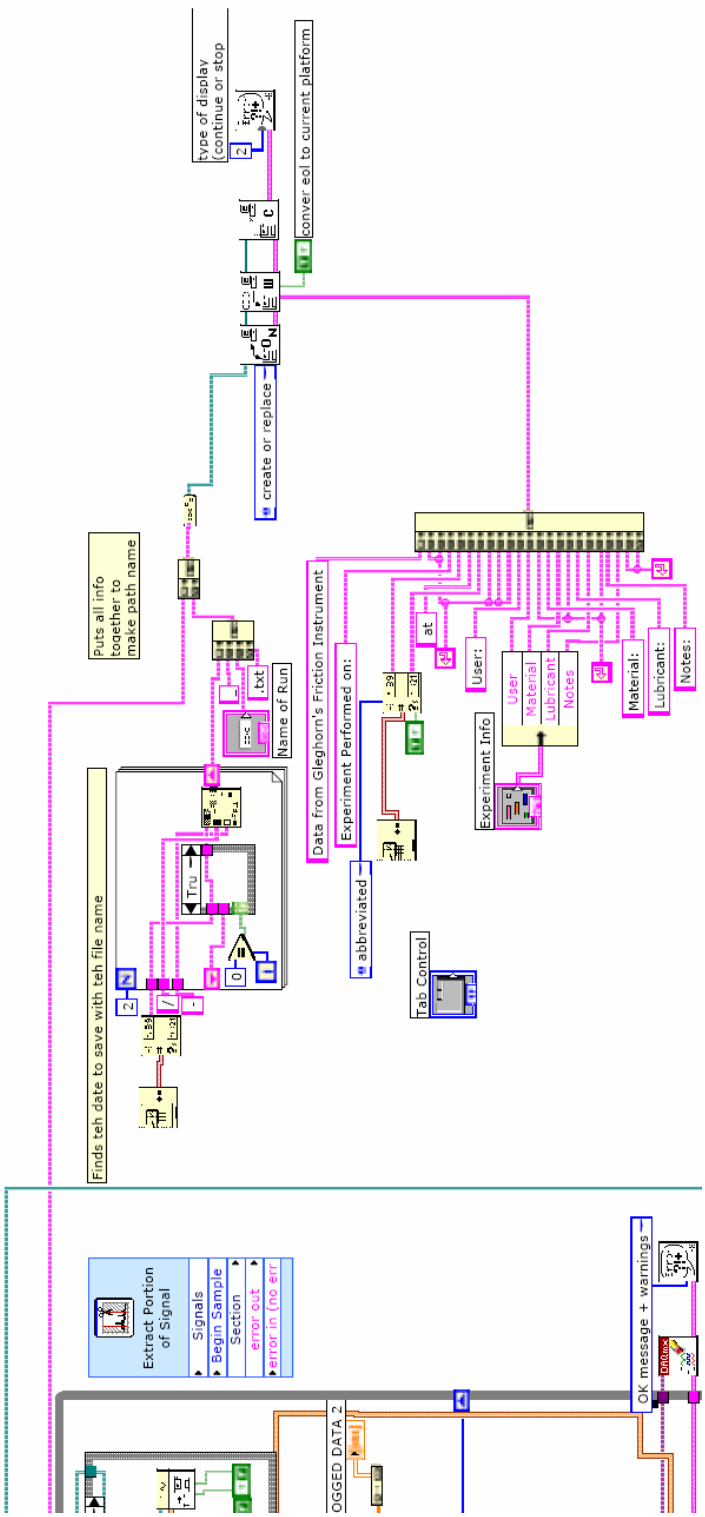

Figure C2: LabView code acquisition[12]

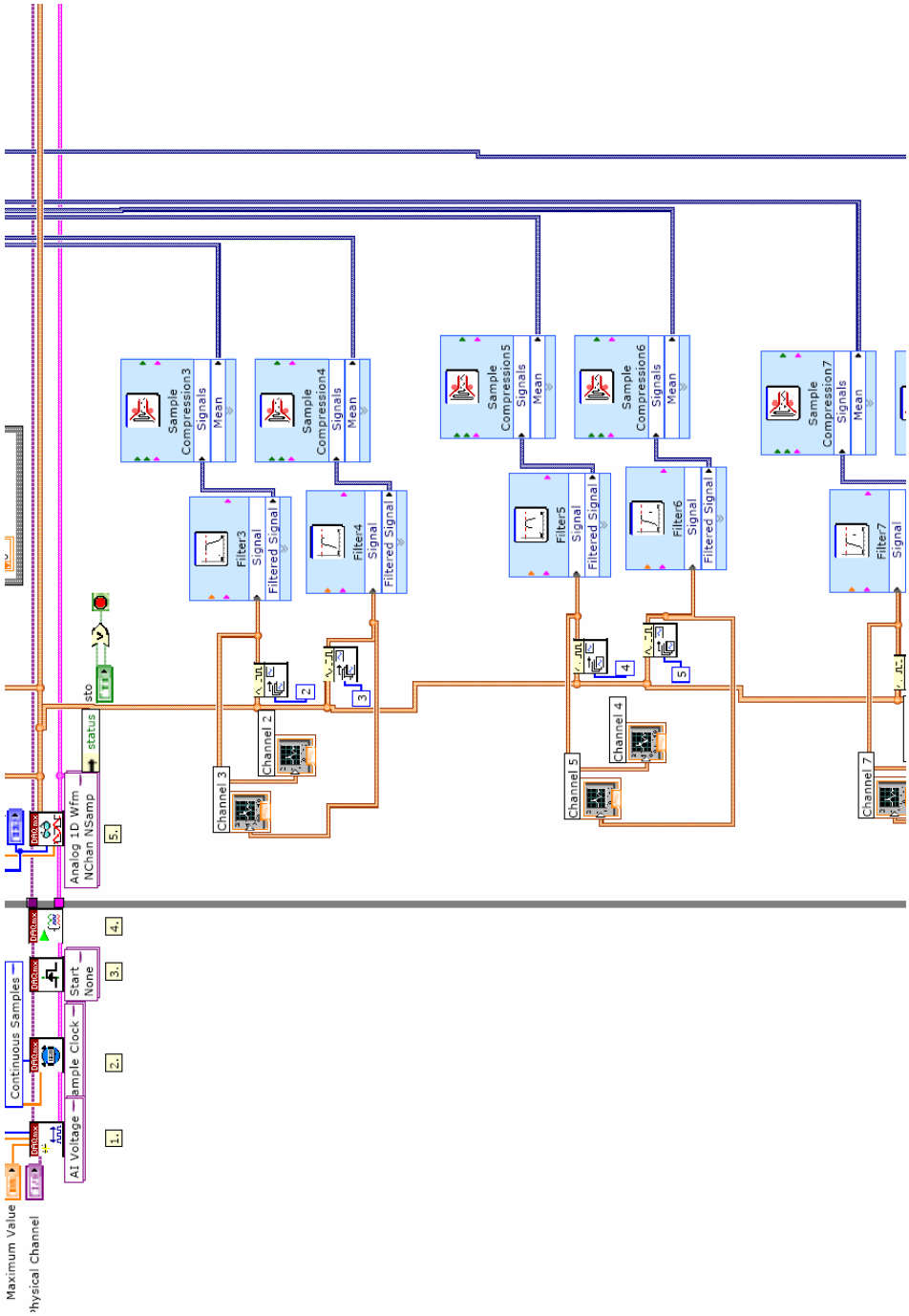

Figure C3: LabView code acqusition[21]

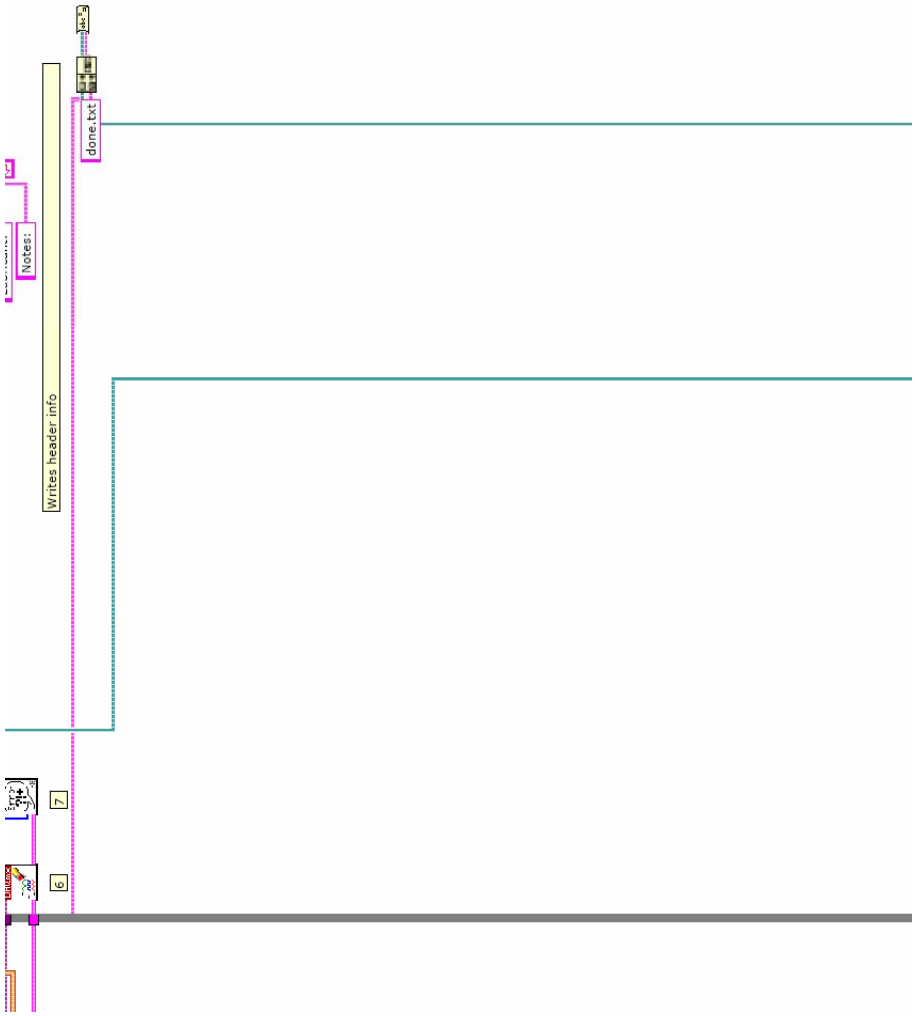

Figure C4: LabView code acqusition[22]

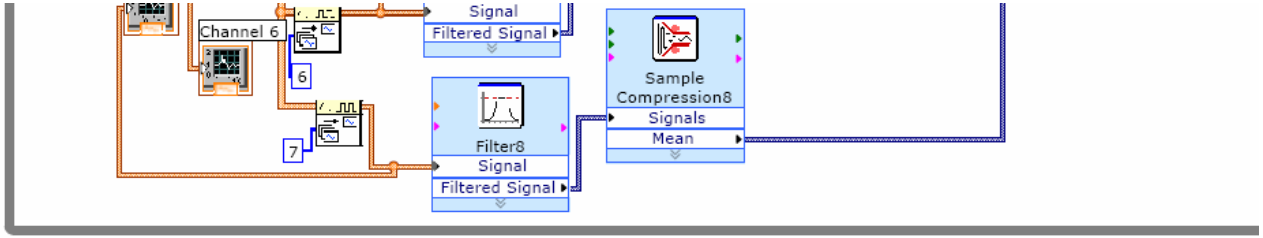

Steps:
1. Create an analog input voltage channel.
2. Set the rate for the sample clock. Additionally, define the sample mode to be continuous.
3. Define the parameters for an Analog Slope Start Trigger.
4. Call the Start VI to start the acquisition.
5. Read the waveform data in a loop until the user hits the stop button or an error occurs.
6. Call the Clear Task VI to clear the Task.
7. Use the popup dialog box to display an error if any.

should run loop once or twice and confirm tat I am averageing the samples per scahn...ie 500 points gets read per scan...that should equate to 1 value for each scan

Figure C5: LabView code acqusition[31]

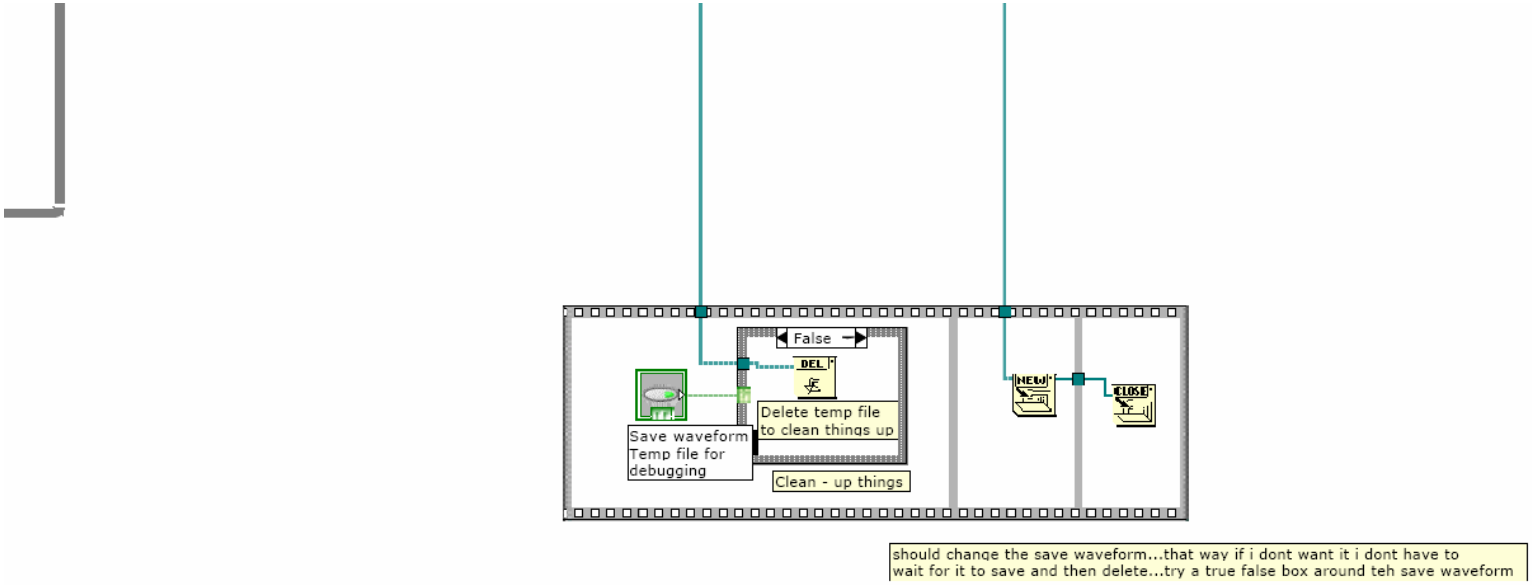

Figure C6: LabView code acqusition[32]

Analysis scripts

<u>Load Cell Calibration Code</u>

```
clear;

%imports data from calibration run into matlab
fid = fopen('Dual channel filtered 100Hz data.txt');
data = load('Dual channel filtered 100Hz data.txt'); %Converts the text file  into martix
A [nx4]
% only grab the data and not the other two parts of the file

%%%%%%%%%%%%%%%%%%%%%%%%%%%%%%%%%%%%%%%
%          ONLY UPDATE IF WEIGHTS USED TO CALIBRATE CHANGE
%hanging masses in normal and shear directions
Ln = [30010.1; 35015.8; 30010.7; 0; 100016.1; 0; 35015.8; 60012.4; 10004.2; 3008;
5005.1; 55013.3; 20006.5; 0; 80018.6; 127987.8; 2003.6; 120022.6; 70014.7; 10004.2;
50008.2; 30010.7; 0; 0; 80018.9; 40012.4; 0; 368828; 368828; 0; 468844.1; 6009.5];

Ls = [320.4; 710.8; 0; 5005.1; 0; 10004.2; 1210.1; 10006.2; 205.7; 825.5; 0; 10006.2;
6009.5; 114.7; 505.1; 320.4; 1509.5; 7008.7; 1004.4; 5005.1; 0; 7008.7; 1829.9;
1004.4; 0; 0; 505.1; 0; 2003.6; 55.4; 8013.1; 14319.9];
%
%%%%%%%%%%%%%%%%%%%%%%%%%%%%%%%%%%%%%%%

%-------------------------------------------------
%UPDATE FOR EVERY CALIBRATION
%interval for zero voltage baseline
baselineinterval = [1.05E4, 1.35E4];
%---------------------------------------------------

% Subtracts off the Baseline y1 voltage
y1= data(1:length(data),3)-mean(data(baselineinterval(1):baselineinterval(2),3));

% Subtracts off the Baseline y2 voltage
y2= data(1:length(data),4)-mean(data(baselineinterval(1):baselineinterval(2),4));

t = linspace (0,length(data)/100,length(data));          % creates a data-point array
according to the length of data
time=t./60;                                    %Converts the data into a time scale

figure(1)
clf
hold on

subplot (3,1,1);                               %plots the data in the time domain
```

```
plot (time,y1,'r',time,y2,'g')
legend('Vs','Vn')
grid on;

subplot (3,1,2);

hold on
plot (y1,'r')                          %plots the data in the datapoint domain for
computation
plot (y2,'g')

legend('Vs','Vn')
grid on;

%-----------------------------------------------
%       UPDATE FOR EVERY CALIBRATION
%Intervals for each loading
intervals =[
   0.60E4,0.85E4;...      %1
   1.9E4,2.2E4;...        %2
   2.9E4,3.1E4;...        %3
   3.9E4,4.2E4;...        %4
   4.9E4,5.2E4;...        %5
   6.0E4,6.3E4;...        %6
   7.3E4,7.6E4;...        %7
   8.5E4,8.7E4;...        %8
   9.6E4,9.8E4;...        %9
   1.05E5,1.08E5;...      %10
   1.15E5,1.18E5;...      %11
   1.26E5,1.30E5;...      %12
   1.37E5,1.39E5;...      %13
   1.46E5,1.49E5;...      %14
   1.57E5,1.59E5;...      %15
   1.67E5,1.69E5;...      %16
   1.77E5,1.79E5;...      %17
   1.87E5,1.89E5;...      %18
   1.97E5,1.99E5;...      %19
   2.05E5,2.07E5;...      %20
   2.13E5,2.16E5;...      %21
   2.23E5,2.26E5;...      %22
   2.34E5,2.36E5;...      %23
   2.43E5,2.45E5;...      %24
   2.49E5,2.52E5;...      %25
   2.57E5,2.60E5;...      %26
   2.67E5,2.70E5;...      %27
   2.75E5,2.77E5;...      %28
   2.83E5,2.85E5;...      %29
```

```
   2.92E5,2.94E5;...       %30
   2.99E5,3.02E5;...       %31
   3.08E5,3.11E5];         %32
%-------------------------------------------------------------------

%Data ranges to be averaged for each point were manually derermined above
Vs =
[mean(y1(intervals(1,1):intervals(1,2)));mean(y1(intervals(2,1):intervals(2,2)));mean(
y1(intervals(3,1):intervals(3,2)));mean(y1(intervals(4,1):intervals(4,2)));mean(y1(inter
vals(5,1):intervals(5,2)));mean(y1(intervals(6,1):intervals(6,2)));...

mean(y1(intervals(7,1):intervals(7,2)));mean(y1(intervals(8,1):intervals(8,2)));mean(y
1(intervals(9,1):intervals(9,2)));mean(y1(intervals(10,1):intervals(10,2)));mean(y1(int
ervals(11,1):intervals(11,2)));mean(y1(intervals(12,1):intervals(12,2)));...


mean(y1(intervals(13,1):intervals(13,2)));mean(y1(intervals(14,1):intervals(14,2)));me
an(y1(intervals(15,1):intervals(15,2)));mean(y1(intervals(16,1):intervals(16,2)));mean
(y1(intervals(17,1):intervals(17,2)));mean(y1(intervals(18,1):intervals(18,2)));...

mean(y1(intervals(19,1):intervals(19,2)));mean(y1(intervals(20,1):intervals(20,2)));me
an(y1(intervals(21,1):intervals(21,2)));mean(y1(intervals(22,1):intervals(22,2)));mean
(y1(intervals(23,1):intervals(23,2)));mean(y1(intervals(24,1):intervals(24,2)));...

mean(y1(intervals(25,1):intervals(25,2)));mean(y1(intervals(26,1):intervals(26,2)));me
an(y1(intervals(27,1):intervals(27,2)));mean(y1(intervals(28,1):intervals(28,2)));mean
(y1(intervals(29,1):intervals(29,2)));mean(y1(intervals(30,1):intervals(30,2)));...

mean(y1(intervals(31,1):intervals(31,2)));mean(y1(intervals(32,1):intervals(32,2)))];

Vn =
[mean(y2(intervals(1,1):intervals(1,2)));mean(y2(intervals(2,1):intervals(2,2)));mean(
y2(intervals(3,1):intervals(3,2)));mean(y2(intervals(4,1):intervals(4,2)));mean(y2(inter
vals(5,1):intervals(5,2)));mean(y2(intervals(6,1):intervals(6,2)));...

mean(y2(intervals(7,1):intervals(7,2)));mean(y2(intervals(8,1):intervals(8,2)));mean(y
2(intervals(9,1):intervals(9,2)));mean(y2(intervals(10,1):intervals(10,2)));mean(y2(int
ervals(11,1):intervals(11,2)));mean(y2(intervals(12,1):intervals(12,2)));...


mean(y2(intervals(13,1):intervals(13,2)));mean(y2(intervals(14,1):intervals(14,2)));me
an(y2(intervals(15,1):intervals(15,2)));mean(y2(intervals(16,1):intervals(16,2)));mean
(y2(intervals(17,1):intervals(17,2)));mean(y2(intervals(18,1):intervals(18,2)));...

mean(y2(intervals(19,1):intervals(19,2)));mean(y2(intervals(20,1):intervals(20,2)));me
an(y2(intervals(21,1):intervals(21,2)));mean(y2(intervals(22,1):intervals(22,2)));mean
(y2(intervals(23,1):intervals(23,2)));mean(y2(intervals(24,1):intervals(24,2)));...
```

```
mean(y2(intervals(25,1):intervals(25,2)));mean(y2(intervals(26,1):intervals(26,2)));me
an(y2(intervals(27,1):intervals(27,2)));mean(y2(intervals(28,1):intervals(28,2)));mean
(y2(intervals(29,1):intervals(29,2)));mean(y2(intervals(30,1):intervals(30,2)));...

mean(y2(intervals(31,1):intervals(31,2)));mean(y2(intervals(32,1):intervals(32,2)))];


Vs = Vs.*1000;                          %Convert Volts to mV
Vn = Vn.*1000;                          %Convert Volts to mV

subplot (3,1,3);

hold on
plot (Vs,'ro')                          %Plots the averaged voltages for each Load
plot (Vn,'g*')
legend('Vs','Vn')


Shearload= [Vs,Vn,Ls];                  % matrix [normal voltage(mV), shear
voltage(mV), shear load(mg)
Normload = [Vs,Vn,Ln];                  % matrix [normal voltage(mV), shear
voltage(mV), normal load(mg)


%MATLAB CODE FOR PLANE OF BEST FIT
% This code determines the best fit plane for both the normal and shear
% loads, graphs them both and also graphs both point coulds from which the
% best fit plane was calculated

Xi = Normload(:,1);
Yi = Normload(:,2);
Zi = Normload(:,3);

Xi2 = Shearload(:,1);
Yi2 = Shearload(:,2);
Zi2 = Shearload(:,3);

n=size(Xi);
n=n(:,1);

n2=size(Xi2);
n2=n2(:,1);

Xb=sum(Xi)/n;
Yb=sum(Yi)/n;
Zb=sum(Zi)/n;
```

```
Xb2=sum(Xi2)/n2;
Yb2=sum(Yi2)/n2;
Zb2=sum(Zi2)/n2;

A(:,1)=Xi-Xb;
A(:,2)=Yi-Yb;
A(:,3)=Zi-Zb;

A2(:,1)=Xi2-Xb2;
A2(:,2)=Yi2-Yb2;
A2(:,3)=Zi2-Zb2;

[U,S,V]=svd(A,0);

[U2,S2,V2]=svd(A2,0);

temp1=S(1,1);
temp2=S(2,2);
temp3=S(3,3);

temp12=S2(1,1);
temp22=S2(2,2);
temp32=S2(3,3);


if(temp1<temp2&temp1<temp3)
  point=1;
elseif(temp2<temp1&temp2<temp3)
  point=2;
elseif(temp3<temp1&temp3<temp2)
  point=3;
end

if(temp12<temp22&temp12<temp32)
  point2=1;
elseif(temp22<temp12&temp22<temp32)
  point2=2;
elseif(temp32<temp12&temp32<temp22)
  point2=3;
end

a=V(1,point)
b=V(2,point)
c=V(3,point)

a2=V2(1,point2)
```

```
b2=V2(2,point2)
c2=V2(3,point2)

X=Xi;
Y=Yi;
Z =Zb-((a/c)*(Xi-Xb))-((b/c)*(Yi-Yb));

X2=Xi2;
Y2=Yi2;
Z2=Zb2-((a2/c2)*(Xi2-Xb2))-((b2/c2)*(Yi2-Yb2));

K_inv = [-a2/c2 -b2/c2;-a/c -b/c]
K = inv(K_inv)

C1 = (((a2*Xb2)/(c2))+((b2*Yb2)/(c2))+((c2*Zb2)/(c2)));
C2 = (((a*Xb)/(c))+((b*Yb)/(c))+((c*Zb)/(c)));
C_matrix = [C1;C2]

[XI,YI]=meshgrid(linspace(min(X),max(X),40),linspace(min(Y),max(Y),40));

ZI1=griddata(X,Y,Z,XI,YI);
ZI2=griddata(X,Y,Zi,XI,YI);

[XI2,YI2]=meshgrid(linspace(min(X2),max(X2),40),linspace(min(Y2),max(Y2),40));

ZI12=griddata(X2,Y2,Z2,XI2,YI2);
ZI22=griddata(X2,Y2,Zi2,XI2,YI2);

figure(3); clf; hold on;
                        %surf(XI,YI,ZI1);
surf(XI,YI,ZI2);
plot3(Xi,Yi,Zi,'r*');

surf(XI2,YI2,ZI12);
plot3(Xi2,Yi2,Zi2,'b*');

grid on;
xlabel('\bfVs(mV)')
ylabel('\bfVn(mV)')
zlabel('\bfLoad(mg)')
legend('Normal','Shear')
```

Friction Analysis Code

```
function [Z]=frictionanalysis(name);
close all
format compact

%Over all program concept...
%   -Have a script which will run multiple analyses...with the individual
%   analysis tasks beng run as functions
%   -Labview will run instrument, filter raw data, and save data for
%   analysis
%   - Analysis program will...
%   1) take filtered data and decouple the directions
%   2) rectify the data
%   3) eliminate points that were aquired in transition of oscillation
%   4) fit the Normal load data to an exponential model
%   5) fit the shear load to a model?
%   6) calculate the instaneous friction coefficent
%   7) fit model to friction coefficent and output min and equlibrium
%      points
%   8) graph filtered raw data, decoupled, rectified data with no
%      transition points for both channels, data with their respective
%      model fits, mu, with model fit.
%

% Get decoupling coefficients for the correct LC
[k11,k12,k21,k22,C1,C2,shiftfact]=getLCdecoupledata(name);

% Get the data and determine shear and normal channels ... voltages are in [mV]
[data,timeminutes,timeaxis,sfreq,rawVs,rawVn]=getvoltagechannels(name);

% The calibration program references an unloaded state and measures the
% diff from the unloaded to loaded state.  So for the friction data I need to
% find the unloaded state and reference everything from there.  To do this I
% will transform the data so that the reference state is zero and then use the
% magnitude of the signal to measure the loaded state.  The reference state is
% found at end of the data set and then the signal is transformed.

refintervalVs=rawVs(end-100:end-30);  %interval is the unloaded end of the data set
(last 10 sec except the very last 3 sec)
refvalueVs=mean(refintervalVs);
refintervalVn=rawVn(end-100:end-30);  %interval is the unloaded end of the data set
(last 10 sec except the very last 3 sec)
refvalueVn=mean(refintervalVn);

Vs=(rawVs-refvalueVs);
Vn=(rawVn-refvalueVn);
```

```
% Decouple the 2 channels ... when done load data is in [g]

Lsraw = (k11*Vs)+(k12*Vn)+C1;
Lnraw = (k21*Vs)+(k22*Vn)+C2;
Lsrawplot = ((k11*Vs)+(k12*Vn)+C1)/1000;
Ls=(Lsraw+(shiftfact*Lnraw))/1000;
Ln=(Lnraw)/1000;

% Calculate the friction coefficient

mu=Ls./Ln;
% figure(10)
% plot(timeaxis,abs(mu),'g', timeaxis, abs(mu1),'r');
% hold;
% title('mu vs time');

figure(3);
hold on;
% subplot(2,1,2);
plot(timeaxis,mu,'b');
refline(0,0);
xlabel('Time (min)');
ylabel('mu');
Title('Friction Coefficient');
% subplot(2,1,2);
% plot(timeaxis,Ln,'r');
% refline(0,0);
% xlabel('Time (min)');
% ylabel('Ln (g)');
% Title('Temporal Normal Load');
hold off;

% Eliminate LC transitions

figure(2)
plot(timeaxis,Ls,'g');
hold;

figure(3)
plot(timeaxis,Ln,'r');
hold;

intervals = [200, 800;...
   1000,   1500;...
   1900,   2200;...
   2700,   3000;...
```

```
   3400,   3700;...
   4200,   4500;...
   5400,   5700];

Lspoints =
[mean(Ls(intervals(1,1):intervals(1,2)));mean(Ls(intervals(2,1):intervals(2,2)));mean(
Ls(intervals(3,1):intervals(3,2)));mean(Ls(intervals(4,1):intervals(4,2)));mean(Ls(inter
vals(5,1):intervals(5,2)));mean(Ls(intervals(6,1):intervals(6,2)));mean(Ls(intervals(7,1
):intervals(7,2)))]
Lnpoints =
[mean(Ln(intervals(1,1):intervals(1,2)));mean(Ln(intervals(2,1):intervals(2,2)));mean(
Ln(intervals(3,1):intervals(3,2)));mean(Ln(intervals(4,1):intervals(4,2)));mean(Ln(inte
rvals(5,1):intervals(5,2)));mean(Ln(intervals(6,1):intervals(6,2)));mean(Ln(intervals(7,
1):intervals(7,2)))]

solun=Fit(Lnpoints,Lspoints,'a*x+b')

figure(4)
plot(Lnpoints,Lspoints,'k');
%ezplot(solun(1)*x+solun(b));
hold;
solun(1)

figure(5)
plot(timeaxis,Ls1,'r');hold;
plot(timeaxis,Ls,'b');

A = [Ls,Ln];

figure(6)
plot(timeaxis,abs(Ls1),'r');hold;

%
% intervals2 = [
%     10.4,10.85;...       %1
%     9.10,9.4;...         %2
%     9.92,10.2;...        %3
%     11.1,11.37;...         %4
%     12.27,13.0;...       %5
%     13.6,14.0;...        %6
%     15.02,15.4];         %7
%

%%%%%%%%%%%%%%%%%%%%%%%%%%%%%%%%%%%%%%%%%%%%%%%%%%%%%%%%%%%%%%%%%%%%%%%
%Create Plots
% Plot the adjusted data for each channel
```

```
figure(1);
hold on;
subplot(2,1,1);
plot(timeaxis,rawVs,'g',timeaxis,Vs,'r');
refline(0,0);
xlabel('Time (min)');
ylabel('Vs (mV)');
Title('Adjusted Vs');
subplot(2,1,2);
plot(timeaxis,rawVn,'g',timeaxis,Vn,'r');
refline(0,0);
xlabel('Time (min)');
ylabel('Vn (mV)');
Title('Adjusted Vn');
hold off;

% Plot the load data for each channel
figure(2);
hold on;
subplot(2,1,1);
plot(timeaxis,Lsrawplot,'g',timeaxis,Ls,'r');
refline(0,0);
xlabel('Time (min)');
ylabel('Ls (g)');
Title('Temporal Shear Load');
subplot(2,1,2);
plot(timeaxis,Ln,'r');
refline(0,0);
xlabel('Time (min)');
ylabel('Ln (g)');
Title('Temporal Normal Load');
hold off;

*****************************************
function [k11,k12,k21,k22,C1,C2,shiftfact]=getLCdecoupledata(name);
format long

mydir=pwd
cd '..';
cd
cd '..';
cd

LCnumb = STRTOK(name,'.txt')
LCdecoupmatrix = [LCnumb 'decouple.txt']
LCdecoupmatrix
K = importdata(LCdecoupmatrix);
```

```
k11=K(1,1);
k12=K(1,2);
k21=K(2,1);
k22=K(2,2);
C1=K(3,1);
C2=K(4,1);
shiftfact=K(5,1);

cd(mydir)

**********************************************************

function [Z]=SplitData;

%%%%%%%%%%%%%%%%%%%%%%%%%%%%%%%%%%%%%%%%%%%%%%%%%%%%%%%%
% SplitData function takes the raw data file from the instrument which
% LabView records of all acquired LC channels and parses the file into
% data from individual LCs.  The file is of the format:
% [arbitary number from timestamp, 1st channel data, 2nd channel data]

% Features to still incorporate:
% 1)some how identifying the true LC number used as opposed to a false number

rawdata = importdata('Dual channel filtered 100Hz data.txt');

nLC = size(rawdata,2);
i=3;

for J=1:(nLC-1)/2,
   A = [rawdata(:,1),rawdata(:,i),rawdata(:,i+1)];
   i=i+2;
   num=int2str(J);
   LCname=[num 'LC.txt'];
   save(LCname,'A','-ascii','-tabs');
end



**********************************************************
%Clean up files subroutine

format compact
clear all
clc

mydir = pwd;
```

```
cd ..;
addpath(pwd);
cd(mydir);

dtop = dir;

sz = size(dtop,1);

% reads the folders in the same folder as the code
if sz >= 3
     disp('Please wait, cleaning up your files')
  for i = 3:sz
    if dtop(i).isdir == 1
      disp(dtop(i).name);
      cd(dtop(i).name);
      dmid = dir;

      szm = size(dmid,1);
      if szm >= 3
        for j = 3:szm
          if dmid(j).isdir == 1
            disp(dmid(j).name)
            cd(dmid(j).name);

            mkdir Raw_Data;
            mkdir Split_LC_Data_Files;

            SplitData;

            [success,msg,msgid] = movefile('Dual*.txt','Raw_Data');
            [success,msg,msgid] = movefile('*LC.txt','Split_LC_Data_Files');

            delete marker.txt;
            delete *.ASV;
            delete done.txt;
            delete full*.txt;

            cd Raw_Data;
            delete *.ASV;
            cd '..';
            cd Split_LC_Data_Files;
            delete *.ASV;
            cd '..';
            disp('complete');
           cd '..';

          end
```

```
      end
    end

    cd '..';
   end
  end
end

 delete *.ASV;
```

****

```
%Plot raw data

% Write the name of the file to be used, Ex. fid = fopen('file_name.ext');
% ext is the extension of the file (Ex. .txt, .dat)

fid = fopen('Dual channel filtered 100Hz data.txt');

% Load Function is used for reading the file and write it under a variable name
% Ex. A (or matrix name) = load('file_name.ext');

A = load('Dual channel filtered 100Hz data.txt');

% The next two commands are use for defining the columns of the data-file Dual
channel filtered 100Hz data to be used
% In this case normal force and shear force resulting voltages, third and fourth column
from the data-file.
% Ex. Variable = matrixload(:,(column_#));

Y = A(:,3);

Z = A(:,4);

% L2 = A(:,5);
%
% L2n = A(:,6);

% Defining a vector so we can plot the variables defined above against a column of
real number recognized by the program.
% Ex. V = starting_number : count_format : last_number
% Last number could be found by loading the file using the load command directly
from the main MATLAB window\Command Window

V = 1:1:length(A(:,1));

% PLOT command is finally use for creating the plot.
```

```
% Ex. plot(x_axis_values , y_axis_values);

figure(1);
plot(V,Y);

figure(2);
plot(V,Z);

figure(3);
plot(V,L2);

figure(4);
plot(V,L2n);
```

D. FRICTION TESTING PROTOCOL

Sample harvest & preparation

Full thickness patellofemoral groove sections were harvested from young bovine stifle joints. The tissue was delaminated from the underlying bone, placed in a 50 ml conical tube, and frozen "dry" at -20 ºC.

At the time of testing the frozen cartilage was removed from the freezer and Dulbecco's Phosphate-Buffered Saline (PBS) was poured into the tube to submerge the cartilage. Sterility of the solutions and handling the cartilage is of little importance as testing occured immediately. The cartilage was thawed in a water bath at 37 ºC, until completely thawed (approx 20 min).

Using a biopsy punch and scalpel, the goal was to create a 6mm diameter by ~2mm tall right cylinder. To do this, the flattest part of the cartilage surface was found and the biopsy punch was held perpendicular to the surface. The cylindrical cut was made and a scalpel was used to undercut the cylinder and release it from the surrounding cartilage. Once the cylinder was cut free, a custom jig or calipers were used to make the final cut with the scalpel. The final cut trimmed the cylinder to the correct height specified by the test. For most tests, a 2mm thick sample was ideal and the final cut was made as close to parallel to the surface as possible. This produced a 6mm diameter by 2mm thick right cylinder. Hereby it is referred to as the "sample."

** At all times, it is very important to keep the tissue hydrated and minimize the time it takes to create the individual samples.

*** If testing will be prolonged or assays will be conducted to investigate biochemical composition, then protease inhibitors should be used in all solutions. In particular

protease inhibitors should be in the initial PBS used for cartilage thawing as large amounts of proteases would be expected to be released at that time.

Running a friction test

The pointed stainless steel rod on the end of the load cell interacts with a brass sample holder. On the one side of the sample holder, a blind conical hole is present which accepts the point from the load cell, and on the reverse of the sample holder a series of circular marks are present. The circular scribes are markings to orient tissue samples of various diameters so that the tissue is concentric with the sample holder. This would allow a uniform normal strain to be applied by the load cell on the tissue.

Take the cartilage sample and glue it onto the sample holder using the circular marks as a guide. It is important to use a "gel" superglue, as regular superglue will wick along the tissue surface due to the hydrated nature of the cartilage, and encase the sample. The gel superglue does not flow like regular superglue and thus there is no significant tissue penetration or encapsulation. As in the case of cutting the samples, it is important to keep the tissue hydrated, so samples with sample holders glued on are stored submerged in a beaker with PBS.

To run a friction test, you must know what axial (normal) strains you wish to apply as well as the surface speeds you want to generate. As the motor control programs to move the stage and load cells are evolving, this section will discuss the principles of running a test rather than specifics about the motor control and acquisition programs.

Place the tissue, articulating surface down against the glass. Turn on the acquisition software so that you can see the live signals from the load cell. Due to the significant difference in sensitivity between the normal and shear channels on the load

cell, the shear channel will have a higher oscillating voltage as a result of random noise/vibration. As you slowly bring the load cell into contact with the sample holder in the conical hole, watch the shear channel. You will know that you are in contact with the sample holder as the noise in the shear channel will dissipate and you will be able to observe a slight tare load in the normal channel. At that point you have set the zero point from which you will apply known displacements to apply strain to the sample. Once the axial zero point has been achieved, start the table oscillating to produce a constant surface speed. Allow the system to equilibrate (~ 2 min) and then start your experiment by applying a given normal strain. Further details of experimental protocols used herein are found in chapters 2-5.

** Other experiments investigating tissue-material interfaces can be conducted by swapping out the glass for the desired material you wish to investigate.

*** Beware of wear. Prolonged friction due to complicated testing paradigms may wear the tissue or the lubricant being tested. Testing paradigms should be randomized to test for hysteresis, which may indicate changes in friction coefficients due to wear.

REFERENCES

1. Akizuki, S., et al., *Tensile properties of human knee joint cartilage: I. Influence of ionic conditions, weight bearing, and fibrillation on the tensile modulus.* J Orthop Res, 1986. **4**(4): p. 379-92.

2. Ateshian, G.A., *A theoretical formulation for boundary friction in articular cartilage.* J Biomech Eng, 1997. **119**(1): p. 81-6.

3. Ateshian, G.A., et al., *The Role of Osmotic Pressure and Tension-Compressio Nonlinearity in the Frictional Response of Articular Cartilage.* Transport in Porous Media, 2003. **50**: p. 5-33.

4. Ateshian, G.A., H.Q. Wang, and W.M. Lai, *The role of interstitial fluid pressurization and surface porosities on the boundary friction of articular cartilage.* Journal of Tribology-Transactions of the Asme, 1998. **120**(2): p. 241-248.

5. Aviad, A.D. and J.B. Houpt, *The Molecular-Weight of Therapeutic Hyaluronan (Sodium Hyaluronate) - How Significant Is It.* Journal of Rheumatology, 1994. **21**(2): p. 297-301.

6. Aydelotte, M.B., R.R. Greenhill, and K.E. Kuettner, *Differences between sub-populations of cultured bovine articular chondrocytes. II. Proteoglycan metabolism.* Connect Tissue Res, 1988. **18**(3): p. 223-34.

7. Aydelotte, M.B. and K.E. Kuettner, *Differences between sub-populations of cultured bovine articular chondrocytes. I. Morphology and cartilage matrix production.* Connect Tissue Res, 1988. **18**(3): p. 205-22.

8. Bailey, A.J., *Molecular mechanisms of ageing in connective tissues.* Mech Ageing Dev, 2001. **122**(7): p. 735-55.

9. Baker, C.L., Jr. and C.M. Ferguson, *Future treatment of osteoarthritis.* Orthopedics, 2005. **28**(2 Suppl): p. s227-34.

10. Ballyns, J.J., et al., *CT-guided injection molding of tissue engineered meniscus.* Trans Orthop Res Soc, 2005. **30**: p. 292.

11. Barnett, C.H. and A.F. Cobbold, *Lubrication within Living Joints.* Journal of Bone and Joint Surgery-British Volume, 1962. **44**(3): p. 662-674.

12. Basalo, I.M., et al., *Chondroitin sulfate reduces the friction coefficient of articular cartilage.* Journal of Biomechanics, 2007. **40**(8): p. 1847-54.

13. Bell, C.J., E. Ingham, and J. Fisher, *Influence of hyaluronic acid on the time-dependent friction response of articular cartilage under different conditions.* Proceedings of the Institution of Mechanical Engineers Part H-Journal of Engineering in Medicine, 2006. **220**(H1): p. 23-31.

14. Benz, M., et al., *Static forces, structure and flow properties of complex fluids in highly confined geometries.* Annals of Biomedical Engineering, 2005. **33**(1): p. 39-51.

15. Bianco, P., et al., *Expression and localization of the two small proteoglycans biglycan and decorin in developing human skeletal and non-skeletal tissues.* J Histochem Cytochem, 1990. **38**(11): p. 1549-63.

16. Bland, J.H. and S.M. Cooper, *Osteoarthritis: a review of the cell biology involved and evidence for reversibility. Management rationally related to known genesis and pathophysiology.* Semin Arthritis Rheum, 1984. **14**(2): p. 106-33.

17. Buckley, M.R., et al., *Mapping the depth dependence of shear properteis in articular cartilage.* J Biomech 2008: p. in press.

18. Buckwalter, J.A., *Osteoarthritis and articular cartilage use, disuse, and abuse: experimental studies.* Journal of Rheumatology. Supplement, 1995. **43**: p. 13-5.

19. Buschmann, M.D. and A.J. Grodzinsky, *A molecular model of proteoglycan-associated electrostatic forces in cartilage mechanics.* J Biomech Eng, 1995. **117**(2): p. 179-92.

20. Carter, M.J., I.M. Basalo, and G.A. Ateshian, *The temporal response of the friction coefficient of articular cartilage depends on the contact area.* J Biomech, 2007.

21. Cassin, G., E. Heinrich, and H.A. Spikes, *The influence of surface roughness on the lubrication properties of adsorbing and non-adsorbing biopolymers.* Tribology Letters, 2001. **11**(2): p. 95-102.

22. Cawston, T.E., et al., *The role of oncostatin M in animal and human connective tissue collagen turnover and its localization within the rheumatoid joint.* Arthritis Rheum, 1998. **41**(10): p. 1760-71.

23. Chang, S.C., et al., *Injection molding of chondrocyte/alginate constructs in the shape of facial implants.* J Biomed Mater Res, 2001. **55**(4): p. 503-11.

24. Charnley, J. *The lubrication of animal joints*. in *Symposium on Biomechanics*. 1959. London, UK: Institute of Mechanical Engineers.

25. Charnley, J., *The lubrication of animal joints.* New Scientist, 1959. **6**: p. 60.

26. Charnley, J., *The lubrication of animal joints in relation to surgical reconstruction by arthroplasty.* Ann Rheum Dis, 1960. **19**: p. 10-9.

27. Charnley, J., *How our joints are lubricated.* Triangle, 1960. **4**: p. 175-9.

28. Chen, A.C., et al., *Depth- and strain-dependent mechanical and electromechanical properties of full-thickness bovine articular cartilage in confined compression.* Journal of Biomechanics, 2001. **34**(1): p. 1-12.

29. Clark, J.M., et al., *The surface contour of articular cartilage in an intact, loaded joint.* Journal of Anatomy, 1999. **195, Pt 1**: p. 45-56.

30. Cooke, T.D., *Rheumatoid arthritis pannus: true or false?* Arthritis Rheum, 1985. **28**(10): p. 1195-8.

31. Cunnane, G., et al., *Mechanism of joint destruction in rheumatoid arthritis.* Arch Immunol Ther Exp (Warsz), 1998. **46**(1): p. 1-7.

32. Darling, E.M. and K.A. Athanasiou, *Growth factor impact on articular cartilage subpopulations.* Cell Tissue Res, 2005. **322**(3): p. 463-73.

33. Darling, E.M. and K.A. Athanasiou, *Retaining zonal chondrocyte phenotype by means of novel growth environments.* Tissue Eng, 2005. **11**(3-4): p. 395-403.

34. Davis, W.H., Jr., S.L. Lee, and L. Sokoloff, *Boundary lubricating ability of synovial fluid in degenerative joint disease.* Arthritis and Rheumatism, 1978. **21**(7): p. 754-6.

35. Dean, D., et al., *Compressive nanomechanics of opposing aggrecan macromolecules.* J Biomech, 2006. **39**(14): p. 2555-65.

36. Dowson, D. *Modes of lubrication in human joints*. in *Symposium on Lubrication and Wear in Living and Artifical Human Joints: Proceedings*. 1966. London: Institute of Mechanical Engineers.

37. Dowson, D., *New joints for the Millennium: wear control in total replacement hip joints.* Proceedings of the Institution of Mechanical Engineers. Part H, 2001. **215**(4): p. 335-58.

38. Dowson, D. and Z.M. Jin, *Micro-elastohydrodynamic lubrication of synovial joints.* Eng Med, 1986. **15**(2): p. 63-5.

39. Dowson, D., V. Wright, and M.D. Longfield, *Human joint lubrication.* Biomed Eng, 1969. **4**: p. 160-165.

40. Durigova, M., P.J. Roughley, and J.S. Mort, *Mechanism of proteoglycan aggregate degradation in cartilage stimulated with oncostatin M.* Osteoarthritis Cartilage, 2007.

41. Eckstein, F., et al., *In vivo cartilage deformation after different types of activity and its dependence on physical training status.* Annals of the Rheumatic Diseases, 2005. **64**(2): p. 291-5.

42. Eisenberg, S.R. and A.J. Grodzinsky, *Swelling of Articular-Cartilage and Other Connective Tissues - Electromechanochemical Forces.* Journal of Orthopaedic Research, 1985. **3**(2): p. 148-159.

43. Elsaid, K.A., G.D. Jay, and C.O. Chichester, *Reduced expression and proteolytic susceptibility of lubricin/superficial zone protein may explain early elevation in the coefficient of friction in the joints of rats with antigen-induced arthritis.* Arthritis Rheum, 2007. **56**(1): p. 108-16.

44. Enobakhare, B.O., D.L. Bader, and D.A. Lee, *Quantification of sulfated glycosaminoglycans in chondrocyte/alginate cultures, by use of 1,9-dimethylmethylene blue.* Anal Biochem, 1996. **243**(1): p. 189-91.

45. Eyre, D., *Collagen of articular cartilage.* Arthritis Research, 2002. **4**(1): p. 30-35.

46. Eyre, D.R., et al., *Covalent cross-linking of the NC1 domain of collagen type IX to collagen type II in cartilage.* J Biol Chem, 2004. **279**(4): p. 2568-74.

47. Fein, R.S., *Are synovail joints squeeze-film lubricated?* Proc Inst Mech Eng [H], 1967. **181**: p. 125-128.

48. Flannery, C.R., et al., *Articular cartilage superficial zone protein (SZP) is homologous to megakaryocyte stimulating factor precursor and Is a multifunctional proteoglycan with potential growth-promoting, cytoprotective, and lubricating properties in cartilage metabolism.* Biochem Biophys Res Commun, 1999. **254**(3): p. 535-41.

49. Forster, H. and J. Fisher, *The influence of loading time and lubricant on the friction of articular cartilage.* Proc Inst Mech Eng [H], 1996. **210**(2): p. 109-19.

50. Forster, H. and J. Fisher, *The influence of continuous sliding and subsequent surface wear on the friction of articular cartilage.* Proceedings of the Institution of Mechanical Engineers. Part H, 1999. **213**(4): p. 329-45.

51. Foundation, A., *Arthritis Foundation: The Facts About Arthritis*. 2006.

52. Garg, H.G. and D.A. Swann, *The structure of the O-glycosylically-linked oligosaccharide chains of LGP-I, a glycoprotein present in articular lubricating fraction of bovine synovial fluid.* Carbohydrate Res, 1979. **78**: p. 79-88.

53. Genes, N.G., et al., *Effect of substrate mechanics on chondrocyte adhesion to modified alginate surfaces.* Arch Biochem Biophys, 2004. **422**(2): p. 161-7.

54. Gleghorn, J.P. and L.J. Bonassar, *Mapping of Cartilage Lubrication Modes Using Stribeck Analysis.* Trans Orthop Res Soc, 2007. **32**: p. 613.

55. Gleghorn, J.P., et al., *Boundary mode frictional properties of engineered cartilaginous tissues.* European Cells and Materials, 2007. **14**: p. 20-8; discussion 28-9.

56. Gleghorn, J.P., et al., *Role of Endogeneous and Exogeneous Lubricin in Lubrication of Articular Cartilage.* Trans Intl Cart Rep Soc, 2006. **7c-6**.

57. Gleghorn, J.P., et al., *Lubrication of Articular Cartilage by Recombinant Human Lubricin.* Trans Orthop Res Soc, 2006. **31**: p. 1502.

58. Grad, S., et al., *Surface motion upregulates superficial zone protein and hyaluronan production in chondrocyte-seeded three-dimensional scaffolds.* Tissue Eng, 2005. **11**(1-2): p. 249-56.

59. Grad, S., et al., *Chondrocyte gene expression under applied surface motion.* Biorheology, 2006. **43**(3-4): p. 259-69.

60. Graindorge, S., et al., *The role of the surface amorphous layer of articular cartilage in joint lubrication.* Proceedings of the Institution of Mechanical Engineers Part H-Journal of Engineering in Medicine, 2006. **220**(H5): p. 597-607.

61. Grodzinsky, A.J., et al., *Cartilage tissue remodeling in response to mechanical forces.* Annu Rev Biomed Eng, 2000. **2**: p. 691-713.

62. Han, L., et al., *Nanoscale shear deformation mechanisms of opposing cartilage aggrecan macromolecules.* Biophys J, 2007. **93**(5): p. L23-5.

63. Han, L., et al., *Lateral nanomechanics of cartilage aggrecan macromolecules.* Biophys J, 2007. **92**(4): p. 1384-98.

64. Hascall, V.C. and J.H. Kimura, *Proteoglycans: isolation and characterization.* Methods Enzymol, 1982. **82 Pt A**: p. 769-800.

65. Hassell, J.R., J.H. Kimura, and V.C. Hascall, *Proteoglycan core protein families.* Annu Rev Biochem, 1986. **55**: p. 539-67.

66. Hersey, M.D., *Laws of Lubrication.* Journal of the Washington Academy of Sciences, 1914. **4**: p. 542-552.

67. Hersey, M.D., *Theory of Lubrication, 2nd Edition*. 1938, New York,: Wiley. xiii, 488.

68. Higginson, G.R. and R. Norman, *A model investigation of squeeze-film lubrication in animal joints.* Physics in Medicine and Biology, 1974. **19**(6): p. 785-92.

69. Hills, B.A., *Oligolamellar lubrication of joints by surface active phospholipid.* J Rheumatol, 1989. **16**(1): p. 82-91.

70. Hills, B.A. and M.K. Monds, *Enzymatic identification of the load-bearing boundary lubricant in the joint.* British Journal of Rheumatology, 1998. **37**(2): p. 137-42.

71. Hlavacek, M., *The Role of Synovial-Fluid Filtration by Cartilage in Lubrication of Synovial Joints .2. Squeeze-Film Lubrication - Homogeneous Filtration.* Journal of Biomechanics, 1993. **26**(10): p. 1151-1160.

72. Hlavacek, M., *Squeeze-film lubrication of the human ankle joint with synovial fluid filtrated by articular cartilage with the superficial zone worn out.* Journal of Biomechanics, 2000. **33**(11): p. 1415-22.

73. Hui, W., M. Bell, and G. Carroll, *Oncostatin M (OSM) stimulates resorption and inhibits synthesis of proteoglycan in porcine articular cartilage explants.* Cytokine, 1996. **8**(6): p. 495-500.

74. Hung, C.T., et al., *A paradigm for functional tissue engineering of articular cartilage via applied physiologic deformational loading.* Ann Biomed Eng, 2004. **32**(1): p. 35-49.

75. Ikegawa, S., et al., *Isolation, characterization and mapping of the mouse and human PRG4 (proteoglycan 4) genes.* Cytogenet Cell Genet, 2000. **90**(3-4): p. 291-7.

76. Jay, G.D., *Characterization of a bovine synovial fluid lubricating factor. I. Chemical, surface activity and lubricating properties.* Connect Tissue Res, 1992. **28**(1-2): p. 71-88.

77. Jay, G.D., *Lubricin and surfacing of articular joints.* Curr Opin Orthop, 2004. **15**: p. 335-359.

78. Jay, G.D., D.E. Britt, and C.J. Cha, *Lubricin is a product of megakaryocyte stimulating factor gene expression by human synovial fibroblasts.* J Rheumatol, 2000. **27**(3): p. 594-600.

79. Jay, G.D. and C.J. Cha, *The effect of phospholipase digestion upon the boundary lubricating ability of synovial fluid.* Journal of Rheumatology, 1999. **26**(11): p. 2454-2457.

80. Jay, G.D., et al., *Lubricating ability of aspirated synovial fluid from emergency department patients with knee joint synovitis.* J Rheumatol, 2004. **31**(3): p. 557-64.

81. Jay, G.D., K. Haberstroh, and C.J. Cha, *Comparison of the boundary-lubricating ability of bovine synovial fluid, lubricin, and Healon.* J Biomed Mater Res, 1998. **40**(3): p. 414-8.

82. Jay, G.D., D.A. Harris, and C.J. Cha, *Boundary lubrication by lubricin is mediated by O-linked beta(1-3)Gal-GalNAc oligosaccharides.* Glycoconj J, 2001. **18**(10): p. 807-15.

83. Jay, G.D. and B.S. Hong, *Characterization of a bovine synovial fluid lubricating factor. II. Comparison with purified ocular and salivary mucin.* Connect Tissue Res, 1992. **28**(1-2): p. 89-98.

84. Jay, G.D., et al., *Homology of lubricin and superficial zone protein (SZP): products of megakaryocyte stimulating factor (MSF) gene expression by human synovial fibroblasts and articular chondrocytes localized to chromosome 1q25.* J Orthop Res, 2001. **19**(4): p. 677-87.

85. Jay, G.D., et al., *The role of lubricin in the mechanical behavior of synovial fluid.* Proc Natl Acad Sci U S A, 2007. **104**(15): p. 6194-9.

86. Jin, M., et al., *Combined effects of dynamic tissue shear deformation and insulin-like growth factor I on chondrocyte biosynthesis in cartilage explants.* Archives of Biochemistry and Biophysics, 2003. **414**(2): p. 223-31.

87. Jin, M., et al., *Tissue shear deformation stimulates proteoglycan and protein biosynthesis in bovine cartilage explants.* Archives of Biochemistry and Biophysics, 2001. **395**(1): p. 41-8.

88. Jones, A.R. and C.R. Flannery, *Bioregulation of lubricin expression by growth factors and cytokines.* Eur Cell Mater, 2007. **13**: p. 40-5; discussion 45.

89. Jones, A.R., et al., *Binding and localization of recombinant lubricin to articular cartilage surfaces.* J Orthop Res, 2007. **25**(3): p. 283-92.

90. Jones, E.S., *Joint Lubrication.* Lancet, 1934. **228**: p. 1426-7.

91. Jones, E.S., *Joint Lubrication.* Lancet, 1936. **230**: p. 1043-4.

92. Kempson, G.E., *Age-related changes in the tensile properties of human articular cartilage: a comparative study between the femoral head of the hip joint and the talus of the ankle joint.* Biochim Biophys Acta, 1991. **1075**(3): p. 223-30.

93. Kempson, G.E., M.A. Freeman, and S.A. Swanson, *Tensile properties of articular cartilage.* Nature, 1968. **220**(5172): p. 1127-8.

94. Khalafi, A., et al., *Increased accumulation of superficial zone protein (SZP) in articular cartilage in response to bone morphogenetic protein-7 and growth factors.* J Orthop Res, 2007. **25**(3): p. 293-303.

95. Kim, Y.J., L.J. Bonassar, and A.J. Grodzinsky, *The role of cartilage streaming potential, fluid flow and pressure in the stimulation of chondrocyte biosynthesis during dynamic compression.* Journal of Biomechanics, 1995. **28**(9): p. 1055-66.

96. Klein, T.J., et al., *Depth-dependent biomechanical and biochemical properties of fetal, newborn, and tissue-engineered articular cartilage.* J Biomech, 2007. **40**(1): p. 182-90.

97. Klein, T.J., et al., *Tailoring secretion of proteoglycan 4 (PRG4) in tissue-engineered cartilage.* Tissue Eng, 2006. **12**(6): p. 1429-39.

98. Klein, T.J., et al., *Tissue engineering of stratified articular cartilage from chondrocyte subpopulations.* Osteoarthritis Cartilage, 2003. **11**(8): p. 595-602.

99. Klippel, J.H., *Primer on Rheumatic Diseases*. 11 ed. 1997, Atlanta: Arthritis Foundation.

100. Knudson, W., et al., *CD44-anchored hyaluronan-rich pericellular matrices: an ultrastructural and biochemical analysis.* Exp Cell Res, 1996. **228**(2): p. 216-28.

101. Knudson, W. and R.F. Loeser, *CD44 and integrin matrix receptors participate in cartilage homeostasis.* Cell Mol Life Sci, 2002. **59**(1): p. 36-44.

102. Krishnan, R., et al., *Removal of the superficial zone of bovine articular cartilage does not increase its frictional coefficient.* Osteoarthritis and Cartilage, 2004. **12**(12): p. 947-55.

103. Krishnan, R., M. Kopacz, and G.A. Ateshian, *Experimental verification of the role of interstitial fluid pressurization in cartilage lubrication.* J Orthop Res, 2004. **22**(3): p. 565-70.

104. Kuettner, K.E., M.B. Aydelotte, and E.J.M.A. Thonar, *Articular-Cartilage Matrix and Structure - a Minireview.* Journal of Rheumatology, 1991. **18**: p. 46-48.

105. Kuroda, M., et al., *Induction of a secreted protein by the myxoid liposarcoma oncogene.* Proc Natl Acad Sci U S A, 1999. **96**(9): p. 5025-30.

106. LeBaron, R.G. and K.A. Athanasiou, *Ex vivo synthesis of articular cartilage.* Biomaterials, 2000. **21**(24): p. 2575-87.

107. Lee, C.S., et al., *Integration of layered chondrocyte-seeded alginate hydrogel scaffolds.* Biomaterials, 2007. **28**(19): p. 2987-93.

108. Lewis, P.R. and C.W. McCutchen, *Experimental evidence for weeping lubrication in mammalian joints.* Nature, 1959. **184**: p. 1285.

109. Linn, F.C., *Lubrication of animal joints. I. The arthrotripsometer.* J Bone Joint Surg Am, 1967. **49**(6): p. 1079-98.

110. Linn, F.C., *Lubrication of animal joints. II. The mechanism.* Journal of Biomechanics, 1968. **1**(3): p. 193-205.

111. Linn, F.C. and E.L. Radin, *Lubrication of animal joints. 3. The effect of certain chemical alterations of the cartilage and lubricant.* Arthritis Rheum, 1968. **11**(5): p. 674-82.

112. Liu, Y.J., et al., *Hemangiopoietin, a novel human growth factor for the primitive cells of both hematopoietic and endothelial cell lineages.* Blood, 2004. **103**(12): p. 4449-56.

113. Loeser, R.F., *Integrin-Mediated Attachment of Articular Chondrocytes to Extracellular-Matrix Proteins.* Arthritis and Rheumatism, 1993. **36**(8): p. 1103-1110.

114. Loeser, R.F., *Chondrocyte integrin expression and function.* Biorheology, 2000. **37**(1-2): p. 109-116.

115. Longfield, M.D., et al., *"Boosted lubrication" of human joints by fluid enrichment and entrapment.* Biomed Eng, 1969. **4**(11): p. 517-22.

116. Lust, G., et al., *Modulation of fibronectin and proteoglycan synthesis by chondrocytes.* J Rheumatol Suppl, 1991. **27**: p. 58-9.

117. Macconaill, M.A., *The Function of Intra-Articular Fibrocartilages, with Special Reference to the Knee and Inferior Radio-Ulnar Joints.* J Anat, 1932. **66**(Pt 2): p. 210-227.

118. Macirowski, T., S. Tepic, and R.W. Mann, *Cartilage stresses in the human hip joint.* J Biomech Eng, 1994. **116**(1): p. 10-8.

119. Marcelino, J., et al., *CACP, encoding a secreted proteoglycan, is mutated in camptodactyly-arthropathy-coxa vara-pericarditis syndrome.* Nat Genet, 1999. **23**(3): p. 319-22.

120. Marcinko, D.E. and M.D. Dollard, *Physical and mechanical properties of joints (the pathomechanics of articular cartilage degeneration).* J Foot Surg, 1986. **25**(1): p. 3-13.

121. Martin, I., et al., *Modulation of the mechanical properties of tissue engineered cartilage.* Biorheology, 2000. **37**(1-2): p. 141-147.

122. Martin, J.A. and J.A. Buckwalter, *Aging, articular cartilage chondrocyte senescence and osteoarthritis.* Biogerontology, 2002. **3**(5): p. 257-264.

123. Martin, J.A., S.M. Ellerbroek, and J.A. Buckwalter, *Age-related decline in chondrocyte response to insulin-like growth factor-I: the role of growth factor binding proteins.* J Orthop Res, 1997. **15**(4): p. 491-8.

124. Mauck, R.L., et al., *Influence of seeding density and dynamic deformational loading on the developing structure/function relationships of chondrocyte-seeded agarose hydrogels.* Ann Biomed Eng, 2002. **30**(8): p. 1046-56.

125. McCutchen, C.W., *Sponge-Hydrostatic and Weeping Bearings.* Nature, 1959. **184**(4695): p. 1284-1285.

126. McCutchen, C.W., *The frictional properties of animal joints.* Wear, 1962. **5**: p. 1-17.

127. McCutchen, C.W., *Boundary Lubrication by Synovial Fluid - Demonstration and Possible Osmotic Explanation.* Federation Proceedings, 1966. **25**(3P1): p. 1061-3.

128. Meachim, G., *Light-Microscopy of Indian Ink Preparations of Fibrillated Cartilage.* Annals of the Rheumatic Diseases, 1972. **31**(6): p. 457.

129. Merberg, D., L.J. Fitz, and P. Temple. *A comparison of vitronectin and megakarocyte stimulating factor*. in *Biology of vitronectins and their receptors: First International Vitronectin Workshop*. 1993. New York: Elsevier Science B.V.

130. Mohr, W., et al., *Proliferation of pannus tissue cells in rheumatoid arthritis.* Rheumatol Int, 1986. **6**(3): p. 127-32.

131. Morales, T.I., *Transforming growth factor-beta 1 stimulates synthesis of proteoglycan aggregates in calf articular cartilage organ cultures.* Arch Biochem Biophys, 1991. **286**(1): p. 99-106.

132. Morales, T.I. and A.B. Roberts, *Transforming growth factor beta regulates the metabolism of proteoglycans in bovine cartilage organ cultures.* J Biol Chem, 1988. **263**(26): p. 12828-31.

133. Mow, V.C., G.A. Ateshian, and R.L. Spilker, *Biomechanics of diarthrodial joints: a review of twenty years of progress.* J Biomech Eng, 1993. **115**(4B): p. 460-7.

134. Mow, V.C., et al., *Biphasic Creep and Stress-Relaxation of Articular-Cartilage in Compression - Theory and Experiments.* Journal of Biomechanical Engineering-Transactions of the Asme, 1980. **102**(1): p. 73-84.

135. Murakami, T., et al., *Adaptive multimode lubrication in natural synovial joints and artificial joints.* Proceedings of the Institution of Mechanical Engineers Part H-Journal of Engineering in Medicine, 1998. **212**(H1): p. 23-35.

136. Nakamura, K., et al., *Stimulation of bone formation by intraosseous application of recombinant basic fibroblast growth factor in normal and ovariectomized rabbits.* J Orthop Res, 1997. **15**(2): p. 307-13.

137. Neuman, R.E. and M.A. Logan, *The determination of hydroxyproline.* J Biol Chem, 1950. **184**(1): p. 299-306.

138. Niikura, T. and A.H. Reddi, *Differential regulation of lubricin/superficial zone protein by transforming growth factor beta/bone morphogenetic protein superfamily members in articular chondrocytes and synoviocytes.* Arthritis Rheum, 2007. **56**(7): p. 2312-21.

139. Nugent, G.E., et al., *Dynamic shear stimulation of bovine cartilage biosynthesis of proteoglycan 4.* Arthritis Rheum, 2006. **54**(6): p. 1888-96.

140. Nugent, G.E., et al., *Static and dynamic compression regulate cartilage metabolism of PRoteoGlycan 4 (PRG4).* Biorheology, 2006. **43**(3-4): p. 191-200.

141. Nugent-Derfus, G.E., et al., *Continuous passive motion applied to whole joints stimulates chondrocyte biosynthesis of PRG4.* Osteoarthritis Cartilage, 2007. **15**(5): p. 566-74.

142. Ohno, S., et al., *Expression of superficial zone protein in mandibular condyle cartilage.* Osteoarthritis Cartilage, 2006. **14**(8): p. 807-13.

143. Pelletier, J.P. and J. Martel-Pelletier, *Oncostatin M: foe or friend?* Arthritis Rheum, 2003. **48**(12): p. 3301-3.

144. Peyron, J.G., *Epidemiological aspects of osteoarthritis.* Scand J Rheumatol Suppl, 1988. **77**: p. 29-33.

145. Peyron, J.G., *Clinical features of osteoarthritis, diffuse idiopathic skeletal hyperostosis, and hypermobility syndromes.* Curr Opin Rheumatol, 1991. **3**(4): p. 653-61.

146. Pickard, J., et al., *Investigation into the effect of proteoglycan molecules on the tribological properties of cartilage joint tissues.* Proceedings of the Institution of Mechanical Engineers. Part H, 1998. **212**(3): p. 177-82.

147. Pickard, J.E., et al., *Investigation into the effects of proteins and lipids on the frictional properties of articular cartilage.* Biomaterials, 1998. **19**(19): p. 1807-1812.

148. Poole, A.R., et al., *Composition and structure of articular cartilage: a template for tissue repair.* Clin Orthop Relat Res, 2001(391 Suppl): p. S26-33.

149. Poole, A.R., et al., *Cartilage macromolecules and the calcification of cartilage matrix.* Anat Rec, 1989. **224**(2): p. 167-79.

150. Quinn, T.M. and A.J. Grodsinsky, *Longitudinal modulus and hydraulic permeability of poly(methacrylic acid) gels - Effects of charge-density and solvent content.* Macromolecules, 1993. **26**(16): p. 4332-4338.

151. Radin, E.L. and I.L. Paul, *Consolidated Concept of Joint Lubrication.* Journal of Bone and Joint Surgery-American Volume, 1972. **54**(3): p. 606-617.

152. Radin, E.L., D.A. Swann, and P.A. Weisser, *Separation of a Hyaluronate-Free Lubricating Fraction from Synovial Fluid.* Nature, 1970. **228**(5269): p. 377.

153. Rees, S.G., et al., *Immunolocalisation and expression of proteoglycan 4 (cartilage superficial zone proteoglycan) in tendon.* Matrix Biol, 2002. **21**(7): p. 593-602.

154. Reid, D.L., M.B. Aydelotte, and J. Mollenhauer, *Cell attachment, collagen binding, and receptor analysis on bovine articular chondrocytes.* J Orthop Res, 2000. **18**(3): p. 364-73.

155. Rhee, D.K., et al., *The secreted glycoprotein lubricin protects cartilage surfaces and inhibits synovial cell overgrowth.* J Clin Invest, 2005. **115**(3): p. 622-31.

156. Roberts, B.J., A. Unsworth, and N. Mian, *Modes of lubrication in human hip joints.* Ann Rheum Dis, 1982. **41**(3): p. 217-24.

157. Roughley, P.J., E. Rodriguez, and E.R. Lee, *The interactions of 'non-aggregating' proteoglycans.* Osteoarthritis Cartilage, 1995. **3**(4): p. 239-48.

158. Sauermann, W. and T.J. Feuerstein, *Some Mathematical Models for Concentration-Response Relationships.* Biometrical J, 1998. **40**(7): p. 865-881.

159. Schinagl, R.M., et al., *Depth-dependent confined compression modulus of full-thickness bovine articular cartilage.* J Orthop Res, 1997. **15**(4): p. 499-506.

160. Schmid, T., et al., *Superficial zone protein (SZP) from human cartilage has lubrication activity.* Trans Orthop Res Soc, 2001. **26**: p. 178.

161. Schmidt, T.A., et al., *Differential regulation of proteoglycan 4 metabolism in cartilage by IL-1α, IGF-1,and TGF-β1.* Osteoarthritis and Cartilage, 2007. doi:10.1016/j.joca.2007.5.009.

162. Schmidt, T.A. and R.L. Sah, *Effect of synovial fluid on boundary lubrication of articular cartilage.* Osteoarthritis Cartilage, 2007. **15**(1): p. 35-47.

163. Schmidt, T.A., et al., *Synthesis of proteoglycan 4 by chondrocyte subpopulations in cartilage explants, monolayer cultures, and resurfaced cartilage cultures.* Arthritis Rheum, 2004. **50**(9): p. 2849-57.

164. Schumacher, B.L., et al., *A novel proteoglycan synthesized and secreted by chondrocytes of the superficial zone of articular cartilage.* Arch Biochem Biophys, 1994. **311**(1): p. 144-52.

165. Schumacher, B.L., et al., *Immunodetection and partial cDNA sequence of the proteoglycan, superficial zone protein, synthesized by cells lining synovial joints.* J Orthop Res, 1999. **17**(1): p. 110-20.

166. Schumacher, B.L., et al., *Proteoglycan 4 (PRG4) synthesis and immunolocalization in bovine meniscus.* J Orthop Res, 2005. **23**(3): p. 562-8.

167. Schwarz, I.M. and B.A. Hills, *Surface-active phospholipid as the lubricating component of lubricin.* British Journal of Rheumatology, 1998. **37**(1): p. 21-6.

168. Seidel, J.O., et al., *Long-term culture of tissue engineered cartilage in a perfused chamber with mechanical stimulation.* Biorheology, 2004. **41**(3-4): p. 445-58.

169. Soltz, M.A., I.M. Basalo, and G.A. Ateshian, *Hydrostatic pressurization and depletion of trapped lubricant pool during creep contact of a rippled indenter against a biphasic articular cartilage layer.* Journal of Biomechanical Engineering-Transactions of the Asme, 2003. **125**(5): p. 585-593.

170. Su, J.L., et al., *Detection of superficial zone protein in human and animal body fluids by cross-species monoclonal antibodies specific to superficial zone protein.* Hybridoma, 2001. **20**(3): p. 149-57.

171. Sun, Y., et al., *Mapping lubricin in canine musculoskeletal tissues.* Connect Tissue Res, 2006. **47**(4): p. 215-21.

172. Swann, D.A., et al., *The lubricating activity of synovial fluid glycoproteins.* Arthritis Rheum, 1981. **24**(1): p. 22-30.

173. Swann, D.A. and E.L. Radin, *The molecular basis of articular lubrication. I. Purification and properties of a lubricating fraction from bovine synovial fluid.* Journal of Biological Chemistry, 1972. **247**(24): p. 8069-73.

174. Swann, D.A., et al., *The molecular structure and lubricating activity of lubricin isolated from bovine and human synovial fluids.* Biochem J, 1985. **225**(1): p. 195-201.

175. Swann, D.A., H.S. Slayter, and F.H. Silver, *The molecular structure of lubricating glycoprotein-I, the boundary lubricant for articular cartilage.* J Biol Chem, 1981. **256**(11): p. 5921-5.

176. Sweigart, M.A. and K.A. Athanasiou, *Toward tissue engineering of the knee meniscus.* Tissue Eng, 2001. **7**(2): p. 111-29.

177. Szeri, A.Z., *Fluid film lubrication: theory and design*. 1998, Cambridge: Cambridge University Press. 412.

178. Tanner, R.I., *An alternative mechanism for the lubrication of synovial joints.* Physics in Medicine and Biology, 1966. **11**: p. 119-127.

179. Torres, J., et al., *Lubricin Network Deposition is Concentration Dependent and Follows the Effective Contact Boundary Length Model.* Trans Orthop Res Soc, 2006. **31**: p. 902.

180. Unsworth, A., D. Dowson, and V. Wright, *Some new evidence on human joint lubrication.* Ann Rheum Dis, 1975. **34**(4): p. 277-85.

181. Waldman, S.D., et al., *Long-term intermittent shear deformation improves the quality of cartilaginous tissue formed in vitro.* J Orthop Res, 2003. **21**(4): p. 590-6.

182. Walker, P.S., et al., *"Boosted lubrication" in synovial joints by fluid entrapment and enrichment.* Annals of the Rheumatic Diseases, 1968. **27**(6): p. 512-20.

183. Wang, H. and G.A. Ateshian, *The normal stress effect and equilibrium friction coefficient of articular cartilage under steady frictional shear.* Journal of Biomechanics, 1997. **30**(8): p. 771-6.

184. Wang, K., et al., *[Ultramicrostructural changes of articular cartilage, subchondral bone and synovium in human osteoarthritis of patellofemoral joint].* Zhongguo Yi Xue Ke Xue Yuan Xue Bao, 1996. **18**(6): p. 450-6.

185. Wang, Y.S., et al., *Development of a set of Stribeck curves for conformal contacts of rough surfaces.* Tribology Transactions, 2006. **49**(4): p. 526-535.

186. Wick, M.C., et al., *Relationship between inflammation and joint destruction in early rheumatoid arthritis: a mathematical description.* Ann Rheum Dis, 2004. **63**(7): p. 848-52.

187. Wilkins, R.J., J.A. Browning, and J.P.G. Urban, *Chondrocyte regulation by mechanical load.* Biorheology, 2000. **37**(1-2): p. 67-74.

188. Wilson, C.G., et al., *Selective and non-selective metalloproteinase inhibitors reduce IL-1-induced cartilage degradation and loss of mechanical properties.* Matrix Biol, 2007. **26**(4): p. 259-68.

189. Worster, A.A., et al., *Chondrocytic differentiation of mesenchymal stem cells sequentially exposed to transforming growth factor-beta1 in monolayer and insulin-like growth factor-I in a three-dimensional matrix.* J Orthop Res, 2001. **19**(4): p. 738-49.

190. Worster, A.A., et al., *Effect of transforming growth factor beta1 on chondrogenic differentiation of cultured equine mesenchymal stem cells.* Am J Vet Res, 2000. **61**(9): p. 1003-10.

191. Wright, V. and D. Dowson, *Lubrication and cartilage.* J Anat, 1976. **121**(Pt 1): p. 107-18.

192. Yao, J.Q. and A. Unsworth, *Asperity lubrication in human joints.* Proc Inst Mech Eng [H], 1993. **207**(4): p. 245-54.

193. Young, A.A., et al., *Proteoglycan 4 downregulation in a sheep meniscectomy model of early osteoarthritis.* Arthritis Res Ther, 2006. **8**(2): p. R41.

194. Zanetti, M., A. Ratcliffe, and F.M. Watt, *Two subpopulations of differentiated chondrocytes identified with a monoclonal antibody to keratan sulfate.* J Cell Biol, 1985. **101**(1): p. 53-9.

195. Zappone, B., et al., *Adsorption, Lubrication, and Wear of Lubricin on Model Surfaces: Polymer Brush-Like Behavior of a Glycoprotein.* Biophys J, 2007. **92**(5): p. 1693-708.